VOLUME 32 AUGUST 1954 NUMBER 8

Canadian Journal of Physics

Published by THE NATIONAL RESEARCH COUNCIL
OTTAWA CANADA

CANADIAN JOURNAL OF PHYSICS

(Formerly Section A, Canadian Journal of Research)

Under the authority of the Chairman of the Committee of the Privy Council on Scientific and Industrial Research, the National Research Council issues annually THE CANADIAN JOURNAL OF PHYSICS and six other journals devoted to the publication of the results of original scientific research. Matters of general policy concerning these journals are the responsibility of a joint Editorial Board consisting of: members representing the National Research Council of Canada; the Editors of the Journals; and members representing the Royal Society of Canada and four other scientific societies.

Manuscripts for publication should be submitted to Dr. Léo Marion, Editor-in-Chief, Canadian Journal of Physics, National Research Council, Ottawa 2, Canada.
(For instructions on preparation of copy, see **Notes to Contributors** (inside back cover).)

Proof, correspondence concerning proof, and *orders for reprints* should be sent to the Manager, Editorial Office (Research Journals), Division of Administration, National Research Council, Ottawa 2, Canada.

Subscriptions, renewals, and orders for single or back numbers should be sent to Division of Administration, National Research Council, Ottawa 2, Canada. Remittances should be made payable to the Receiver General of Canada, credit National Research Council.

The journals published, frequency of publication, and prices are:

Canadian Journal of Biochemistry and Physiology	Bimonthly	$3.00 a year
Canadian Journal of Botany	Bimonthly	$4.00 a year
Canadian Journal of Chemistry	Monthly	$5.00 a year
Canadian Journal of Microbiology*	Bimonthly	$3.00 a year
Canadian Journal of Physics	Monthly	$4.00 a year
Canadian Journal of Technology	Bimonthly	$3.00 a year
Canadian Journal of Zoology	Bimonthly	$3.00 a year

The price of single numbers of all journals is 75 cents.

*Volume 1 will combine three numbers published in 1954 with six published in 1955 and will be available at the regular annual subscription rate of $3.00.

Canadian Journal of Physics

Issued by THE NATIONAL RESEARCH COUNCIL OF CANADA

VOLUME 32 AUGUST 1954 NUMBER 8

FURTHER CALCULATIONS ON THE NUCLEAR RESONANCE SPECTRUM OF Al^{27} IN SPODUMENE[1]

BY G. M. VOLKOFF AND G. LAMARCHE

ABSTRACT

Calculations of the expected dependence of the relative intensities of nuclear quadrupole resonance lines of Al^{27} on the orientation of a single crystal of spodumene with respect to a linearly polarized resonant magnetic field H_1 show that a suitably oriented single crystal should give rise to lines which are approximately twice as strong as those in a randomly oriented polycrystalline sample. The dependence of the matrix elements, which determine expected nuclear magnetic resonance line intensities, on the strength of a uniform external magnetic field H_0 is also given for one particular crystal orientation with respect to both H_0 and a linearly polarized field H_1.

In a previous paper (1) we reported our calculations regarding the expected dependence on the external uniform magnetic field H_0 of the energy levels, the transition frequencies, and the matrix elements entering into the corresponding transition probabilities, for the Al^{27} nuclear magnetic resonance spectrum in a single crystal of $LiAl(SiO_3)_2$ (spodumene). Only one crystal position was considered explicitly in which the z principal axis (corresponding to the largest eigenvalue) of the non axially symmetric electric field gradient tensor at the Al sites in spodumene was coincident with the external magnetic field H_0. The perturbing energy operator whose matrix elements were calculated was taken to be proportional to $\mathbf{I}_+ \equiv \mathbf{I}_x + i\mathbf{I}_y$. This operator corresponds to a resonant radiofrequency magnetic field H_1, *circularly* polarized in the xy plane (normal to the external field H_0). A case of greater experimental interest, however, is one in which H_1 is a *linearly* polarized radiofrequency field, such as the one produced along the axis of a radiofrequency oscillator coil. Also it is of interest to investigate the dependence of the transition probabilities on the orientation of such a linearly polarized H_1 with respect to the crystal axes. In the present paper we report the extension of our calculations of Ref. (1) to: (I) H_1 linearly polarized along the x principal axis of the field gradient tensor, with arbitrary values of H_0 directed along the z axis, and (II) H_1 linearly polarized along an arbitrary direction with respect to the principal axes, for the case $H_0 = 0$. This second case represents a theoretical estimate of the dependence of the relative line intensities of the expected pure quadrupole

[1]*Manuscript received May 17, 1954.*
Contribution from the Department of Physics, University of British Columbia, Vancouver, B.C.
Work supported by grants from the National Research Council.

spectrum of Al^{27} in spodumene on the orientation of a single crystal of spodumene with respect to the axis of the coil producing the radiofrequency field H_1.

I. H_1 LINEARLY POLARIZED ALONG x AXIS; $H_0 \gtrless 0$ ALONG z AXIS

A linearly polarized field H_1 may, of course, be decomposed into two circularly polarized fields rotating in opposite directions. At values of H_0 sufficiently high to make the magnetic interaction of the nucleus the dominant one, while the electric quadrupole interaction represents just a small perturbation, only that circularly polarized component of H_1 will be effective which rotates in the sense determined by the Larmor precession of the nucleus caused by the interaction of the nuclear magnetic moment with the external field H_0. However, in the case of weak H_0, and particularly in the case of pure quadrupole spectra ($H_0 = 0$), both circularly polarized components of H_1

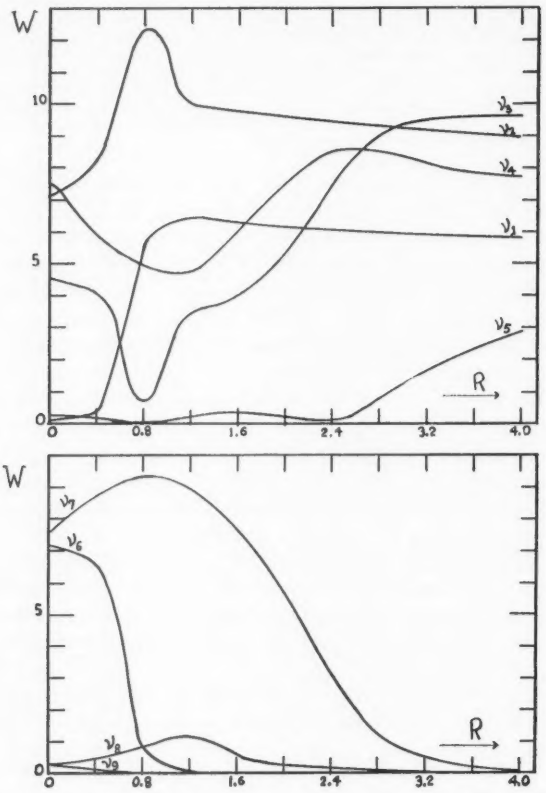

FIG. 1. Squares W of the matrix elements (in arbitrary units) of the perturbing operator proportional to $2\mathbf{I}_z$, as a function of $R = 4\mu H_0/eQ\phi_{zz}$.

are effective because the torque produced by the inhomogeneous electric field makes possible both senses of precession of the nuclear magnetic moment (e.g. around the axis of symmetry in an axially symmetric electric field). We therefore have calculated the squares of the matrix elements of the operator $2\mathbf{I}_x \equiv \mathbf{I}_+ + \mathbf{I}_-$, corresponding to H_1 linearly polarized along the x axis of the electric field gradient tensor, using the eigenfunctions obtained in our previous paper (1). Fig. 1 of this paper should be compared with Fig. 3 of Ref. (1). At high values of H_0 ($R > 3$) comparison of the two figures shows that the squares of the absolute values of the matrix elements of $2\mathbf{I}_x$ approach those of $\mathbf{I}_+ \equiv \mathbf{I}_x + i\mathbf{I}_y$, the contribution of $\mathbf{I}_- \equiv \mathbf{I}_x - i\mathbf{I}_y$ becoming negligible. This is because the corresponding eigenstates of the total energy operator for high values of H_0 directed along the z axis become almost pure eigenfunctions of the $\mathbf{I}_z$ operator, and the selection rule $m' - m = 1$ for the nonvanishing elements of $\mathbf{I}_+$ leads to zero elements of $\mathbf{I}_-$. On the other hand at lower fields the eigenstates of the total energy operator are mixtures of eigenfunctions of $\mathbf{I}_z$, and the contributions of $\mathbf{I}_+$ and $\mathbf{I}_-$ interfere sometimes constructively and sometimes destructively. Comparison of Fig. 1 of this paper with Fig. 3 of Ref. (1) shows the following differences expected in the absorption of energy from a linearly and a circularly polarized field H_1. The transition denoted by ν_1 is not appreciably affected. The transitions denoted by ν_2 and ν_3 are markedly different in the two cases, showing in the linearly polarized case strong interference effects around $R = 0.8$. ν_4 is stronger and ν_5 is weaker at low fields in the case of linearly polarized as compared with circularly polarized H_1. ν_6, ν_7, ν_8 are all stronger at low fields in the linearly polarized case. ν_9 is practically unaffected. For the linearly polarized case Fig. 2 of Ref. (1) should be modified by making the ν_2, ν_4 curves solid for all R values shown. The ν_3, ν_7 curves should also be made solid at the lowest R values. The other curves are essentially not affected.

II. PURE QUADRUPOLE SPECTRUM; $H_0 = 0$

To investigate the dependence of the relative intensities of the pure quadrupole lines on the orientation of the direction of polarization of H_1 with respect to the principal axes of the electric field gradient tensor we introduce the polar angle α and the azimuthal angle β of the direction of H_1 with respect to the principal axes. We then examine the squares W of the absolute values of the matrix elements of the operator:

$$[1] \quad 2(\mathbf{I}_x \sin\alpha\cos\beta + \mathbf{I}_y \sin\alpha\sin\beta + \mathbf{I}_z\cos\alpha) \equiv (\mathbf{I}_+ + \mathbf{I}_-)\sin\alpha\cos\beta - i(\mathbf{I}_+ - \mathbf{I}_-)\sin\alpha\sin\beta + 2\mathbf{I}_z\cos\alpha.$$

Let C, D, G (which, with the eigenstates used, are all real quantities) denote respectively the matrix elements of $\mathbf{I}_+$, $\mathbf{I}_-$, $2\mathbf{I}_z$ between the initial and final states for the transition in question. Then

$$[2] \quad W = [(C + D)\sin\alpha\cos\beta + G\cos\alpha]^2 + (C - D)^2\sin^2\alpha\sin^2\beta.$$

It was shown in Ref. (1) that the pure quadrupole eigenfunctions for half-integral I are of two classes: L involving ψ_m with $m = \frac{1}{2} + 2n$ and M involving

ψ_m with $m = -\frac{1}{2} + 2n$, where n is an integer and ψ_m are eigenfunctions of $\mathbf{I}_z$. Then in view of the well-known properties of $\mathbf{I}_+$, $\mathbf{I}_-$, $\mathbf{I}_z$ we have for transitions between states of the same class: $C = D = 0$ and

$$W = G^2\cos^2\alpha, \tag{3}$$

and for transitions between states of different classes: $G = 0$ and

$$W = [(C + D)^2\cos^2\beta + (C - D)^2\sin^2\beta]\sin^2\alpha. \tag{4}$$

The pure quadrupole energy levels for half-integral I are doubly degenerate, each energy value corresponding to a class L, and also to a class M eigenfunction. If the states are numbered 1, 2, 3, . . . in order of decreasing energy (the total number is equal to $I + \frac{1}{2}$), then the corresponding eigenfunctions may be denoted by $L_1, L_2, L_3, \ldots$ and $M_1, M_2, M_3, \ldots$. For transitions of the type $L_i \leftrightarrow M_j$ it may be shown that

$$\begin{aligned}(C + D)^2_{L_i,M_j} &= (D + C)^2_{M_i,L_j} \equiv P_{ij},\\ (C - D)^2_{L_i,M_j} &= (D - C)^2_{M_i,L_j} \equiv Q_{ij},\end{aligned} \tag{5}$$

while for transitions of the type $L_i \leftrightarrow L_j$, $M_i \leftrightarrow M_j$:

$$G^2_{L_i,L_j} = G^2_{M_i,M_j} \equiv S_{ij}. \tag{6}$$

The total intensity of a line of frequency $\nu = (E_i - E_j)/h$ arising from all the transitions between the energy levels i and j is then proportional to:

$$(P_{ij}\cos^2\beta + Q_{ij}\sin^2\beta)\sin^2\alpha + S_{ij}\cos^2\alpha. \tag{7}$$

From this we see that the intensities of transitions induced by H_1 linearly polarized along the x, y, and z principal axes are respectively proportional to P_{ij}, Q_{ij}, and S_{ij}. For other orientations of the direction of the linearly polarized H_1, eq. [7] shows that relative intensities are symmetric with respect to reflections of H_1 in the three principal co-ordinate planes. The maximum and the minimum intensities with respect to all possible orientations of H_1 correspond respectively to the largest and the smallest of the three numbers P_{ij}, Q_{ij}, S_{ij}.

It is clear from equation [7] that an investigation of the dependence of the line intensities on crystal orientation with respect to a linearly polarized H_1 can determine the orientation of the principal axes of the field gradient tensor. For a collection of randomly oriented small single crystals the averaged out intensity turns out to be proportional to $(P_{ij} + Q_{ij} + S_{ij})/3$. For a single crystal with an axially symmetric field gradient it can be shown that $S_{ij} = 0$ and $P_{ij} = Q_{ij}$, so that the line intensity is proportional to $P\sin^2\alpha$. The above results apply to any nucleus of half-integral spin.

With the eigenfunctions obtained in Ref. (1) we have calculated the expected relative intensities of the three lines of the pure quadrupole spectrum of Al^{27} in spodumene for the cases that the radiofrequency field H_1 is along each of the principal axes of the field gradient tensor, and also for the case that the sample is polycrystalline. The results are given in Table I. For other orientations of the crystal eq. [7] combined with Table I will give the result.

TABLE I

CALCULATED RELATIVE INTENSITIES W OF THE THREE PURE NUCLEAR QUADRUPOLE LINES ($H_0 = 0$) OF Al^{27} IN SPODUMENE, FOR THE CASES THAT THE LINEARLY POLARIZED RADIO-FREQUENCY MAGNETIC FIELD H_1 IS ALONG THE PRINCIPAL AXES OF THE FIELD GRADIENT TENSOR AT THE Al SITES, AND FOR THE CASE OF A POLYCRYSTALLINE SAMPLE. $W(1\leftrightarrow 2)$ CORRESPONDS TO THE TRANSITIONS $\nu_2 = \nu_6 = 0.789$ MC./SEC. $W(2\leftrightarrow 3)$ TO $\nu_4 = \nu_7 = 0.758$ MC./SEC., AND $W(1\leftrightarrow 3)$ TO $\nu_8 = \nu_9 = 1.547$ MC./SEC. (CF. REF. (1)).

Orientation of crystal with respect to H_1	Relative intensities of equation [7]	$W(1\leftrightarrow 2)$	$W(2\leftrightarrow 3)$	$W(1\leftrightarrow 3)$
H_1 along x axis	P	7.2	7.5	0.33
H_1 along y axis	Q	2.8	0.6	0.19
H_1 along z axis	S	0.5	2.6	0.18
Polycrystalline sample (random)	$\frac{1}{3}(P+Q+S)$	3.5	3.6	0.23

Thus we see that by properly orienting one or more large single crystals of spodumene with respect to the axis of the coil producing the H_1 field, we can increase the expected line intensity of pure quadrupole transitions approximately by a factor 2 over that expected for a polycrystalline sample. For an axially symmetric field gradient this factor is 1.5. In no case can this factor exceed 3.

One of the authors (G.M.V.) is indebted to the National Research Council for the financial support of the experimental program which gave rise to these calculations.

REFERENCE

1. LAMARCHE, G. and VOLKOFF, G. M. Can. J. Phys. 31: 1010. 1953.

THE MULTIPLICITY OF NEUTRON PRODUCTION BY SPONTANEOUS FISSION OF URANIUM[1]

By K. W. Geiger[2] and D. C. Rose

ABSTRACT

Metallic uranium was placed in a paraffin pile containing two $B^{10}F_3$ neutron counters. The mean life of thermal neutrons in this pile was measured (140 μsec.). Neutron counter pulses occurring within a time interval of this order can be assumed to come from an individual fission event and statistical analysis makes it possible to obtain information concerning the actual number of neutrons released in one fission event. The efficiency of the pile for neutron counting was found to be 2.5% using the known neutron rate from spontaneous fission of uranium. Without further assumption, the method does not give the mean multiplicity directly, but the higher moments of the multiplicity spectrum. A Poisson distribution for the multiplicity spectrum fits our data well and gives an average of 2.3 ± 0.2 neutrons per spontaneous fission. This value is in good agreement with the mean multiplicity from other methods.

I. INTRODUCTION

Though measurements have been published on the rate of spontaneous fission of uranium (5, 7) and on the total neutron production by spontaneous fission (3), a direct measure of the multiplicity of the neutrons produced is not available. An apparatus designed primarily to study neutron production by cosmic rays in various materials has proved very useful in studying the multiplicity of neutron production by spontaneous fission of uranium in a direct way.

The present measurements are not absolute in that without some independent measure of the efficiency of the apparatus the multiplicity cannot be calculated without reference to other measurements, for instance the total neutron production by spontaneous fission. The combination of our results with other published work and certain assumptions about the multiplicity spectrum have resulted in a measure of the mean multiplicity which is considered reliable and is consistent with available measurements on total neutron production and the spontaneous fission rate.

II. APPARATUS AND METHOD OF EXPERIMENT

(*a*) *Description of Apparatus*

Fig. 1 is a schematic diagram of the apparatus. Freshly refined natural uranium metal was used in the form of seven flat strips 40 cm. long, 3.4 cm. wide, and 0.45 cm. thick. These were placed together in two flat layers (three strips on top of four strips). This amount was chosen since it gave a convenient counting rate in the apparatus. The uranium was surrounded by paraffin wax, and in holes in the wax two $B^{10}F_3$ neutron counters were placed as shown, centered about 9 cm. below the uranium. The counters were 6.4 cm. in diameter and the active length was about 50 cm. This pile was built on a steel

[1]*Manuscript received April 9, 1954.*
Contribution from the Division of Physics, National Research Council, Ottawa, Canada. Issued as N.R.C. No. 3320.
[2]*National Research Laboratories Postdoctorate Fellow.*

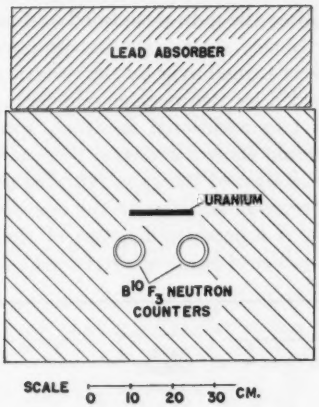

FIG. 1. Arrangement of uranium and neutron counters in the paraffin pile.

frame, the paraffin being contained in light steel tanks so that the whole was demountable. A lead absorber could be placed on top of the pile up to 25 cm. in thickness.

The neutrons which come from one fission event are slowed down in the paraffin and with a mean life of about 150 μsec. will be captured in the paraffin or in the boron of the counters. Neutrons recorded in a suitable time interval after the nuclear event will therefore have a common origin. But because of the low efficiency of such an arrangement, only a few of the released neutrons will be recorded. This makes the statistical analysis of the data somewhat difficult. The method is similar to that used by Cocconi *et al.* (1) in the study of neutron production by penetrating cosmic ray showers.

The counters in the present experiment were connected in parallel to an amplifier and a discriminator which was normally blocked by a gate circuit. The gate circuit was opened after a fixed delay by the first pulse from the neutron counters from each event. The linear amplifier, discriminator, and gate circuits were conventional and need not be described here except to say that they were very rugged, designed for continuous operation, and were built in the laboratory.

The recording of multiple neutrons during the period of the gate opening was arranged by using a series of two binary scaling stages. The two stages were in series but the output from each was recorded on a message register and on an Esterline-Angus 20-pen operations recorder. The sequence of operations was as follows. An event which occurred in the uranium in such a way that a neutron was picked up by one of the counters would cause the gate to be opened after a delay of 6 μsec. The length of the gate was normally 320 μsec., but for one experiment a variable gate length was used so that the mean life of the neutrons could be measured. Any further neutrons collected while

the gate was open would then set the two binary scalar circuits according to the number collected. After the gate was closed and after a further delay of a few microseconds, the binary scaler circuits were reset automatically. The binary circuits which were turned over by the resetting circuit would send out a pulse which was recorded by the message registers and the Esterline-Angus recorder. Therefore, if two additional neutrons appeared in the gate, the second binary circuit would show a count; if three neutrons were collected in addition to the one which opened the gate, both binary circuits would show a count. Up to three neutrons in addition to the one opening the gate could be counted for any event. A schematic diagram of the circuit arrangement is shown in Fig. 2. The number of gates was recorded using a suitable scaler, the

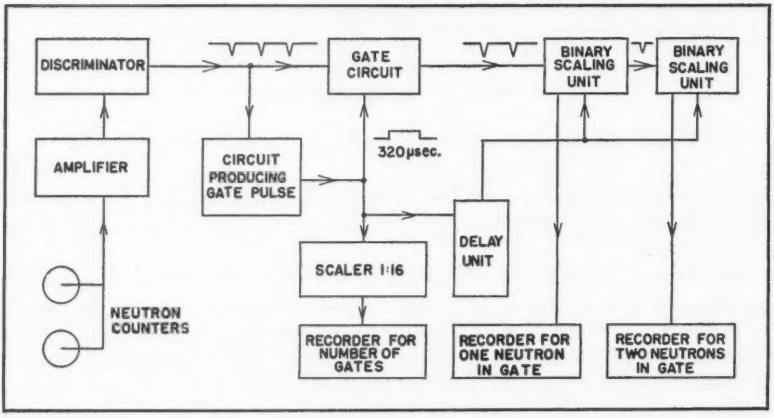

FIG. 2. Schematic circuit diagram.

output of which was fed to one of the pens of the 20-pen operations recorder and to a message register. The recorder chart was operated at a rate of one foot per hour, time marks being put on the chart every minute.

(*b*) *Analysis of the Experimental Method*

The efficiency of the apparatus, ϵ, is defined as the probability of any one neutron produced in the uranium being captured in the boron trifluoride and producing a pulse from the counter, not just while the gate is open but at any time after the event which produced the neutron. In any fission event the number ν of neutrons produced is an integer, but to calculate a mean multiplicity $\bar{\nu}$ the various moments of ν, defined as follows, must be considered:

$$[1] \qquad \sum_{\nu=0}^{\infty} \nu\, I(\nu) = \bar{\nu}, \quad \sum_{\nu=0}^{\infty} \nu^2 I(\nu) = \overline{\nu^2}, \quad \text{etc.},$$

$$\sum_{\nu=0}^{\infty} I(\nu) = 1.$$

$I(\nu)$ is the probability that ν neutrons are released from a fission event.

If for the present the effect of the finite gate length is omitted, the probability that n of the ν neutrons released in one fission event reach the counters and are captured follows a binomial distribution

$$P(n, \nu) = \binom{\nu}{n} \epsilon^n (1 - \epsilon)^{\nu - n}.$$

Then where F is the spontaneous fission rate and R_1 the counting rate for events wherein only one neutron from each event is collected, R_2 that for exactly two neutrons, etc.,

$$R_n = F \sum_{\nu=n}^{\infty} I(\nu) \binom{\nu}{n} \epsilon^n (1 - \epsilon)^{\nu - n}.$$

Since ϵ is small (~ 0.03) and it is difficult to get statistics such that errors are smaller than a few per cent, the factor $(1-\epsilon)^{\nu-n}$ can be considered equal to unity. Then

$$R_1 = F \bar{\nu} \epsilon, \quad R_2 = F \frac{\overline{\nu^2} - \bar{\nu}}{2} \epsilon^2, \quad R_3 = F \frac{\overline{\nu^3} - 3\overline{\nu^2} + 2\bar{\nu}}{6} \epsilon^3$$

or, using the ratios R_2/R_1 and R_3/R_2,

[2] $$\frac{\overline{\nu^2}}{\bar{\nu}} = \frac{2R_2}{\epsilon R_1} + 1, \quad \frac{\overline{\nu^3} - \overline{\nu^2}}{\overline{\nu^2} - \bar{\nu}} = \frac{3R_3}{\epsilon R_2} + 2.$$

ϵ is assumed to be a constant over the area of the neutron producer or sufficiently so that $\overline{\epsilon^2} = \bar{\epsilon}^2$ and similarly for the higher moments. A rough experiment performed by moving strips of uranium across the area occupied by the producer showed that variation in efficiency was sufficiently small for this to be the case.

To obtain the values for the R's from the measured results, it is necessary to correct for the gate length. The neutrons have a mean lifetime τ in the paraffin and counters, and the probable number at a time t after the event has the usual exponential form

$$N = N_0 e^{-t/\tau}.$$

The probability of a neutron being recorded is proportional to the number present and therefore decays with time according to the same law. Therefore, there is an additional efficiency factor f represented by

$$f = \frac{1}{\tau} \int_{t_1}^{t_2} e^{-t/\tau} \, dt$$

where t_1 represents the time the gate opens after the first opening neutron and t_2 the time the gate closes.

If a total of n neutrons would have reached the counters had the gate opened immediately the first one was detected and had it remained open a long time, the probability $P(m, n)$ that m neutrons of those n would be recorded is

$$P(m, n) = \binom{n-1}{m-1} f^{m-1} (1 - f)^{n-m}.$$

An observed counting rate O_m, that is one in which m neutrons are recorded for each event including the one that opens the gate, is made up of $f^{m-1} R_m$ as defined in previous paragraphs plus fractions of R_{m+1}, R_{m+2}, etc., the recorded number of neutrons being reduced to m by the finite gate length. It is readily seen that

$$[3] \qquad \begin{aligned} O_1 &= R_1 + (1-f) R_2 + (1-f)^2 R_3 \ldots, \\ O_2 &= fR_2 + 2f(1-f) R_3 + 3f(1-f)^2 R_4 \ldots, \\ O_3 &= f^2 R_3 + 3f^2(1-f) R_4 + 6f^2(1-f)^2 R_5 \ldots, \end{aligned}$$

etc.

Since the rate of observed multiplicities above three was negligibly small, the contribution of R_4 and higher can be neglected. The gate correction f was calculated from the gate length measured with a suitable oscilloscope. Actually an experiment was performed using three gate lengths so that the mean life τ could be measured; the gate lengths were 320, 120, and 70 μsec. and by a comparison of the counting rates N_1, N_2, and N_3, three measures of the mean life were obtained as follows:

from N_1/N_2, $\tau = 141 \pm 13$ μsec.;

N_2/N_3, $\tau = 122 \pm 40$ μsec.;

N_1/N_3, $\tau = 136 \pm 10$ μsec.

These are in general agreement with published values for similar types of experiments. The actual value will depend on the geometrical arrangement of counters in the wax since BF_3 counters are very strong absorbers of slow neutrons. In calculating the value of f, 140 μsec. was used for τ. This makes $f = 0.861$.

To make the measurements independent of other knowledge of the fission of uranium, the efficiency ϵ would have to be measured by other means. Accurate calculation of ϵ is impossible and the use of sources of known strength, even if one had been available, would be uncertain unless the spectrum was the same as the spontaneous fission spectrum. It seemed therefore reasonable to use the uranium itself to evaluate the efficiency. This method has the additional advantage that it takes into account the small neutron loss due to absorption within the uranium. Measurements have been published on the total neutron production by spontaneous fission which vary from 1.5 to 1.75×10^{-2} neutrons per gram per sec. (3, 5, 7). The most recent value given by Littler (3) is $(1.65 \pm 0.09) \times 10^{-2}$ neutrons per gram per sec. and this has been chosen to calculate ϵ for the present experiment. The amount of uranium was 8.05 kgm. and with the total number of neutrons collected an efficiency of $(2.51 \pm 0.17)\%$ was obtained. Another estimate of the efficiency was made by comparing the effects of cosmic rays on a lead producer (in place of the uranium) with the results of Tobey and Montgomery (6) who measured the neutron production by cosmic rays in lead. This method gives an efficiency of $(2.9 \pm 0.4)\%$, but there is considerable uncertainty in using it because of absorption and barometer corrections for the neutron-producing cosmic

radiation and because the average neutron energy from lead is known to be higher than that from fission.

It was found that the paraffin on top of the uranium increased the efficiency appreciably. This is due to reflection of the neutrons by the top paraffin and thus permits the assumption that any anisotropy in the emission of the fission neutrons is sufficiently smeared out that the results are not affected.

Though the counting efficiency has now been evaluated, the mean multiplicity still cannot be obtained directly. Using published data (for instance, Segrè's (5) value for the fission rate and Littler's (3) value for the total neutron production), the resulting mean multiplicity put in equation [2] will give the second and third moments of the multiplicity. These could then be compared with possible analytical expressions for the multiplicity spectrum. Alternatively, analytical expressions can be chosen for the multiplicity spectrum and the ratios of the moments obtained from them can be used with equation [2] to obtain the mean multiplicity. The latter way has been chosen to treat the data.

III. RESULTS

(*a*) *Numerical Results and Corrections*

To obtain the counting rate the background was always measured by removing the producer and subtracting the rate without it. Corrections were also necessary for accidental counts and for dead times of the circuits wherever they applied. A typical set of data showing the correction is shown in Table I.

TABLE I

TYPICAL SET OF DATA SHOWING CORRECTIONS

	Gates per hour	Double events per hour	Triple events per hour
8.05 kgm. of uranium, no absorber on top of pile (6 days of operation)	12019 ± 50	274.7 ± 1.6	7.49 ± 0.23
Correction due to dead time of message registers	—	$+32.8$	—
Correction due to time constant of the gate circuit	$+22$	—	—
Corrections due to accidental counts		-12.8	-0.33
Background without producer	-303 ± 3	-3.0 ± 0.2	$-0 \quad +0.05$
Uranium	11738 ± 51	291.7 ± 1.7	7.16 ± 0.24

The amount of uranium (8.05 kgm.) used was much too small to produce a substantial number of thermal-neutron-induced fissions in U^{235} by spontaneous fission neutrons slowed down in the paraffin. This was checked by surrounding the uranium with cadmium which lowered the counting efficiency without producing a significant effect on the final results. We have also neglected

the small contribution to the neutron production due to secondary fission events in uranium 238 induced by fast neutrons from spontaneous fission. Their number would be too small to have an appreciable influence on the mean multiplicity, but because the two events would be effectively simultaneous, they may have some influence on the multiplicity distribution at high values of ν.

The correction for the dead time of the message registers only applied where shown, since a scaler was used on the number of gates and in the case of triple events the rate was low enough for the dead time corrections to be negligible. The dead time used to make this correction was carefully measured. The correction due to the time constant of the gate circuit was necessary since the clearing of the scalers and recovery of the circuit made it impossible to repeat a gate until 550 μsec. after a gate pulse started. This time was measured by setting up a circuit giving two pulses, the interval between them being variable. This correction would, of course, only apply to the number of gates. For accidental double counts the correction was taken to be $N_1^2 g$ where N_1 is the counting rate for gates and g the gate length. The corresponding correction for triple events was calculated from $N_1 N_2 g$ where N_2 is the rate for double events.

Table II shows a set of results for uranium and lead neutron producers after these corrections have been made, the rate using the lead producer being

TABLE II

NEUTRON PRODUCTION FROM URANIUM AND LEAD

	Gates per hour	Double events per hour	Triple events per hour
No absorber on top			
8.05 kgm. of uranium	11738 ± 51	291.7 ± 1.7	7.16 ± 0.24
5.65 kgm. of lead as producer but data corrected to be equivalent to 8.05 kgm. of lead	70 ± 10	6.5 ± 0.7	0.60 ± 0.17
Difference, uranium − lead	11668 ± 55	285 ± 2	6.56 ± 0.30
Absorber, 25 cm. of lead			
8.05 kgm. of uranium	11655 ± 31	284 ± 1.7	5.76 ± 0.27
Lead producer as above	31 ± 9	3.46 ± 0.57	0.34 ± 0.14
Difference, uranium − lead	11624 ± 33	281 ± 2	5.42 ± 0.31

included so that the cosmic ray correction for uranium can be explained. Barometer corrections were, of course, necessary when using the lead producer. Examining Table II it is noted that the lead absorber has little effect on the number of gates, hardly a significant effect on the number of double events, but probably a significant effect on the number of triple events. This is the result that would be expected if the multiplicity of neutrons produced by cosmic rays in uranium is somewhat greater than that in lead. It is also noted that the effect of the lead absorber on neutrons from a lead producer is to cut the intensity by approximately 50%. If one assumes for a first approximation

that the cross section for neutron-producing collisions by cosmic rays is the same for uranium and lead, a correction can be made for the effects of cosmic rays on the uranium. The difference in the number of triple events without and with the lead absorber is 7.16 − 5.76. This represents 50% of the effect of cosmic rays. The cosmic ray correction, therefore, is twice this difference or 2.80 counts per hour, making the true number of triple events 4.36 per hour. A similar correction can be made for the double events. Since the number of gates includes double and triple events, these must be subtracted to get the number of single events. The results, therefore, are:

O_1 = rate of single events = 11341 ± 35 per hour,

O_2 = rate of double events = 279 ± 4 per hour,

O_3 = rate of triple events = 4.36 ± 0.60 per hour.

From these data and equation [3], neglecting higher multiplicities than three, the values of R_1, R_2, and R_3 can be calculated as

$$R_1 = 11296 \pm 35 \text{ per hour},$$
$$R_2 = 321 \pm 5 \text{ per hour},$$
$$R_3 = 5.9 \pm 0.8 \text{ per hour}.$$

From these figures and the efficiency using equation [2], the ratios $\overline{\nu^2}/\bar{\nu}$ and $\overline{\nu^3}/\bar{\nu}$ can be calculated, giving

[4] $$\overline{\nu^2}/\bar{\nu} = 3.26, \qquad \overline{\nu^3}/\bar{\nu} = 12.73.$$

(*b*) *The Mean Multiplicity and the Multiplicity Spectrum*

Since the experimental method gives only these ratios of the moments of the multiplicity spectrum, the best procedure seemed to be to assume a multiplicity function and try to fit the results to it. The multiplicity spectrum will, of course, be a histogram or discontinuous type of distribution because only integral values of ν are possible. A Poisson distribution suggests itself as follows:

$$I(\nu) = \bar{\nu}^{\nu} e^{-\bar{\nu}}/\nu! .$$

For this distribution

$$\overline{\nu^2} = \bar{\nu}^2 + \bar{\nu}$$

and

$$\overline{\nu^3} = \bar{\nu}^3 + 3\bar{\nu}^2 + \bar{\nu}.$$

Applying this to our results gives

$$\bar{\nu} = 2.26 \pm 0.16$$

and

$$\overline{\nu^3} = 29.1 \pm 4.8.$$

From equation [4], using $\bar{\nu} = 2.26$, $\overline{\nu^3}$ would be 28.8.

This agreement indicates that a Poisson distribution is a good approximation. The average neutron multiplicity of $\bar{\nu} = 2.3 \pm 0.2$ agrees well with other more indirect measurements. For instance, combining Segrè's (5) figure for the spontaneous fission rate $(6.90 \pm 0.24) \times 10^{-3}$ fissions gm.$^{-1}$ sec.$^{-1}$, and Littler's (3) value for the total neutron production of

$(1.65 \pm 0.09) \times 10^{-2}$ neutrons gm.$^{-1}$ sec.$^{-1}$ yields an average multiplicity of $\bar{\nu} = 2.4 \pm 0.2$. A value of $\bar{\nu} = 2.55$ (4) is usually accepted as the mean multiplicity of neutrons by fast neutron fission in uranium, but spontaneous fission would be expected to produce a slightly lower value.

Fig. 3 shows the Poisson distribution function. It is noted that the probability $I(\nu = 0)$ is not 0, or if this is the true distribution about 10% of the sponta-

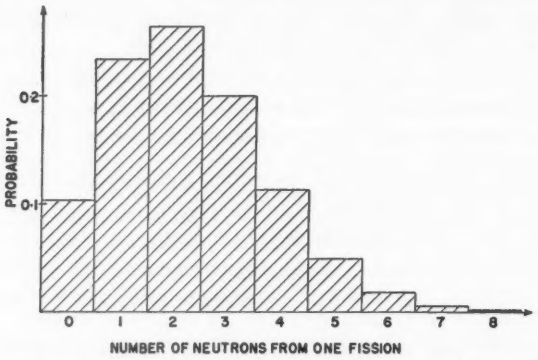

FIG. 3. Poisson distribution for neutron multiplicity.

neous fission events do not produce prompt neutrons. To see if the present results make such a conclusion necessary, other distributions were tried. Following the method of Widgoff (8) for studying neutron production by mesons, a histogram having the following properties was tried:

$$I(0) = 0, \quad I(1) = I(2) = a, \quad I(3) = I(4) = b,$$

$$I(5) = I(6) = I(7) = c, \quad I(\geqslant 8) = 0,$$

$$\sum_{\nu=0}^{\infty} I(\nu) = 1.$$

With these equations and our data, a, b, and c can be evaluated. The results yield

$$\bar{\nu} = 2.54,$$
$$a = 0.270,$$
$$b = 0.205,$$
$$c = 0.0165.$$

The value of $\bar{\nu}$ is rather high, but probably not too high to exclude such a distribution.

A distribution of the form

$$I(\nu) \propto e^{-a\nu}$$

was also tried. This gives a value of $\bar{\nu} = 1.1$ which is improbably low.

Using this expression but imposing the condition that $I(0) = 0$ leads to a value of 2.13 for $\bar{\nu}$ which is quite a possible value. It also yields a reasonable value for $\overline{\nu^3}$ ($=32.9$) since applying the ratio $\overline{\nu^3}/\bar{\nu}$ in equation [4] to this distribution gives $\overline{\nu^3} = 27.1$, the error being such that this difference is hardly significant.

The results therefore are not sufficiently accurate to show whether or not spontaneous fission can occur without neutron emission. In fact, the measurements are comparatively insensitive to the shape of the multiplicity spectrum for low values of ν.

IV. SUMMARY AND DISCUSSION

We have derived the mean multiplicity of neutron production by spontaneous fission of natural uranium. The measurements are considered to apply to U^{238} since the amount of U^{235} and other isotopes is known to be less than 1% and their spontaneous fission rate is too small to contribute appreciably. The mean multiplicity $\bar{\nu}$ is obtained from these measurements and Littler's value (3) for the total neutron production due to spontaneous fission. The data do not give the value of $\bar{\nu}$ directly, but the ratio of $\bar{\nu}$ to the higher moments of ν. To determine $\bar{\nu}$ it is necessary to assume a multiplicity distribution. A number of distributions were tried. A Poisson distribution gives results which fit the data well and indicates a mean multiplicity of $\bar{\nu} = 2.3 \pm 0.2$ neutrons per fission event. This requires however that about 10% of the fission events occur with no prompt neutron emission, a value which seems relatively high.

Other multiplicity distributions, resembling a Poisson distribution at high values of ν but with $I(\nu = 0) = 0$, are not inconsistent with our data. Therefore a Poisson distribution is not necessarily correct, particularly for low values of ν. The results require, however, an appreciable probability for values of ν above, say, 3 and in this region the distribution must resemble the Poisson distribution as shown in Fig. 3. Even if a few per cent of the events are in cascade involving fast neutron fission of uranium^{238} this conclusion will not be altered.*

Fission neutrons have two substantially different origins: First the prompt neutrons which are emitted during the fission act itself or from the excited fragments immediately after division. Secondly the delayed neutrons which are due to re-excitation of the fragments after beta-decay. The contribution of the delayed neutrons is only 1% of the total and is therefore negligible in the present experiment. They will not seriously affect the shape of the multiplicity spectrum.

Fraser's (2) experiments on the angular distribution of prompt neutrons from fission are consistent with the hypothesis that the neutrons are emitted from moving fission fragments with a spread in number and energy characteristic of nuclear evaporation. The distribution in mass and excitation energy

*NOTE: *H. H. Clayton and S. A. Kushneriuk (private communication) have calculated the number of neutrons produced in such a block of uranium by fission of U^{238} caused by fast neutrons from spontaneous fission. The increase in production is estimated to be 3%.*

of the fission fragments will further complicate the multiplicity spectrum and therefore a simple distribution in multiplicity should hardly be expected.

ACKNOWLEDGMENTS

The uranium used in this experiment was loaned to the authors by Atomic Energy of Canada Limited. We are grateful to Dr. W. B. Lewis for arranging this loan and for discussion of the results and advice. Thanks are also due Dr. D. Jakeman and Mr. E. P. Hincks for discussions on some parts of the experiment, and to Mr. H. H. Clayton and Dr. S. A. Kushneriuk for calculations on cascade processes.

REFERENCES

1. COCCONI, G., COCCONI TONGIORGI, V., and WIDGOFF, M. Phys. Rev. 79: 768. 1950.
2. FRASER, J. S. Phys. Rev. 88: 536. 1952.
3. LITTLER, D. J. Proc. Phys. Soc. (London), A, 65: 203. 1952.
4. Release of Information on Atomic Energy. Nature, 169: 871. 1952.
5. SEGRÈ, E. Phys. Rev. 86: 21. 1952.
6. TOBEY, A. R. and MONTGOMERY, C. G. Phys. Rev. 81: 517. 1951.
7. WHITEHOUSE, W. J. and GALBRAITH, W. Phil. Mag. 41: 429. 1950.
8. WIDGOFF, M. Phys. Rev. 90: 891. 1953.

ON THE EVALUATION OF CERTAIN LATTICE SERIES[1]

By S. K. Roy[2]

ABSTRACT

Lattice series of the Madelung type are at best conditionally convergent; the values of such series, therefore, depend on the method of summation. A criterion is indicated for the choice of a method of summation leading to a physically significant value consistent with the problem in which such a series occurs. Evjen's method of grouping the terms of the series into particular units is discussed in detail for the CsCl type of lattice. It is found that in this case, his method fails to yield directly the unique physically significant value. An alternative method is proposed which leads at once to the unique value and is applicable to any series of the Madelung type.

1. INTRODUCTION

Lattice series of the type

$$[1] \qquad S = \sum_{(xyz)} (-1)^{x+y+z} \frac{x^m + y^m + z^m}{(x^2 + y^2 + z^2)^{\frac{1}{2}(m+1)}}$$

occur in the calculation of the elastic constants and anharmonicities of the lattice oscillations of alkali halide crystals on the basis of the Born dynamic model of a lattice (Wasastjerna (8, 9), Löwdin (6), Krishnan and Roy (3, 4)). In the case of the NaCl type of lattice the summation extends over all integral values of x, y, z, while in the CsCl type x, y, z are restricted to values which are either all odd or all even; the term corresponding to $x = y = z = 0$ is to be excluded for both crystal types. In the series [1] m is an integer. For lattices with a center of symmetry, such as the NaCl and the CsCl types, an odd value of m leads to a zero value for the series.

The cases $m = 0$ and $m = 2$—which are evidently identical apart from a trivial multiplying factor—correspond to the well-known Madelung series which appears in the calculation of the average electrostatic potential energy per ion in a crystal:

$$[2] \qquad S_0 = \sum_{(xyz)} \frac{(-1)^s}{(x^2 + y^2 + z^2)^{\frac{1}{2}}}$$

where

$$s = x + y + z.$$

In fact, the electrostatic potential at any lattice point—say the point occupied by an alkali ion in an alkali halide crystal—due to the charges of all the other ions in the crystal is given by $S_0|e|/a$, where $|e|$ is the electronic charge and $2a$ the side of the unit cell containing four alkali and four halide ions in the NaCl type and one of each in the CsCl type.

It is evident that the series [1] and [2] are at best conditionally convergent. Hence the values of the series depend on the method of summation.

Any particular method of summing these series has to be consistent with

[1]*Manuscript received April 27, 1954.*
Contribution from the Division of Physics, National Research Council, Ottawa. Issued as N.R.C. No. 3327.
[2]*National Research Laboratories Postdoctorate Fellow.*

the physical problem in which they occur. As has already been mentioned, the series [2] has a direct physical significance, and the method of summation must be chosen such that the value S_0, which is the potential energy per ion in units of $|e|^2/a$, is the same for every ion in a unit cell of the crystal. The same criterion will be extended for defining a physically significant sum of the series [1].

Various methods are available for summing series [2]; the earlier ones have been reviewed by Sherman (7). The methods of Madelung, Ewald, and Born cannot be applied to the general series [1]. Evjen (1) has suggested a method for the summation of the Madelung series which can also be applied to general series of the type [1]. The main idea of Evjen's method is to regard the crystal as built up of different electrically neutral unit cells. When summing the Madelung series [2], he first groups the terms of the series into unit cells and then sums the contributions from different unit cells. (The ions in a particular unit cell are assigned proper weights to make it electrically neutral.) This method gives S_0 as defined for the NaCl type of lattice, but for the CsCl type it fails to yield a unique value. For the CsCl type of lattice, in which the unit cell is a body-centered cube containing two ions per cell, Evjen's method gives different values for the potential at the center and at one of the corners of the unit cell. Indeed, the physically-interesting *average* potential energy per ion is evidently the arithmetic mean of these two values.*

The procedure described above is equivalent to the following: to find the potential at a point occupied by, say, a positive ion of a CsCl type of crystal, we group the ions into unit cells. It is readily seen that for the CsCl type of lattice the choice of a cubic unit cell can be made in two different ways, either with a positive ion at the center and negative ions at the eight corners, or with a negative ion at the center of the cube and eight positive ions at the corners. Depending on this choice, the sum of the resulting series S_{I} and S_{II}, say, will be different, and the two sums will be different from the actual sum S_0 defined above. The physical reason for the difference between S_{I} and S_{II} lies in the fact that by choosing the origin at two distinct lattice points in the crystal, S_{I} will differ from S_{II} by the potential contributed by the corresponding electrical double layer at the surface of the crystal.

In this paper we discuss in detail the implications of Evjen's method when applied to the series [1] and [2] for the CsCl type of lattice. Further, we shall find a criterion for grouping the terms of the series in such a manner that *unique* values are obtained.

2. EVJEN'S METHOD OF SUMMING THE MADELUNG SERIES FOR THE CsCl TYPE OF CRYSTAL, AND THE CONTRIBUTION TO THE POTENTIAL FROM THE IONS IN A DOUBLE LAYER

From now onwards we shall discuss the case of the CsCl type of crystals, postponing that of the NaCl type to the last section. In the present section we shall consider only the simpler series [2] (cf. Krishnan and Roy (5), Gurney (2)).

As is well known, the positive and the negative ions in a CsCl type of lattice

**Evjen's reason for taking the arithmetic mean of these values is somewhat obscure.*

separate in alternate layers parallel to {100}. Hence the distribution of the ions about the origin (supposed occupied by a positive ion, with the co-ordinate axes parallel to the cubic axes of the crystal) may be regarded in the following manner. We group the ions in such a way that all of them lie on the surfaces of cubes having their centers at the origin and their edges along the cubic axes of the crystal, with their semisides equal to 1, 2, . . . n, . . ., all distances being expressed in units of a; the corners and edges are included in the surface of the cubes. The ions on the surface of a particular cube of semiside n are all positive when n is even, and all negative when n is odd.

Denoting the potential at the origin contributed by all ions on the surface of the cube of semiside n by $(-1)^n\Delta_n$, where Δ_n is positive, we have for large n:

$$\Delta_n = 6\sum_{(yz)} (n^2 + y^2 + z^2)^{-\frac{1}{2}}, \tag{3}$$

in which both y and z vary from $-n$ to $+n$ at intervals of 2. Since the minimum value of any term of [3] is $1/(n\sqrt{3})$, and the number of such terms in the expression for Δ_n is proportional to n^2, it is readily seen that $\Delta_n \to \infty$ when $n \to \infty$.

On the other hand, for large n the contribution to the potential at the origin from the ions on the surfaces of any two adjacent cubes is $(-1)^{n+1}(\Delta_{n+1}-\Delta_n)$. When n is large, the double layer of charged particles may be regarded as a homogeneous electric shell, the surface charge per unit area being $\frac{1}{4}$ and the thickness unity. The electric moment of the shell is $\frac{1}{4}$ per unit area, and directed away from the center when n is odd and towards the center when n is even. According to the theorem of Gauss, the potential at the origin of such a shell is

$$(-1)^{n+1}(\Delta_{n+1} - \Delta_n) = (-1)^{n+1}\Omega/4 = (-1)^{n+1}\pi, \tag{4}$$

where Ω is the total solid angle subtended at the origin by the shell—i.e. 4π. The contribution to the potential at the origin from any two adjacent layers is therefore finite and equal to $\pm\pi$, even when Δ_n and Δ_{n+1} tend separately to infinity.

In order to sum the series [2] according to Evjen's method, we first group the ions into cubic unit cells, and then regroup these unit cells into cubic shells each of thickness 2 (in units of a). Following this method of grouping, the series [2] can be written in the form

$$\sum_{\text{shells}} \sum_{\text{cells}} \Psi_p$$

where Ψ_p denotes the contribution to the series from the ions in a unit cell, the inner summation is over all such cells included in a cubic shell of thickness 2, and the outer summation is over all such shells. Now the sum over the cells represents the contribution from the ions on the three cubic layers of semisides, say, n, $n + 1$, and $n + 2$, the two extremal layers n and $n + 2$ being shared with adjacent shells. The contribution to the potential at the origin due to one such shell is, for large n,

$$\begin{aligned}(-1)^n[\tfrac{1}{2}\Delta_n - \Delta_{n+1} + \tfrac{1}{2}\Delta_{n+2}] &= (-1)^n\tfrac{1}{2}[(\Delta_n - \Delta_{n+1}) - (\Delta_{n+1} - \Delta_{n+2})] \\ &= U_N, \text{ say,}\end{aligned} \tag{5}$$

in which the subscript N initially has the value of n but increases in steps of 2. U_N tends to zero when $N \to \infty$.

In the above sequence (U_N), N is consistently even or odd depending on the original choice of the unit cell—i.e. on whether the cell contains a positive or a negative ion at its center. Thus depending on the choice of the unit cell, the sum of the resultant series is either S_{I} or S_{II} and the two sums differ by $(\Delta_{n+1} - \Delta_n)/2$, i.e. by $\pi/2$ (cf. [4]).

3. THE GENERAL CASE WHEN m IS ANY INTEGER

Instead of taking cubic shells as before, we shall for simplicity consider infinite layers of ions perpendicular to one of the cubic axes of the crystal. Numbering the layers as $\ldots -n, \ldots -2, -1, 1, 2, \ldots n, \ldots$, about the origin, we consider the contribution to the series [1] from the ions in any given infinite layer $x = n$. Denoting this contribution by $(-1)^n\sigma_n$, we have

$$\sigma_n = \sum_{(yz)} \frac{n^m + y^m + z^m}{r^{m+1}}, \tag{6}$$

where $r^2 = n^2 + y^2 + z^2$. Obviously σ_n is infinite for all n. On the other hand, the joint contribution from any two adjacent layers $x = n$ and $x = n + 1$ is, for large n,

$$(-1)^{n+1}(\sigma_{n+1} - \sigma_n) = (-1)^{n+1} \times 2l, \tag{7}$$

where

$$2l = \frac{1}{4}\int \frac{\partial}{\partial n}\left\{\frac{n^m + y^m + z^m}{r^{m+1}}\right\} ds. \tag{8}$$

In [8] ds is an element of area on the plane $x = n$ (or the plane $x = n + 1$), and the integration extends over the whole of one of these planes. Eq. [8] can be written in the form

$$2l = \frac{1}{4}\left[(m+1)\int \frac{n^m + y^m + z^m}{r^{m+1}} d\tilde{\omega} - m\int \frac{n^{m-2}}{r^{m-2}} d\tilde{\omega}\right], \tag{9}$$

where $d\tilde{\omega}$ is the element of solid angle subtended at the origin by ds. The integration in [9] is readily performed, leading to the result

$$2l = \frac{2m-3}{m-1}\cdot\frac{\pi}{2}. \tag{10}$$

Hence the contribution to S (eq. [1]) from any two layers jointly is finite and equal to $\pm 2l$, even when σ_n and σ_{n+1} separately tend to infinity.

By grouping the contributions from the infinite layers into terms of the type

$$V_N = (-1)^n(\tfrac{1}{2}\sigma_n - \sigma_{n+1} + \tfrac{1}{2}\sigma_{n+2}), \tag{11}$$

we obtain two different sums according as N is even or odd; thus

$$\begin{cases} S'_{\mathrm{I}} = S + l, \\ S'_{\mathrm{II}} = S - l, \end{cases} \tag{12}$$

l being defined by [10].

Putting $m = 0$ in [10], we find that $l = 3\pi/4$, which is indeed just thrice the corresponding value of l calculated for the Madelung series in the previous section.

4. IMPLICATION OF GROUPING THE IONS INTO CUBIC UNIT CELLS, AND THE CRITERION FOR THE CHOICE OF CELLS LEADING TO A UNIQUE SUM

We have seen that Evjen's method of summation can indeed be used to give the two sums S_I and S_{II} and hence their arithmetic mean S_0 (cf. Introduction), not only for the Madelung series but also for the general case when m is any integer.

We may mention here that for the Madelung series Evjen's method of grouping the terms into unit cells yields two *absolutely* convergent series for S_I and S_{II}, but this fact is of no particular advantage, as can be seen from the consideration that, for the general case (m any integer), after the terms have been grouped into unit cells the resulting series may not be absolutely convergent; yet we may still group the terms of [1] in the same manner as Evjen and obtain therefrom values S'_I and S'_{II} the arithmetic mean of which still gives S.

From the considerations in the previous section, we have found that the consequences of grouping the terms of the series [1] into unit cells and further regrouping these unit cells as done by Evjen are as follows:

(1) The unit cells can be further regrouped in such a manner that the positive and negative ions separate out into alternate parallel layers.

(2) The contribution to the sum from any two adjacent layers remains finite, and is positive or negative according as the positive layer of the pair is the one on the further side or on that facing the origin.

(3) Since the unit cell has to be electrically neutral, three such adjacent layers have to be grouped together, the outer layer of this composite three-layered shell being shared equally with the adjacent shells. Whether it is the central layer in the shell which is positive or the one on the sides is determined uniquely by the type of cubic cell chosen.

(4) Though the net contribution to the sum from such a triple layer tends to zero, and the series obtained by grouping the terms of the original series in such triple layers is convergent, the sum to which the resulting series converges depends on whether the triple layer has positive ions in the central plane and negative ions in the outer planes, or *vice versa*. The difference between the two sums is obviously half the joint contribution from two adjacent layers.

The above results immediately suggest a criterion for grouping the terms of the original series such that a unique result is obtained. For if the cell obtained by grouping together particular terms of the original series is such that any regrouping of such cells cannot lead to a separation of positive and negative charges in parallel layers, the resulting series will lead to the correct sum. This can be achieved by choosing a cell of the following type: Consider a parallelepiped whose three adjacent edges are the lines joining the center of the cubic cell to any three adjacent corners of the cube, i.e. the lines joining,

say, the origin (0, 0, 0) to points (1, 1, 1), (1, 1, −1), and (1, −1, 1). The surfaces of this cell do not carry any *net* charge since the positive and negative charges are alternately situated at the eight corners, and so a separation of charges in parallel layers can never occur by any regrouping of the cells. *The electrical neutrality of the faces of the cell is thus a sufficient condition for a unique sum.* The condition is also necessary; for the terms of the series [1] are of the order of $1/R$, and hence the contribution from a pair of adjacent positive and negative layers is of the order of the solid angle subtended at the origin by the layers, and will therefore remain finite. Hence the cell chosen should be such that the separation of charges into parallel layers cannot occur by any regrouping of the cells.

It may be easily seen that the resulting triple series obtained by grouping the terms into such cells is rapidly and absolutely convergent, so that this method can conveniently be used for the numerical evaluation of [1] for any value of m. In actual practice, instead of taking ions at the eight corners of this elementary cell as each contributing $\frac{1}{8}$ to the cell, we may equally well regard them as belonging wholly to the cell, and regard every alternate cell as unoccupied.

The position is very different when we are dealing with a double series of the type [1], or with a triple series in which the terms are of the order of $1/R^{\nu}$, when $\nu > 1$. In these cases, the contribution from two adjacent lines or layers (as the case may be) into which the positive and negative terms separate tends to zero, and hence the sum of the series remains unaltered even if the grouping leads to such a separation.

5. THE NaCl TYPE OF LATTICE

In this case the lattice cell chosen is a cube consisting of four positive and four negative ions situated alternately at the eight corners; the side of this cell is then half the side of the usual cubic cell. Such a cell satisfies the condition mentioned in the last section, and the triple series [1] can be evaluated for any value of m by adding up contributions from such cells. For this lattice type and for certain special values of m, series [1] has been evaluated by Wasastjerna (8) and Löwdin (6).

ACKNOWLEDGMENTS

I wish to thank Sir. K. S. Krishnan, F.R.S., Dr. D. K. C. MacDonald, Dr. R. B. Dingle, and Dr. A. B. Bhatia for many useful comments.

REFERENCES

1. Evjen, H. M. Phys. Rev. 39: 675. 1932.
2. Gurney, I. D. C. Phys. Rev. 90: 317. 1953.
3. Krishnan, K. S. and Roy, S. K. Nature, 168: 869, 983. 1951.
4. Krishnan, K. S. and Roy, S. K. Proc. Roy. Soc. (London), A, 210: 481. 1951.
5. Krishnan, K. S. and Roy, S. K. Phys. Rev. 87: 581. 1952.
6. Löwdin, P. O. A theoretical investigation into some properties of ionic crystals. Dissertation, University of Uppsala. 1948.
7. Sherman, J. Chem. Revs. 11: 93. 1932.
8. Wasastjerna, J. A. Comment. Phys. Math. Helsingf. 8: No. 21. 1935.
9. Wasastjerna, J. A. Trans. Roy. Soc. (London), A, 237: 105. 1938.

A METHOD OF DETERMINING THE ELECTRONIC TRANSITION MOMENT FOR DIATOMIC MOLECULES[1]

By P. A. Fraser

ABSTRACT

A method is described that will give the variation, as a function of internuclear distance, of the electronic transition moment governing intensities in diatomic molecular band systems. Reliable theoretical results and good experimental intensities are used conjointly to find this variation. Once smoothed, the trend may be replaced into the overlap integrals to give relative vibrational transition probabilities better than those given by the approximation 'overlap integrals squared', and presumably better than those deduced directly from experiment, since the latter are not smoothed. Limits on the application of the method are suggested; however many band systems fall within these limits.

I. INTRODUCTION

A well-known approximation is the removal of an average value of $R_e(r)$, the electronic transition moment,* from the integrals that govern band intensities in the electronic spectra of diatomic molecules (7), i.e.

$$[1] \qquad \int_0^\infty \psi_1^{(v')}(r)\, R_e(r)\, \psi_2^{(v'')}(r)\, dr \approx \bar{R}_e \int_0^\infty \psi_1^{(v')} \psi_2^{(v'')} dr.$$

In other words, $R_e(r)$ is assumed to be slowly varying over the important range of r, the internuclear separation co-ordinate. The average, $\bar{R}_e$, is assumed to be the same for all bands of the system, and the implication in this approximation is that intensities of bands are controlled (among other factors involving physical constants and wavelengths) by squares of the so-called overlap integrals,

$$[2] \qquad (v', v'') = \int_0^\infty \psi_1^{(v')} \psi_2^{(v'')} dr;$$

$\psi_1^{(v')}$ and $\psi_2^{(v'')}$ are vibrational wave functions in the electronic states 1 and 2, between which the transition takes place, and v' and v'' are vibrational quantum numbers in the upper and lower states, respectively.

Some investigations have been made to take account of the variation of the transition moment and to determine its possible effect on the theoretical band intensities (see, for example, the work of Bates (1, 2), Poots (12), and Shuler (13)). This paper presents a method which uses both reliable theoretical results and good experimental relative band intensities to give the dependence of $R_e(r)$ on r, but not the magnitude, which could be estimated from lifetime measurements, for example.

[1]*Manuscript received April 2, 1954.*
Contribution from the Department of Physics, University of Western Ontario, London, Ontario.

**The electronic transition moment may be written as a product of two parts, one depending on r and the other a function of angles. The angular part is concerned with the nuclear rotation, and on integration, squaring, and summing over rotational levels gives the same result for each band, in the approximation that rotational effects on the vibrational wave functions are ignored (7). The radial part alone is considered in this paper.*

II. A PROPERTY OF THE OVERLAP INTEGRALS

Jarmain and Nicholls (10) have obtained by numerical methods extensive tables of overlap integrals of Morse type vibrational wave functions for the first and second positive systems of N_2. At the same time, for these band systems, the integrals

$$[3] \qquad (v', rv'') = \int_0^\infty \psi_1^{(v')} r \, \psi_2^{(v'')} dr,$$

$$(v', r^2v'') = \int_0^\infty \psi_1^{(v')} r^2 \psi_2^{(v'')} dr$$

were calculated with the hope that they could be used in conjunction with experimental intensities to find a parabolic form for $R_e(r)$. Such methods fail for reasons that are described in Section III. It was noticed by Jarmain (8) that these integrals exhibited the following property:

$$[4] \qquad \frac{(v', rv'')}{(v', v'')} = \frac{(v', r^2v'')}{(v', rv'')},$$

to within an accuracy in almost all cases of better than 0.2%. This led to the conjecture that the equality of this ratio could probably be extended to higher (or lower) powers of r,

$$[5] \qquad \frac{(v', rv'')}{(v', v'')} = \frac{(v', r^nv'')}{(v', r^{n-1}v'')}.$$

There must be some limit on the power of r for which this holds, as can be seen by the weighting effect of a large power of r on the rest of the integrand. There is an indication (see below) that the upper limit on the power is of order 10. A quantity $\bar{r}_{v'v''}$, which may be considered as an average r for the $(v' \rightarrow v'')$ transition, may be defined:

$$[6] \qquad \bar{r}_{v'v''} = (v', rv'')/(v', v'');$$

and then

$$[7] \qquad (v', r^nv'') = \bar{r}^n_{v'v''}(v', v'').$$

Naturally then, for any function $f(r)$ expressible in a reasonable number of powers of r

$$[8] \qquad (v', f(r)v'') = f(\bar{r}_{v'v''})(v', v'').$$

The possibility of writing equation [8] leads to the method of finding the variation of $R_e(r)$ which is described below. First, however, some indication of the validity of the conjecture should be made.

For values of integrals calculated by numerical methods the ratios for a few bands of the first positive system of N_2 are given in Table I (8). The considerable variation of the ratios for the $(1 \rightarrow 1)$ transition may be attributed in part to uncertainties in the values of the $(1 \rightarrow 1)$ integrals, these uncertainties arising from the loss of significant figures on numerical integration which, for example, makes (1, 1) one of the smallest overlaps in the array. (1, 1) is known to perhaps two figures, and the ratios agree to two figures. However,

TABLE I

THE CONSTANCY OF RATIOS OF CERTAIN INTEGRALS FOR A FEW BANDS OF THE FIRST POSITIVE SYSTEM OF NITROGEN (8); THE SYMBOLS ARE DEFINED IN THE TEXT. THE MOLECULAR CONSTANTS ARE FROM HERZBERG (7).

v'	v''	$\frac{(v', rv'')}{(v', v'')}$	$\frac{(v', r^2v'')}{(v', rv'')}$	$\frac{(v', v'')}{(v', r^{-1}v'')}$
0	0	1.257 Å	1.258 Å	..
0	1	1.222	1.222	1.221 Å
0	2	1.191	1.191	..
1	1	1.205	1.170	..
		(1.2)	(1.2)	
1	3	1.201	1.201	1.200

it is also possible that equation [7] breaks down when the overlap integral is small. The constancy of the ratios in the first two columns has been shown for all of the remaining bands calculated for the first positive system (8).

As one test of the above conjecture (equation [7]), the integrals

$$\int \psi_1^{(v')}(\exp -\alpha r)\, \psi_2^{(v'')} dr = (v', [\exp -\alpha r]v''),$$

[9]
$$\int \psi_1^{(v')}(\alpha r \exp -\alpha r)\, \psi_2^{(v'')} dr = (v', [\alpha r \exp -\alpha r]v''),$$

and
$$\int \psi_1^{(v')}(\alpha^2 r^2 \exp -\alpha r)\, \psi_2^{(v'')} dr = (v', [\alpha^2 r^2 \exp -\alpha r]v'')$$

were calculated for the (0, 0), (0, 1), and (0, 2) bands of the first positive system of N_2. The integrals were calculated using the approximation appropriate to Morse vibrational potentials described elsewhere (6, 9, 11), the approximation allowing analytic evaluation of these integrals, as well as of the overlap integrals. α is the mean value of the parameters in the Morse potentials of the two states of the transition, this adjustment of the α_1 and α_2 to a mean value being the basis of the approximation. The three forms chosen for $f(r)$ thus have the typical behavior of physically reasonable functions. The results of these integrations were compared respectively with

$$(\exp -\alpha \bar{r}_{v'v''})(v', v''),$$

[10]
$$(\alpha \bar{r}_{v'v''} \exp -\alpha \bar{r}_{v'v''})(v', v''),$$

and
$$(\alpha^2 \bar{r}^2_{v'v''} \exp -\alpha \bar{r}_{v'v''})(v', v''),$$

the $\bar{r}_{v'v''}$ for each band being given by [6]. The argument, $-(\alpha r)$, of the exponential is of such a magnitude that 12 or more terms in a power series expansion would be needed to represent the functions to two significant figures in the important range of integration. The comparison is made in Table II, and the agreement between the two calculations is excellent.

The reason for the validity of equation [7] is the concentration, in general, of the product $\psi_1^{(v')}\, \psi_2^{(v'')}$ into a small part of the range of integration. It could be expected then that the equation would break down under at least

TABLE II

TEST OF THE CONJECTURE THAT $(v', f(r)v'') = f(\bar{r}_{v'v''})(v', v'')$ (EQUATION 8) FOR A FEW BANDS OF THE FIRST POSITIVE SYSTEM OF NITROGEN. AN APPROXIMATION DESCRIBED ELSEWHERE (11, 6) ALLOWS ANALYTIC INTEGRATION FOR THE CHOSEN FORMS OF $f(r)$, WHEN THE MORSE MODEL IS USED. THE ADJUSTED MOLECULAR CONSTANTS ARE AS IN REFERENCE (6).

$\alpha = 2.4269$ Å^{-1}; $\bar{r}_{00} = 1.257$ Å, $\bar{r}_{01} = 1.222$ Å, $\bar{r}_{02} = 1.192$ Å;
$|r_{e1} - r_{e2}| \approx 0.08$ Å, $\mu_A\omega_e \approx 10^4$.

$f(r)$	v'	v''	$(v', f(r)v'')$	$f(\bar{r}_{v'v''})(v', v'')$
$\exp -\alpha r$	0	0	.0276	.0275
	0	1	.0293	.0294
	0	2	.0241	.0242
$\alpha r \exp -\alpha r$	0	0	.0840	.0838
	0	1	.0870	.0870
	0	2	.0699	.0699
$(\alpha r)^2 \exp -\alpha r$	0	0	.256	.256
	0	1	.258	.258
	0	2	.202	.202

two circumstances: (i) the potentials being wide, which implies spread-out wave functions; and (ii) the difference between the equilibrium internuclear distances being large. There is one other circumstance under which the equation could break down, and this is when the overlap integral is very small. The introduction of other factors (e.g. r and r^2) to the integrand could then seriously disturb the situation. Off-diagonal overlap integrals are very small when the difference between the equilibrium internuclear distances is very small, and the equation would not be valid, in general, for such band systems. In systems for which the equation generally applies, there is the occasional very small overlap integral for which the equation would not specifically apply. There must also be a limit on the quantum numbers for which the equation is valid, since the vibrational amplitude increases with the energy.

A crude analysis of the conditions on the validity of equation [7] was made using a harmonic oscillator model of the vibrating molecule. The analysis confirmed that the equation broke down under the circumstances mentioned above, and through the calculation it was possible to put approximate numerical limits on transitions for which the equation was valid. These may be summarized as follows:

(i) $\mu_A\omega_e \sim 10^4$; where μ_A is the reduced mass of the molecule in atomic weight units, and where ω_e is the vibrational quantum in kaysers;

and

(ii) 0.01 Å $< |r_{e1} - r_{e2}| < 0.25$ Å; where r_{e1} and r_{e2} are the two equilibrium internuclear distances concerned in the transition.

The analysis also shows that the equation breaks down for powers of r of order 10 or greater, and also for quantum numbers of order 10 or greater. The validity of equation [7] was explored for the $(0 \rightarrow 0)$ band of a Morse vibrator with a similar result. There is no clear way of testing the equation for the general band on this model, and it is unnecessary to do so, since the

harmonic oscillator wave functions bear all the necessary general features. These calculations on the harmonic oscillator model, and on the $(0 \rightarrow 0)$ band of the Morse model, are presented elsewhere (5).

III. DETERMINATION OF THE VARIATION OF $R_e(r)$

The measured intensity of a band in emission (electric dipole) may be represented by the formula

$$[11] \qquad I_{v'v''} = \frac{DN_{v'}}{\lambda^4_{v'v''}} \left| \int_0^\infty \psi_1^{(v')}(r)\, R_e(r)\, \psi_2^{(v'')}(r)\, dr \right|^2,$$

where D is a constant, $N_{v'}$ is the relative population of the vibrational level v' in the upper state, and $\lambda_{v'v''}$ is taken as some wavelength characteristic of the band, chosen consistently throughout the band system (14).

In the following it is assumed that $R_e(r)$ does not change sign in the important part of the range of integration, and the sign of the overlap integrals is ignored. By choosing one of the larger intensities from each v''-progression (v' constant), $I_{v'n}$ say, the following sets of ratios are constructed for each such progression

$$[12] \qquad \lambda^2_{v'v''} \surd I_{v'v''}/\lambda^2_{v'n} \surd I_{v'n}.$$

The procedure of taking ratios is not necessary, but is convenient in that for each progression, one ratio takes on the value unity. From [11],

$$[13] \qquad \lambda^2_{v'v''} \surd I_{v'v''}/\lambda^2_{v'n} \surd I_{v'n} = (v', R_e(r)v'')/(v', R_e(r)n)$$

$$= \frac{(v', v'')}{(v', n)} \times \frac{R_e(\bar{r}_{v'v''})}{R_e(\bar{r}_{v'n})},$$

if [8] applies. Thus with a knowledge of the overlap integrals and the $\bar{r}_{v'v''}$, one is able to plot, for each v''-progression, a set of points which represent the trend of $R_e(r)$ with r in the range of r covered by the $\bar{r}_{v'v''}$ of the progression. There are methods available for the computation of overlap integrals (3, 6, 9), and a rapid method of finding the $\bar{r}_{v'v''}$ without the labor of computing the (v', rv'') integrals is described in an appendix.

Points far off the general trend in the plots for each v''-progression of $R_e(\bar{r}_{v'v''})/R_e(\bar{r}_{v'n})$ should be discarded. It will be found that in practice such points arise from small and uncertain overlap integrals or intensities. The separate plots may be reduced to a common scale by the objective procedure of joining the points by straight lines, and multiplying the ordinates of each plot by a factor which will equalize areas contained in common ranges of r of neighboring progressions. There is considerable overlap in the ranges of r covered by the $\bar{r}_{v'v''}$ of neighboring v''-progressions, as is shown by Fig. 1 of the paper by Turner and Nicholls (15) who describe this procedure in more detail in connection with the application of the present method to the first positive system of N_2. Turner and Nicholls find a definite trend for $R_e(r)$ of the first positive system suggested by the scatter of points. Results from the application of the method to the second positive system are encouraging (16).

A 'least-squares' curve could be fitted to the scatter of points representing

the trend of $R_e(r)$. In doing so it may be advisable to weight each point by a factor proportional to the corresponding overlap integral, since the larger overlap integrals are more reliable, as are the larger intensities. Once this smoothed variation of $R_e(r)$ is obtained, better relative vibrational transition probabilities for use in the interpretation of spectra may be calculated by use of the relation

$$[14] \qquad \left| \int_0^\infty \psi_1^{(v')} R_e(r)\, \psi_2^{(v'')} dr \right|^2 = R_e^2(\bar{r}_{v'v''})(v', v'')^2.$$

Vibrational transition probabilities so obtained are presumably better than those obtained directly from experiment, since they are obtained from smoothed data, and $R_e(r)$ would be expected to be a smooth function of r.*

The scatter of points that arises from the application of this method shows clearly why attempts at fitting a parabolic or linear form to $R_e(r)$ will fail. The procedure followed is to attempt to fit a linear combination of (v', v''), (v', rv''), and (v', r^2v'') to the reduced intensities of a single v''-progression, say

$$(v', v'') + a(v', rv'') + b(v', r^2v'').$$

The points on the present plots are equivalent to those to be fitted by the form $(1 + ar + br^2)$. It is seen from Fig. 2 of the paper by Turner and Nicholls that this procedure will give widely different values of the coefficients from different choices of three consistent points. The present method picks out a trend rather than attempting to fit a specific curve to $R_e(r)$, and uses almost all experimental results simultaneously rather than in groups of three points. The present method is also relatively insensitive to the model chosen to evaluate the overlap integrals, as long as the model is a good representation of the anharmonic vibration of the molecule.

D. R. Bates has mentioned (4) that the transition moment could change sign in some cases. If this be so in a certain transition the method outlined above will lead to a scatter of points which would show a suggestion of a cusp touching the horizontal axis. The points to the right of the cusp could be reflected in the horizontal axis to give a final smooth curve.

ACKNOWLEDGMENTS

The author wishes to acknowledge valuable discussion with Drs. R. W. Nicholls, R. G. Turner, J. H. Blackwell, and R. H. Cole, and wishes to thank Mr. W. R. Jarmain for suggesting the rapid method of finding the $\bar{r}_{v'v''}$ which is described in an appendix to this paper.

The research reported in this paper has been sponsored by the Geophysics Research Directorate, Air Force Cambridge Research Centre, under Contract AF 19(122)-470.

Appendix

A METHOD OF CALCULATING THE $\bar{r}_{v'v''}$ FOR A BAND SYSTEM†

The vibrational wave equations for the electronic states involved in a transition may be shown quite readily to lead to the general relation:

**It should be pointed out that equation [14] may be used, when applicable, to calculate vibrational transition probabilities when $R_e(r)$ is known from theoretical calculations.*

†The author is greatly indebted to Mr. W. R. Jarmain for suggesting this labor-saving method of calculating the $\bar{r}_{v'v''}$.

$$(E_1^{(v')} - E_2^{(v'')}) \int_0^\infty \psi_1^{(v')} \psi_2^{(v'')} dr = \int_0^\infty \psi_1^{(v')} [V_1(r) - V_2(r)] \psi_2^{(v'')} dr,$$

where V_1 and V_2 are vibrational potential functions for the two states, and $E_1^{(v')}$ and $E_2^{(v'')}$ are the corresponding vibrational energies for the v' and v'' levels. Wu (17) suggested this relation as a useful check on the accuracy of wave functions obtained by approximate methods.

Equation [8], when applicable, permits writing the above equality in the form:

$$(E_1^{(v')} - E_2^{(v'')}) \int_0^\infty \psi_1^{(v')} \psi_2^{(v'')} dr = [V_1(\bar{r}_{v'v''}) - V_2(\bar{r}_{v'v''})] \int_0^\infty \psi_1^{(v')} \psi_2^{(v'')} dr,$$

since $[V_1(r) - V_2(r)]$ is generally a very smooth, slowly varying function. If, as is usual, Morse functions are chosen, then for any particular band $(v' \rightarrow v'')$,

$$D_1[1 - \exp -\alpha_1(\bar{r}_{v'v''} - r_{e1})]^2 - D_2[1 - \exp -\alpha_2(\bar{r}_{v'v''} - r_{e2})]^2 = E_1^{(v')} - E_2^{(v'')},$$

in which $D_1 = (\omega_e)_1^2/4(\omega_e x_e)_1$, $E_1^{(v')} = (\omega_e)_1(v' + \frac{1}{2}) - (\omega_e x_e)_1(v' + \frac{1}{2})^2$,

with similar expressions for D_2 and $E_2^{(v'')}$.

When the approximate method for computing overlaps is used (6), with α_1 and α_2 each adjusted to a mean α, this equation is quadratic in $(\exp -\alpha \bar{r}_{v'v''})$. Otherwise it is easy to set up a graphical solution for $\bar{r}_{v'v''}$. Tests of the method have shown good agreement with values of $\bar{r}_{v'v''}$ obtained numerically, which is in itself a further indication of the validity of equation [7] in the paper.

The method, of course, will fail to provide an adequate set of $\bar{r}_{v'v''}$ for those bands or those systems for which equation [7] of the paper is not valid. This is not serious as the method of finding $R_e(r)$ also breaks down in these circumstances. Indeed, the failure of this method of finding the $\bar{r}_{v'v''}$ for any one band system would indicate that the suggested method of finding the dependence of $R_e(r)$ upon r will also fail for the system.

REFERENCES

1. BATES, D. R. Proc. Roy. Soc. (London), A, 196: 217. 1949.
2. BATES, D. R. J. Chem. Phys. 19:1122. 1951.
3. BATES, D. R. Monthly Notices Roy. Astron. Soc. 112: 614. 1952.
4. BATES, D. R. Private communication.
5. FRASER, P. A. Sci. Rept. No. 12. Contract No. AF 19(122-470). Jan. 1954. Dept. of Phys., University of Western Ontario.
6. FRASER, P. A. and JARMAIN, W. R. Proc. Phys. Soc. (London), A, 66: 1145. 1953.
7. HERZBERG, G. Spectra of diatomic molecules. D. Van Nostrand Company, Inc., New York, 1950.
8. JARMAIN, W. R. Private communication.
9. JARMAIN, W. R. and FRASER, P. A. Proc. Phys. Soc. (London), A, 66: 1153. 1953.
10. JARMAIN, W. R. and NICHOLLS, R. W. Can. J. Phys. 32: 201. 1954.
11. NICHOLLS, R. W., JARMAIN, W. R., and FRASER, P. A. Can. J. Phys. 31: 1019. 1953.
12. POOTS, G. Proc. Phys. Soc. (London), A, 66: 1181. 1953.
13. SHULER, K. E. J. Chem. Phys. 18: 1221. 1950.
14. TURNER, R. G. and NICHOLLS. R. W. Can. J. Phys. 32: 468. 1954.
15. TURNER, R. G. and NICHOLLS, R. W. Can. J. Phys. 32: 475. 1954.
16. WALLACE, L. V. Private communication.
17. WU, TA-YOU. Proc. Phys. Soc. (London), A, 65: 965. 1952.

THE FISSION YIELDS OF THE STABLE AND LONG-LIVED ISOTOPES OF XENON, CESIUM, AND KRYPTON IN NEUTRON FISSION OF U^{233} [1]

By W. Fleming, R. H. Tomlinson, and H. G. Thode

ABSTRACT

The fission yields of Xe^{131}, Xe^{132}, Xe^{134}, Xe^{136}, Cs^{133}, Cs^{135}, Cs^{137}, Kr^{83}, Kr^{84}, 10.27 year Kr^{85}, and Kr^{86} in the neutron fission of U^{233} have been determined by mass spectrometer methods. The very pronounced fine structure in the mass yield curve in the mass range 131 to 137 found in U^{235} fission does not occur in the fission of U^{233}. This disappearance of fine structure would not have been predicted by any of the mechanisms which have been suggested to explain the fine structure in U^{235} fission. The fission yield of the 10.27 year isomer of Kr^{85} relative to the other krypton isotopes is considerably higher in U^{233} fission than in U^{235} fission, indicating some fine structure in this mass range which may be related to the closed shell of 50 neutrons.

INTRODUCTION

Early mass spectrometer studies of fission product xenon and krypton resulting from neutron fission of U^{235} revealed for the first time the existence of "fine structure in the mass yield curve" (8, 10). Xe^{133} and Xe^{134} have much higher fission yields and Xe^{136} a slightly lower yield than would have been expected from the smooth fission yield curve determined by radiochemical methods. A study of the fission yields of the stable and long-lived isotopes of cesium in $U^{235} + n$ fission indicates that the yield of the 137 mass chain is also slightly lower than the smooth mass yield curve (14). In the case of neutron fission of U^{238}, it has been found that the yields of Xe^{132} and Xe^{131} are abnormally high and that the yields of Xe^{134} and Xe^{136} are much lower than those observed in U^{235} fission (13). This fine structure is undoubtedly related to the extra stability of the closed shell of 82 neutrons which occurs in this mass region. The relative fission yields of Cs^{133}, Cs^{135}, and Cs^{137} in neutron fission of U^{238} have been determined (11). Although these yields have not been normalized to the xenon data, there is no indication of any large fine structure at these masses in U^{238} fission.

Recently abnormal yields of Kr^{84} and Kr^{85} have been observed in neutron fission of U^{235} and U^{238} (13) which may be related to the occurrence of the closed shell of 50 neutrons in this mass region. Fine structure has also been observed (6) in the neighborhood of mass 100 in neutron fission of U^{235}. Since the complimentary fragments to the 133 and 134 mass chains fall in this region, it is quite probable that the fine structure observed at mass 100 is the result of the same effects that produced the high yields in the xenon mass range.

It is desirable to determine the variation of the fine structure with mass and charge of the fissioning nucleus since such knowledge will be helpful in developing a satisfactory theory of the fission process. There is also considerable interest in the yield of 135 mass chain because the high neutron capture

[1] *Manuscript received February 17, 1954.*
Contribution from the Departments of Chemistry and Physics, Hamilton College, McMaster University, Hamilton, Ontario.

cross section of Xe^{135} (3.5×10^6 barns) (2) must be considered in reactor design. If there should be an abnormal yield of this mass chain for a given fissionable nucleus, it would greatly affect the suitability of this nucleus for fuel purposes.

The fission yields of the stable and long-lived isotopes of krypton, xenon, and cesium in neutron fission of U^{233} have been determined by mass spectrometer analysis of fission product samples and are reported in this paper.

EXPERIMENTAL

The U^{233} used in this work was obtained from Atomic Energy of Canada Limited in the form of U_3O_8 containing 14.4 atom per cent U^{233} determined by mass spectrometer analysis. The remainder was natural uranium. If the fission cross sections of U^{233} and U^{235} are equal, the contribution of U^{235} fission in this material will be 4.28% of the total. Samples of the oxide, weighing roughly 50 mgm., were sealed in quartz tubes and irradiated in the N.R.X. reactor at Chalk River at two widely differing neutron fluxes for a time sufficient to produce approximately 10^{17} fissions. The samples were allowed to cool for one year after which the radioactivity presented no serious health problem.

(*a*) *Preparation of Krypton and Xenon Samples*

Since it was possible that an appreciable part of the rare gas fission products might have diffused out of the finely powdered oxide, the quartz tube in which each sample was irradiated was placed unopened in the flask in which the dissolution was to be carried out. The flask was connected to the sample preparation line and evacuated. The quartz tube was then broken with a magnetic breaker and approximately 3 ml. of 10 *N* nitric acid which had been previously thoroughly degassed was transferred to the dissolution flask. Approximately 15 min. were required to complete the dissolution. The gases released were passed through a drying train containing potassium hydroxide pellets and magnesium perchlorate and collected in a charcoal trap cooled with liquid oxygen. When the dissolution was completed, the samples were purified in a calcium furnace, condensed into a sample tube containing charcoal, and removed from the preparation line for mass spectrometer analysis. The purified samples, about two cubic millimeters at S.T.P., contained only fission product xenon and krypton and atmospheric argon from the small amount of air trapped in the quartz tubes when they were originally sealed.

The rare gas samples were analyzed on a 180° direction focusing mass spectrometer which had previously been calibrated with standard mixtures of xenon and krypton so that the ratio of fission product xenon to fission product krypton could be determined from the mass spectrometer results. The ion currents were amplified by a vibrating reed electrometer.

(*b*) *Preparation of Cesium Samples*

The uranyl nitrate from which the fission gases had been removed was evaporated to dryness to remove the excess nitric acid and dissolved in a few milliliters of water. The uranyl nitrate and fission products were then adsorbed

on a 10 cm. column of Dowex 50 ion exchange resin. The uranium was eluted first from the column with ether saturated with 6 *M* nitric acid. The cesium was then obtained by a further elution of the resin column with 0.3 *M* hydrochloric acid. A concentrate of this solution was evaporated on the source filament of the mass spectrometer.

The cesium isotope ratios were obtained with a conventional 90° sector instrument with a hot filament ion source. Magnetic scanning was employed.

RESULTS

The fission yield of I^{132} in neutron fission of U^{233} was found to be 4.9% by Grummitt and Wilkinson (7) using radiochemical methods. This value for the yield of the 132 mass chain in $U^{233} + n$ fission was chosen for the normalization point of the mass spectrometer fission yield measurements. Assuming the fission cross sections of U^{235} and U^{233} to be equal, there will be a 4.28% contribution of $U^{235} + n$ fission in the material used (14.4% U^{233}, 85.6 natural uranium). The yield of the 132 mass chain in U^{235} fission is 4.79% (13).* Therefore the observed yield of the 132 mass chain in our samples will be $0.043 \times 4.79 + 0.957 \times 4.90 = 4.90\%$. The observed xenon fission yields for the two samples calculated relative to this value for Xe^{132} are given in Table I,

TABLE I

XENON FISSION YIELD DATA

Sample	Mass	Observed yield, %	Yield U^{235} fission (13), %	Corrected yield U^{233} fission, %
Low neutron flux	131	3.58 ± .01	3.20[a]	3.59 ± .01
	132	4.90[a]	4.79	4.90[a]
	134	6.38 ± .01	8.76	6.28 ± .01
	136	8.51 ± .04	?	8.51 ± .04[b]
High neutron flux	131	3.54 ± .03	3.20[a]	3.55 ± .03
	132	4.90[a]	4.79	4.90[a]
	134	6.39 ± .05	8.76	6.29 ± .05
	136	11.24 ± .07	?	11.24 ± .07[b]

[a] *Normalization point.*
[b] *Not corrected for contribution of $U^{235} + n$ fission.*

Column 3. The deviations shown are average deviations. The much higher yield of Xe^{136} in the sample irradiated at the higher neutron flux is due to the increased importance of neutron capture by Xe^{135} in this sample. Column 4 gives the yields observed in $U^{235} + n$ fission and Column 5 shows the fission yields calculated for U^{233} fission making correction for the contribution of U^{235} fission. No correction has been made to yields of the 136 mass chain because the neutron flux was not known accurately enough to estimate the Xe^{136} yield for the $U^{235} + n$ fission contribution. However, this correction would

**Recently the fission yield of I^{131} in U^{235} fission has been found to be 3.10% relative to 6.10% for Ba^{140} (4). The absolute fission yield of Ba^{140} is now given as 6.30% (3). The corresponding value of 3.20% for the fission yield of I^{131} in $U^{235} + n$ fission has been used as a normalization point for the yields reported by Wiles et al. (14) and Wanless and Thode (13).*

certainly be less than 2% since the U^{235} fission contribution is only 4.28% of the total and the Xe^{135} yields before neutron capture are not very widely different in U^{235} and U^{233} fission.

The cesium and krypton isotope abundance ratios are given in Table II.

TABLE II

CESIUM AND KRYPTON ISOTOPE ABUNDANCE DATA

Sample	Isotope ratios						
	Cs^{133}	Cs^{135}	Cs^{137}	Kr^{83}	Kr^{84}	Kr^{85}	Kr^{86}
Low neutron flux	1.000	0.792 ± .012	1.15 ± .02	16.77 ± .18	27.75 ± .16	8.26 ± .13	47.22 ± .25
High neutron flux	1.000	0.336 ± .005	1.124 ± .007	16.87 ± .18	27.71 ± .05	8.51 ± .12	46.90 ± .14

The results for Cs^{137} and Kr^{85} have been corrected for decay using half lives of 33 years (14) and 10.27 years (12) respectively.

It can be seen that, except for Cs^{135} which is affected by neutron capture in Xe^{135}, the results for the two samples are in agreement within the limits of precision.

The cesium fission yields may be normalized to the xenon data by means of the difference in the extent of the "burning" of Xe^{135} to Xe^{136} in the two samples. The increase in the Xe^{136} fission yield in the high flux sample over that found in the low flux sample is $11.24 - 8.51 = 2.73\%$. Since this increase is entirely due to the reaction $Xe^{135} + n \rightarrow Xe^{136}$, the decrease in the Cs^{135} yield in the high flux sample compared to the low flux sample must also be 2.73%. If "x" is the fission yield of Cs^{133}, it follows from the results in Table II that:

$$2.73 = 0.792x - 0.336x$$

or

$$x = 5.99 \pm 0.23.$$

The deviation is calculated from the individual deviations of the xenon and cesium results by standard methods. The error in the cesium normalization is roughly four per cent.

The ratio of fission product xenon to fission product krypton for the low flux sample was determined from the mass spectrometer results to be 3.31. This ratio is probably accurate to 5%. Using this ratio, the krypton fission yields can be normalized to the xenon fission yield data.

Table III gives the krypton and cesium observed fission yields in Column 3. The errors introduced by the normalization process (4% for cesium and 5% for krypton) are not included in the deviations. Column 4 gives the observed yields for $U^{235} + n$ fission and Column 5 the fission yields for $U^{233} + n$ fission corrected for the contribution of U^{235} fission. As in the case of the xenon results, no correction has been made to the Cs^{135} values because of the uncertainty in the neutron flux.

TABLE III

CESIUM AND KRYPTON FISSION YIELD DATA

Sample	Isotope	Observed yield, %	Yield $U^{235} + n$ fission (13, 14), %	Corrected yield $U^{233} + n$ fission, %
Low neutron flux	Cs^{133}	5.99	7.25	5.93
	Cs^{135}	4.74 ± .06	?	4.74 ± .06[a]
	Cs^{137}	6.87 ± .12	6.66	6.87 ± .12
	Kr^{83}	1.18 ± .01	0.66	1.20 ± .01
	Kr^{84}	1.96 ± .01	1.24	0.200 ± .01
	Kr^{85}	0.583 ± .009	0.355	0.593 ± .009
	Kr^{86}	3.33 ± .02	2.46	3.36 ± .02
High neutron flux	Cs^{133}	5.99	7.25	5.93
	Cs^{135}	2.01 ± .03	?	2.01 ± .03[a]
	Cs^{137}	6.73 ± .05	6.66	6.73 ± .05

[a] *Not corrected for* $U^{235} + n$ *fission.*

DISCUSSION

The xenon and cesium fission yield data for U^{233} fission are plotted in Fig. 1. The vertical lines on the experimental points at masses 133, 135, and 137 represent the error introduced by the process used to normalize the cesium results to the xenon data. The uncertainty in the relative values of these three yields and in the yields of masses 131, 132, 134, and 136 is smaller than the size of the experimental points. It can be seen that all the points lie on a smooth curve with the exception of masses 135 and 136 which have not been corrected

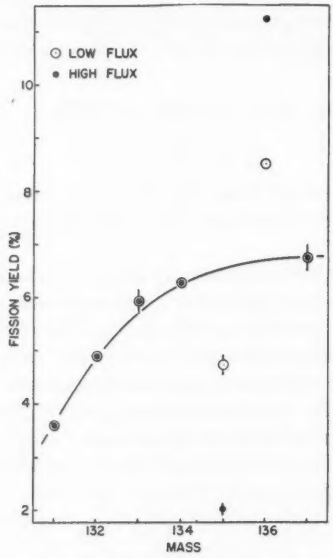

FIG. 1. U^{233} fission yields for masses 131 to 137.

for neutron capture in Xe^{135}. It can be seen from Fig. 1 that the yields of Xe^{136} for the two samples are as far above the smooth curve as the corresponding yields of Cs^{135} are below, indicating that the correction for neutron capture could result in these points falling on the curve. A rough correction for neutron capture places both Xe^{136} and Cs^{135} on the smooth curve. However, since the neutron fluxes at which the samples were irradiated are not known accurately, the exact values of the corrected yields are uncertain.

Fig. 2 shows the yields observed in this mass range for U^{235} and U^{238} fission (corrected for neutron capture). It is apparent in the case of these two fission-

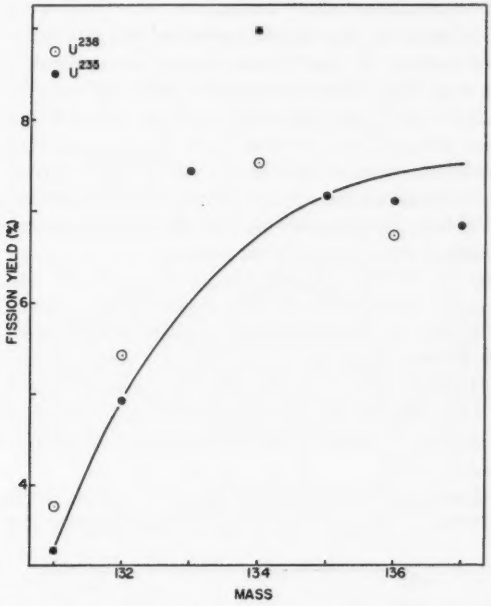

FIG. 2. U^{235} and U^{238} fission yields for masses 131 to 137.

ing nuclei that the fission yields do not lie on a smooth curve. The occurrence of the abnormally high yields observed in U^{235} fission has been explained qualitatively by two mechanisms both of which depend on the extra stability of the closed shell of 82 neutrons which occurs in this mass range. The first, suggested by Glendenin (5), involves the emission of the loosely held 83rd neutron by the highly excited primary fission products with this configuration. Alternately, it has been suggested (14) that nuclei with 82 neutrons may be favored in the primary fission process. Recently Pappas (9) has succeeded in giving a quantitative explanation of the observed U^{235} fission yields by combining both of the above effects with an improved version of the theory of equal charge displacement and making allowance for the delayed neutron emission.

Either of the original mechanisms and the more detailed treatment of Pappas predict abnormal yields of masses 132 and 133 in U^{238} fission and of 134 and 135 in U^{233} fission. In the case of U^{238} fission, the experimental results (Fig. 2) indicate that the 132 mass chain actually has an abnormal yield but there is no quantitative agreement between the predicted and observed values. In the case of U^{233} fission (Fig. 1) there is no indication of the predicted high yields of masses 134 and 135. It is difficult to understand why a decrease of two mass units in the mass of the fissioning nucleus should result in a complete disappearance of the "fine structure" and the disappearance would certainly not have been predicted by any of the mechanisms which have been suggested to explain the fine structure in U^{235} fission.

The 4% uncertainty in the normalization of the cesium results and the effect of neutron capture in Xe^{135} may conceal some small amount of fine structure but it is certain that there are no yields differing from the smooth curve by an amount nearly as large as observed in U^{235} or U^{238} fission. Samples of U^{233} have been prepared for irradiation at very low neutron flux to determine the 135 and 136 yields in the absence of neutron capture, and the yield of Xe^{133} is being determined directly by the method used in the earlier work on U^{235} fission (8). These samples will give definite information on the possible occurrence of a small amount of fine structure.

Measurements of the fission yields for Th^{232} and Pu^{239} fission are now in progress. The charge distribution of the primary fission products in each mass chain for Pu^{239} fission should be somewhat similar to that for U^{233}, and Th^{232} should resemble U^{238} in this respect. The results of these studies should provide much additional information on the relation between the nature of the fissioning nucleus and the observed fine structure and in particular should indicate whether the charge division or the mass difference produces the changes in fine structure observed.

The krypton fission yield data for U^{233} fission are plotted in Fig. 3. The results for U^{235} and U^{238} fission determined by Wanless and Thode (13) are shown for

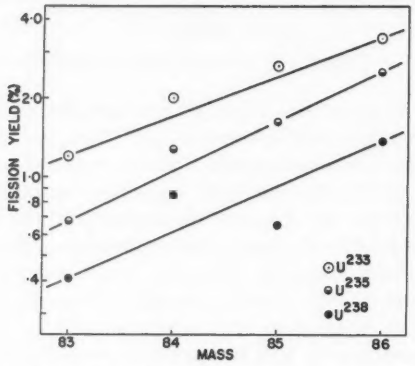

FIG. 3. The fission yields of the krypton isotopes from U^{233}, U^{235}, and U^{238} fission.

comparison. The U^{233} and U^{235} results are normalized by using values of 3.31 and 5.05 (1) respectively for the ratio of xenon to krypton. The U^{238} results are normalized by the method previously described (13). Kr^{85} exists as two isomers, one with a half-life of 10.27 years, the other with a 4.4 hr. half-life. Since the short-lived isomer will have completely decayed before the mass spectrometer analysis was carried out, the results given in Tables II and III for Kr^{85} represent the yield of the 10.27 year isomer only. The values plotted in Fig. 3 for Kr^{85} are calculated on the assumption that 22.5% of the 85 mass chain decays through the long-lived isomer.

It can be seen from Fig. 3 that the krypton fission yields do not lie on a smooth curve. In general, the yield of Kr^{84} is high and the deviation from the smooth curve increases slowly as the mass of the fissioning nucleus increases. The yield of Kr^{85} is high in U^{233} fission, about normal in U^{235} fission, and markedly low in U^{238} fission. The krypton fission yield data for U^{233} fission therefore confirm the variations in "fine structure" in this mass range first reported by Wanless and Thode.

It is noted that the yields for U^{233} fission in this mass range are considerably higher and the slope of the mass yield curve is less than for U^{235} fission, indicating a shift of the low mass hump of the fission yield curve towards the lower masses in U^{233} fission as was found in early radiochemical studies.

ACKNOWLEDGMENTS

We wish to thank Atomic Energy of Canada Limited for supplying the U^{233} and carrying out the irradiation of samples. The financial support of the National Research Council of Canada and Atomic Energy of Canada Limited is gratefully acknowledged. The assistance of Dr. J. Macnamara and Mr. B. W. Smith in early stages of this work is appreciated.

REFERENCES

1. Arrol, W. J., Chackett, K. F., and Epstein, S. Can. J. Research, B, 27: 757. 1949.
2. Atomic Energy of Canada Limited, Technical Release. Can. J. Phys. 30: 624. 1952.
3. Bartholomew, R. M., Brown, F., Hawkings, R. C., Merritt, W. F., Thode, H. G., and Yaffe, L. Forthcoming publication.
4. Bartholomew, R. M., Brown, F., Hawkings, R. C., Merritt, W. F., and Yaffe, L. Can. J. Chem. 31: 120. 1953.
5. Glendenin, L. E. Lab. for Nuclear Science Tech. Rept. No. 35. Mass. Inst. Technol. December, 1949.
6. Glendenin, L. E., Steinberg, E. P., Inghram, M. G., and Hess, D. C. Phys. Rev. 84: 860. 1951.
7. Grummitt, W. E. and Wilkinson, G. Nature, 161: 520. 1948.
8. Macnamara, J., Collins, C. B., and Thode, H. G. Phys. Rev. 70: 129. 1950.
9. Pappas, A. C. Lab. for Nuclear Science Tech. Rept. No. 63. Mass. Inst. Technol. September, 1953.
10. Thode, H. G. and Graham, R. L. Can. J. Research, A, 25: 1. 1947.
11. Tomlinson, R. H. Unpublished work, McMaster University. September, 1953.
12. Wanless, R. K. and Thode, H. G. Can. J. Phys. 31: 517. 1953.
13. Wanless, R. K. and Thode, H. G. Forthcoming publication.
14. Wiles, D. R., Smith, B. W., Horsley, R., and Thode, H. G. Can. J. Phys. 31: 419. 1953.

ON THE RELATION BETWEEN QUANTUM HYDRODYNAMICS AND CONVENTIONAL QUANTUM FIELD THEORY[1]

By F. A. Kaempffer

ABSTRACT

The conditions are examined under which the procedure of quantum hydrodynamics would be a consequence of the conventional quantization procedure, and vice versa. Using the classical nonrelativistic theory of a charged medium as an example, it is shown that the commutation rules of the two procedures differ by a factor 2, if in accordance with an idea by Geilikman the wave function of the classical theory is expanded as $\psi = \psi_0 + \psi_1$, with ψ_0 a constant and $\psi_1 \ll \psi_0$, and if terms of higher than second order in ψ_1 are neglected in the hydrodynamical description of the theory.

There exist at present two entirely different approaches towards quantization of classical field theories.

In the conventional approach the field under consideration is described in terms of, say, a wave function ψ and its complex conjugate ψ^*, and these are subjected to commutation relations of the type

$$[\psi(x); \psi^*(x')] = \delta(x - x'). \tag{1}$$

(This paper deals exclusively with quantization leading to Bose-statistics, and all commutators are therefore understood to contain the minus-sign.) The eigenvalues of the operator $\int \psi^* \psi \, dx$ turn out to be integers and are therefore interpreted as the number of particles present in a given state of the field.

In the approach of quantum hydrodynamics, on the other hand, the same field is described in terms of suitably chosen density ρ and velocity potential ϕ, and these are subjected, on the strength of the fact that they are canonically conjugate variables, to commutation relations of the type

$$[\phi(x); \rho(x')] = \delta(x - x'), \tag{2}$$

thus giving rise to a description in terms of an exciton gas of Bose particles, which is made responsible for all observable effects of the field, while the ψ-field, in this case, is demoted to the somewhat inferior rôle of the underlying fluid, in which observable effects appear as excitations of the motion.

Although there is no a priori reason for preferring one or the other of these possible approaches towards quantization of a given classical field theory, there is still considerable doubt about the justification for the quantum hydrodynamical approach, though the procedure of quantum hydrodynamics, which was first suggested by Landau (3) almost 15 years ago, has been applied successfully in recent work by Ziman (7) regarding the theory of superfluidity and by Geilikman (1) regarding the theory of superconductivity. The reason for the general reluctance to accept quantum hydrodynamics as a legitimate quantization procedure for a classical field theory is the belief, supported by a number of strong arguments, that the conventional quantization method

[1]*Manuscript received May 27, 1954.*
Contribution from the Department of Physics, University of British Columbia, Vancouver 8, B.C.

gives an essentially correct many-particle quantum theory, and that a justification for the procedure of quantum hydrodynamics would have to consist of a proof that the commutation relations [2] follow from the commutation relations [1] or, if such a proof turns out to be impossible, that quantum hydrodynamics could at best yield only an approximate description of a many-particle system. In this respect Tomonaga has made a notable contribution (5) by showing that a one-dimensional assembly of Fermi particles can be represented by an equivalent assembly of phonons, which obey Bose-statistics, provided the consideration is restricted to excitations of the degenerate Fermi gas which do not go beyond the appearance of, so to speak, ripples on the surface of the Fermi sea.

Hereafter, all expressions referring to the point of view that the conventional quantization method is the basic procedure will be labelled "*a*".

It seems feasible, however, to take the reversed view by assuming that for at least certain types of classical field theories the procedure of quantum hydrodynamics yields the correct quantum theory of a many-particle system (2), and by considering the conventional quantization procedure as legitimate only in the approximation in which the commutation relations [1] can be derived from the commutation relations [2].

Hereafter, all expressions referring to the point of view that the quantum hydrodynamical method is the basic procedure will be labelled "*b*".

In view of the fact that the domain of quantum hydrodynamics is largely unexplored it would appear premature to decide here which of these two possible points of view will eventually prevail in specific cases, and this question must be left for future investigation. In the meantime it seems worth while to establish more clearly under which conditions both quantization procedures will yield the same results, and at which point in the development differences, if any, between the two approaches will appear. The establishment of such a relation between quantum hydrodynamics and conventional quantization of a specific classical field theory was the object of the work reported in this paper.

Perhaps the simplest classical field theory that can be subjected equally well to both quantization procedures is the nonrelativistic field theory of a charged medium, characterized by the Lagrangian density

$$[3] \qquad L = \frac{i\hbar}{2}(\psi^*\dot{\psi} - \dot{\psi}^*\psi) - \frac{\hbar^2}{2m}(\operatorname{grad}\psi^* \cdot \operatorname{grad}\psi)$$

from which by independent variation of the wave functions ψ and ψ^* follow the field equations

$$[4] \qquad \frac{\hbar}{i}\dot{\psi} = \frac{\hbar^2}{2m}\nabla^2\psi, \qquad -\frac{\hbar}{i}\dot{\psi}^* = \frac{\hbar^2}{2m}\nabla^2\psi^*.$$

As a consequence of the field equations one has the equation of continuity

$$[5] \qquad \frac{\partial\rho}{\partial t} + \operatorname{div}\mathbf{j} = 0$$

with

$$[6] \qquad \rho = m\psi^*\psi, \qquad \mathbf{j} = \frac{\hbar}{2i}(\psi^* \operatorname{grad} \psi - \psi \operatorname{grad} \psi^*);$$

the law of conservation of energy

$$[7] \qquad \frac{\partial u}{\partial t} + \operatorname{div} \mathbf{s} = 0$$

with

$$[8] \qquad u = \frac{\hbar^2}{2m}(\operatorname{grad} \psi^* \cdot \operatorname{grad} \psi), \qquad \mathbf{s} = \frac{\hbar^3}{4im^2}(\nabla^2\psi \operatorname{grad} \psi^* - \nabla^2\psi^* \operatorname{grad} \psi);$$

and the law of conservation of momentum

$$[9] \qquad \frac{\partial j_k}{\partial t} + \sum_i \frac{\partial T_{ik}}{\partial x_i} = 0$$

with

$$[10] \qquad T_{ik} = \frac{\hbar^2}{4m}\left(\frac{\partial \psi}{\partial x_i}\frac{\partial \psi^*}{\partial x_k} + \frac{\partial \psi^*}{\partial x_i}\frac{\partial \psi}{\partial x_k} - \psi\frac{\partial^2 \psi^*}{\partial x_i \partial x_k} - \psi^*\frac{\partial^2 \psi}{\partial x_i \partial x_k}\right).$$

It should be stressed that at this stage only the ratio $\hbar/m$ of the constants appearing in the equations [3] and [4] has an experimental meaning, and one may imagine this ratio to be determined by diffraction experiments. The constants $\hbar$ and m separately can be defined only after quantization of the theory. In fact, the equations [4], [5], [7], and [9] contain only this ratio, while the appearance of $\hbar$ and m separately in the definitions [6], [8], and [10] is merely a convenience.

The transition to the Hamiltonian formulation is now accomplished by introduction of canonically conjugate variables (6)

$$[11] \qquad \pi_\psi{}^* = \frac{\partial L}{\partial \dot{\psi}^*} = -\frac{i\hbar}{2}\psi, \qquad \pi_\psi = \frac{\partial L}{\partial \dot{\psi}} = \frac{i\hbar}{2}\psi^*,$$

yielding as Hamiltonian density of the field

$$[12] \qquad H_a = \pi_\psi{}^*\dot{\psi}^* + \pi_\psi\dot{\psi} - L = \frac{\hbar^2}{2m}(\operatorname{grad} \psi^* \cdot \operatorname{grad} \psi).$$

The canonical field equations following from [12] are identical with [4], and this formulation is the starting point for the conventional quantization procedure, in which the fact that ψ and ψ^* are canonically conjugate variables is used to postulate for these variables commutation relations of the type [1].

The starting point for the quantum hydrodynamical treatment, on the other hand, is the description of the same classical theory in terms of the density ρ and a velocity potential ϕ defined by

$$[13] \qquad \rho = m\psi^*\psi, \qquad i\phi = \ln \psi - \ln \psi^*.$$

The justification for calling ϕ the velocity potential stems from the observation that in this terminology the vector of the current density $\mathbf{j}$ takes the form

$$[14] \qquad \mathbf{j} = \frac{\hbar}{2m}\rho \operatorname{grad} \phi$$

which implies definition of a velocity vector $\mathbf{v}$ by

[15] $$\mathbf{v} = \frac{\hbar}{2m} \operatorname{grad} \phi.$$

The Lagrangian density [3] may now be rewritten in terms of ρ and ϕ as

[16] $$L = -\frac{\hbar}{2m}\rho\dot{\phi} - \frac{\hbar^2}{8m^2}\left\{\frac{1}{\rho}(\operatorname{grad}\rho)^2 + \rho(\operatorname{grad}\phi)^2\right\}$$

from which follow upon independent variation of ρ and ϕ the equations

[17] $$\dot{\phi} + \frac{\hbar}{2m}\left\{\left(\frac{\operatorname{grad}\rho}{\rho}\right)^2 - \frac{1}{\rho}\nabla^2\rho + \tfrac{1}{2}(\operatorname{grad}\phi)^2\right\} = 0$$

and

[18] $$\dot{\rho} + \frac{\hbar}{2m}\{(\operatorname{grad}\rho\cdot\operatorname{grad}\phi) + \rho\nabla^2\phi\} = 0.$$

It is readily seen that [18] is identical with [5], while [17] is the Bernouilli equation, as it were, which follows upon integration from the Euler equations [9].

Although the physical content of the theory has not been changed by this reinterpretation in hydrodynamical terms, the transition to the Hamiltonian formulation is now quite different from the conventional treatment, because [13] is not a canonical transformation. Looking upon ϕ as field variable one sees that ρ is its canonical conjugate

[19] $$\pi_\phi = \frac{\partial L}{\partial\dot{\phi}} = -\frac{\hbar}{2m}\rho,$$

and one obtains as Hamiltonian density

[20] $$H_b = \pi_\phi\dot{\phi} - L = \frac{\hbar^2}{8m^2}\left\{\frac{1}{\rho}(\operatorname{grad}\rho)^2 + \rho(\operatorname{grad}\phi)^2\right\}.$$

In view of the definition [15] one may therefore look upon

$$(\hbar^2/8m^2)\,\rho(\operatorname{grad}\phi)^2 = \tfrac{1}{2}\rho v^2$$

as the kinetic energy density of the field, while $(\hbar^2/8m^2\rho)(\operatorname{grad}\rho)^2 = U(\rho)$ plays the part of a potential energy density of the field (4).

Quantizations of both descriptions can now be carried out by postulating for the canonically conjugate variables the commutation relations

[21] $$\left[\psi(x);\ \frac{i\hbar}{2}\psi^*(x')\right]_a = i\hbar\delta(x - x'), \text{ or } [\psi(x);\ \psi^*(x')]_a = 2\delta(x - x')$$

and

[22] $$\left[\phi(x);\ -\frac{\hbar}{2m}\rho(x')\right]_b = i\hbar\delta(x - x'), \text{ or } \left[i\phi(x);\ \frac{1}{m}\rho(x')\right]_b = 2\delta(x - x')$$

respectively, with all other commutators vanishing.

Now it is clear immediately from the relations

[23a] $$\rho = m\psi^*\psi, \qquad i\phi = \ln(\psi/\psi^*)$$

or

[23b] $$\psi = \exp\tfrac{1}{2}\{\ln(\rho/m) + i\phi\}, \qquad \psi^* = \exp\tfrac{1}{2}\{\ln(\rho/m) - i\phi\}$$

that the two possible quantization procedures are entirely different, because neither is [22] a general consequence of [21], nor is [21] a general consequence of [22], whichever of the two postulates one considers as the basic one. Consequently, the eigenvalues of the respective Hamiltonians will in general describe entirely different physical situations. In fact, the eigenvalues of the Hamiltonian resulting from [12] can be obtained in a representation in which the operator "number of particles" $N = \int \psi^* \psi \, dx$ is diagonal with integer eigenvalues, and $\mathfrak{H}_a = \int H_a \, dx$ yields the total kinetic energy of all noninteracting "particles" present, with each "particle" of momentum $\mathbf{p}$ contributing the amount $p^2/2m$ to the sum total, while the much more difficult eigenvalue problem posed by the Hamiltonian density [20] is usually attacked (7) by expanding ρ in powers of $\rho - \rho_0$ (ρ_0 being a c-number and identified with the equilibrium density of the fluid), and an interpretation in terms of a system of coupled oscillators or "phonons" that represent possible excitations of the motion of the underlying ψ-fluid is thus obtained.

There exists, however, a certain approximation of the conventional treatment, first introduced by Geilikman (1), in which the commutation relations [22], up to a factor 2, are a consequence of [21], and which consists of the assumption that the operators ψ and ψ^* can be split into

[24] $$\psi = \psi_0 + \psi_1, \qquad \psi^* = \psi_0^* + \psi_1^*$$

with ψ_0 and ψ_0^* constant c-numbers and ψ_1 and ψ_1^* operators such that in the classical theory

[25] $$\psi_1 \ll \psi_0, \qquad \psi_1^* \ll \psi_0^*.$$

This approximation is identical, as will be seen later, with the approximation procedure employed in quantum hydrodynamics, mentioned above, which consists of an expansion of ρ in powers of $\rho - \rho_0$, with ρ_0 a constant; and $\int \psi_0^* \psi_0 \, dx = N_0$ may be considered as the number of particles in the ground state which do not participate in the dynamical behavior of the system. Geilikman's approximation is consistent within the framework of the theory characterized by the Hamiltonian density [12], because with ψ_0 a constant this Hamiltonian density takes the form

[26] $$H_a^{(2)} = \frac{\hbar^2}{2m} (\text{grad } \psi_1^* \cdot \text{grad } \psi_1)$$

and since now ψ_1 and ψ_1^* are canonically conjugate variables, the commutation relations [21] may be replaced by

[27] $$[\psi_1(x); \psi_1^*(x')]_a = 2\delta(x - x').$$

If one expands now ρ/m and $i\phi$ in powers of ψ_1/ψ_0,

[28] $$\frac{\rho}{m} = \frac{1}{m} (\rho_0 + \rho_1 + \rho_2), \qquad i\phi = i(\phi_0 + \phi_1 + \phi_2 + \ldots)$$

with

[29] $$\frac{\rho_0}{m} = \psi_0^* \psi_0 = \text{const.}, \qquad \frac{\rho_1}{m} = \psi_0^* \psi_1 + \psi_0 \psi_1^*, \qquad \frac{\rho_2}{m} = \psi_1^* \psi_1$$

and

$$[30]\quad i\phi_0 = \ln\left(\frac{\psi_0}{\psi_0^*}\right) = \text{const.},\quad i\phi_1 = \left(\frac{\psi_1}{\psi_0} - \frac{\psi_1^*}{\psi_0^*}\right),\quad i\phi_2 = -\frac{1}{2}\left(\frac{\psi_1^2}{\psi_0^2} - \frac{\psi_1^{*2}}{\psi_0^{*2}}\right),$$

it is seen that up to terms quadratic in ψ_1 and ψ_1^* the following commutation relation holds:

$$[31]\quad \left[i\phi_1(x);\ \frac{1}{m}\rho_1(x')\right]_a^{(2)} = \frac{\psi_0^*}{\psi_0}[\psi_1(x);\ \psi_1(x')]_a - \frac{\psi_0}{\psi_0^*}[\psi_1^*(x);\ \psi_1^*(x')]_a + [\psi_1(x);\ \psi_1^*(x')]_a + [\psi_1(x');\ \psi_1^*(x)]_a$$

or, as a consequence of [27],

$$[32]\quad \left[i\phi_1(x);\ \frac{1}{m}\rho_1(x')\right]_a^{(2)} = 4\delta(x - x'),$$

which proves that in this approximation, up to a factor 2, quantum hydrodynamics is a legitimate consequence of the conventional quantization procedure. (Thus one may look upon [23*a*] as a transformation which is almost canonical in this approximation.)

A quite similar proof is possible if one adopts point of view "*b*", namely that quantum hydrodynamics is the basic procedure, and that the conventional treatment can at best only yield an approximate description of the exciton gas. Assume for that purpose that ρ and ϕ may be written as

$$[33]\quad \rho = \rho_0 + \rho_1,\qquad \phi = \phi_0 + \phi_1$$

with the understanding that ρ_0 and ϕ_0 are constant c-numbers, and that

$$[34]\quad \rho_1 \ll \rho_0$$

in the classical theory. Accordingly, the Hamiltonian density [20] can be expanded in terms of increasing order in the field variables ρ_1 and ϕ_1:

$$[35]\quad H_b = H_b^{(2)} + H_b^{(3)} + H_b^{(4)} + \ldots$$

with

$$[36a]\quad H_b^{(2)} = \frac{\hbar^2}{8m^2}\left\{\frac{1}{\rho_0}(\text{grad}\ \rho_1)^2 + \rho_0(\text{grad}\ \phi_1)^2\right\},$$

$$[36b]\quad H_b^{(3)} = \frac{\hbar^2}{8m^2}\left\{-\frac{1}{\rho_0^2}\rho_1(\text{grad}\ \rho_1)^2 + \rho_1(\text{grad}\ \phi_1)^2\right\},$$

$$[36c]\quad H_b^{(4)} = \frac{\hbar^2}{8m^2}\frac{1}{\rho_0^3}\rho_1^2(\text{grad}\ \rho_1)^2,\ \text{etc.}$$

which is the approximation method usually employed in quantum hydrodynamics. Since now ρ_1 and ϕ_1 are canonically conjugate variables, the commutation relations take the form

$$[37]\quad \left[i\phi_1(x);\ \frac{1}{m}\rho_1(x')\right]_b = 2\delta(x - x')$$

and the commutation relations for the ψ-operators can be obtained by using the expansions

[38] $$\psi = \psi_0 + \psi_1 + \psi_2 + \ldots, \qquad \psi^* = \psi_0^* + \psi_1^* + \psi_2^* + \ldots,$$

which according to [23*b*] contain the terms

[39*a*] $$\psi_0 = \exp\frac{1}{2}\left\{\ln\left(\frac{\rho_0}{m}\right) + i\phi_0\right\}, \qquad \psi_0^* = \exp\frac{1}{2}\left\{\ln\left(\frac{\rho_0}{m}\right) - i\phi_0\right\};$$

[39*b*] $$\psi_1 = \psi_0\frac{1}{2}\left(\frac{\rho_1}{\rho_0} + i\phi_1\right), \qquad \psi_1^* = \psi_0^*\frac{1}{2}\left(\frac{\rho_1}{\rho_0} - i\phi_1\right);$$

[39*c*] $$\psi_2 = \psi_0\left\{-\frac{1}{8}\left(\frac{\rho_1^2}{\rho_0^2} + \phi_1^2\right) + \frac{1}{8}\frac{i}{\rho_0}(\rho_1\phi_1 + \phi_1\rho_1)\right\}, \qquad \psi_2^* = \ldots.$$

It is seen that up to terms quadratic in ρ_1 and ϕ_1 the commutation relation holds:

[40] $$[\psi_1(x);\ \psi_1^*(x')]_b^{(2)} = \frac{1}{4m\rho_0}[\rho_1(x);\ \rho_1(x')]_b + \frac{\rho_0}{4m}[\phi_1(x);\ \phi_1(x')]_b + \frac{1}{4}\left[i\phi_1(x);\ \frac{1}{m}\rho_1(x')\right]_b + \frac{1}{4}\left[i\phi_1(x');\ \frac{1}{m}\rho_1(x)\right]_b$$

or, as a consequence of [37],

[41] $$[\psi_1(x);\ \psi_1^*(x')]_b^{(2)} = \delta(x - x'),$$

which proves that in this approximation, again up to the factor 2, the conventional quantization procedure is a legitimate consequence of quantum hydrodynamics.

Taking again point of view "*a*", it can be concluded that in the approximation in which higher than quadratic terms in the field variables are negligible the Hamiltonian density

[36*a*] $$H_b^{(2)} = \frac{\hbar^2}{8m^2}\left\{\frac{1}{\rho_0}(\text{grad}\ \rho_1)^2 + \rho_0(\text{grad}\ \phi_1)^2\right\}$$

is adequate to describe the excitations of the motion of the many-particle system under consideration. The classical canonical equations following from the Hamiltonian resulting from [36*a*] are

[42*a*] $$\dot{\phi}_1 - \frac{\hbar}{2m}\frac{1}{\rho_0}\nabla^2\rho_1 = 0,$$

[42*b*] $$\dot{\rho}_1 + \frac{\hbar}{2m}\rho_0\nabla^2\phi_1 = 0.$$

They have been treated previously by Takabayasi (4), and permit plane wave solutions

[43*a*] $$\phi_1 = \gamma\sin\left\{(\mathbf{k}.\mathbf{r}) \mp \frac{\hbar}{2m}k^2t\right\}, \qquad \rho_1 = \mp\gamma\rho_0\cos\left\{(\mathbf{k}.\mathbf{r}) \mp \frac{\hbar}{2m}k^2t\right\}$$

and

[43*b*] $$\phi_1 = \gamma\cos\left\{(\mathbf{k}.\mathbf{r}) \mp \frac{\hbar}{2m}k^2t\right\}, \qquad \rho_1 = \mp\gamma\rho_0\sin\left\{(\mathbf{k}.\mathbf{r}) \mp \frac{\hbar}{2m}k^2t\right\}$$

which correspond, in this approximation, to solutions of the ψ-field equations

[44a] $$\psi_1 = \pm\, \psi_0 \frac{\gamma}{2} \exp \pm i \left\{ (\mathbf{k}.\mathbf{r}) \mp \frac{\hbar}{2m} k^2 t \right\}$$

and

[44b] $$\psi_1 = i\, \psi_0 \frac{\gamma}{2} \exp \pm i \left\{ (\mathbf{k}.\mathbf{r}) \mp \frac{\hbar}{2m} k^2 t \right\}$$

respectively.

The transition to quantum theory can be carried out in the well-known way (6), and will be omitted here. It suffices to say that the system of uncoupled "phonons" represented by the Hamiltonian density [36a] corresponds to the particle excitations of the ψ-field represented by the Hamiltonian density [26] in the manner indicated by equations [43] and [44].

Finally, it should be noted that deviations from the usual procedure of quantum hydrodynamics will occur, according to point of view "a", if in the expansions [28] higher than quadratic terms in ψ_1 and ψ_1^* are taken into account. In the third approximation the commutation relation of ϕ and ρ, as an example, takes the form

[45] $$\left[i\phi(x); \frac{1}{m} \rho(x') \right]_a^{(3)} = \left[i\phi_1(x); \frac{1}{m} \rho_1(x') \right]_a + \left[i\phi_2(x); \frac{1}{m} \rho_1(x') \right]_a + \left[i\phi_1(x); \frac{1}{m} \rho_2(x') \right]_a$$

$$= 4\, \delta(x - x') \left\{ 1 - \frac{1}{2} \left[\frac{\rho_1(x)}{\rho_0} + i\phi_1(x) \right] \right\},$$

and similar relations for ψ and ψ^* can be derived if point of view "b" is adopted. In either case the canonical equations corresponding to this approximation are rather complicated and require use of perturbation methods.

A detailed application of point of view "a" to the theory of the complex scalar meson field, including higher order effects in the hydrodynamical description, is under way, and will be submitted for publication at a later date.

REFERENCES

1. GEILIKMAN, B. T. Doklady Akad. Nauk S.S.S.R. 94: 199, 659. 1954.
2. KAEMPFFER, F. A. Can. J. Phys. 32: 259. 1954.
3. LANDAU, L. D. J. Phys. U.S.S.R. 5: 71. 1941.
4. TAKABAYASI, T. Progr. Theoret. Phys. (Japan), 8: 143. 1952.
5. TOMONAGA, S. Progr. Theoret. Phys. (Japan), 5: 544. 1950.
6. WENTZEL, G. Quantentheorie der Wellenfelder. Wien. 1943.
7. ZIMAN, J. M. Proc. Roy. Soc. (London), A, 219: 257. 1953.

COSMIC RAY PHENOMENA AT MINIMUM IONIZATION IN A NEW NUCLEAR EMULSION HAVING A FINE GRAIN, MADE IN THE LABORATORY[1]

By Pierre Demers

ABSTRACT

The preparation of a silver bromide emulsion in the form of baseless sheets and their use in thick homogeneous stacks are described. In these sheets, a suitable development brings out minimum ionization tracks with a grain diameter 0.1 to 0.2 μ, and a linear grain density of 15 per 100 μ. The sequence of observations which led to the positive identification of minimum tracks is discussed. Short recoils and delta rays are visible, and excellent discrimination is available at all ionizing powers. The influence of grain size on fog is analyzed.

Several cosmic ray phenomena containing minimum tracks are presented: single tracks, hard showers, $\pi\mu e$ events, and an electron pair. Distortion is very small, and it is shown that the small grain size renders feasible better scattering measurements on higher energy particles. With this emulsion, nearly every possible measurement should become feasible with greater accuracy.

I. INTRODUCTION

Our first experiments in 1945 (4, 5), whose publication (6) (dated 28 December 1945) was retarded for security reasons until July 1946, were followed by the commercial making of Ilford "New Concentrated Halftone" type A, described by Powell, Occhialini, Livesey, and Chilton (27), and later by the production of the Ilford Series B, C, D, E, F. In those experiments (7), concentrated emulsions were made with a fine grain, showing considerably improved fission and proton tracks, and occasionally tracks of electrons measuring as much as 180 μ, see Demers (7). See also further papers on emulsion making by Demers (12).

Berriman (1) was the first to achieve sensitivity to minimum ionization in NT4, then Waller and Dodd in Ilford G5, and Spence, Webb, and Yutzi in Eastman NTB3 (circulars of Ilford, of Eastman Kodak, private communications, and also (24)). Jenny (19) obtained it for the first time outside an industry and described his formula. The appearance of NT4, G5, and NTB3 brought about very rapid progress in cosmic ray research, as these emulsions showed the tracks of fast protons, of relativistic mesons single or in the hard showers, and of the electrons in the soft showers.

However, as Occhialini has noted (24), these very sensitive commercial layers might be improved, in particular by reducing the grain size and enhancing their discriminating properties at moderate and high energy losses. At present the grain size is usually more than 0.5 μ in observed tracks in G5, and light nucleons showing as branches of less than 3000 μ can usually not be identified. Nucleonic branches are readily distinguished in C2, which on the other hand is not sensitive to less than two or three times minimum.

The present emulsion shows the differences between H, α, and heavier

[1]*Manuscript received April 2, 1954.*
Contribution from Institut de Physique, Faculté des Sciences, Université de Montréal, Province de Québec.

tracks that can be seen only with a fine grain, and at the same time, it shows hard showers and electron pairs. A first note on the subject was published earlier (14).

II. EMULSION MAKING

Tests on Preparation

Several tests were made using the three-jet formula in which continuous precipitation is ensured by the simultaneous pouring of the three solutions A, B, and C into a stirred vessel having an overflow (8).

Solution A: $AgNO_3$, 600 gm. per liter of solution weighing 1482 gm.
Solution B: KBr, 420 gm. per liter of solution weighing 1288 gm.
Solution C: gelatine solution in water and alcohol, for exact proportions see (12) or below.

Sensitivity was evaluated after irradiation with an old emanation needle, from the longest electron tracks that could be recognized. It was apparently improved by this three-jet procedure, but at the cost of a larger grain size, 0.2 to 0.4 μ before and 0.3 to 0.6 μ after development; careful tests with the two-jet formula gave as long electron tracks with the usual fine grain of formula 2 (7). All these tests were carried out with metering pumps to deliver the required volumes.

Attempts to improve sensitivity were made by changing the gelatine. Instead of 2191 American Agricultural Chemical Company Keystone brand, we tried several samples of known photographic properties, which were specially prepared and kindly sent to us by Dr. Steigmann of Atlantic Gelatine Co. However all of these failed to procure the smallest gain and most of them gave heavy fog, clumps, and coarse precipitates. This is taken as proof of the radical differences between our procedures and those current in the photographic trade.

In our emulsions, the grain size is nearly fixed at the end of the precipitation stage and there is no purposeful heat treatment. Sensitivity is raised instantaneously by the addition of triethanolamine, later it rises slowly when the emulsions are kept in cold storage. This is at variance with the "ordinary" fast emulsions, which are considerably altered in the first and in the second ripening especially if the bromide is mixed with 1 to 3% iodide. Here, on the contrary, iodide brings about a coarser grain and a lesser sensitivity, and the presence of a small amount of potassium bromide in the finished product, which acts as a stabilizer in other cases, makes little difference and is rather detrimental. According to a private communication of Mr. Waller, it seems that sensitivity in Ilford Nuclear Series is obtained by ordinary or normal procedures involving sulphur bearing complexes.

Gelatine 2191 is described by its makers as a slow positive type, which gives no clue to its peculiar properties. Dr. Steigmann has found that it contains some $\frac{1}{2}$% of chloride ions, which means, in the formula used, a ratio of about $\frac{1}{4}$% chloride/bromide by weight at the end of precipitation. It is not clear whether this chloride may have a bearing on the properties of our emulsions; early tests (7) with chloride–bromide–iodide mixtures have shown that

several per cent chloride in bromide, or chloride alone, gave a good sensitivity with a fog that increased rapidly with time. The chloride alone would probably not explain the good colloidal protection afforded by this gelatine in preventing coarse grain formation.

Present Formula 2 Modified

Several substances have been tested as sensitizers (16), including gold salts; by now a few dozen gelatine samples have been tried from several makers in the United States, Great Britain, and France. It seems reasonable to conclude that the conditions of our two-jet formula represent an optimum, and that changing these conditions can only lead to more fog and less sensitivity. Practically all the parameters which enter into the two-jet equation have been changed slightly once, by chance or by will, in the course of the last few years. Therefore under the broad conditions defining this formula and ensuring a very small grain size, it seems useless to try further changes in the making.

Such considerations led us to try out changes in the processing, which did bring out minimum ionization tracks. The exact formula used in the making is probably not extremely critical but we give it as follows for record.

Solutions A and B see above. *Solution C* contains 225 gm. gelatine 2191 added to 1500 gm. cold water in a stainless steel pot 20 cm. in diameter, 27 cm. high, holding 7.5 l. The gelatine is allowed to swell for an hour, then melted in a hot water bath at 50–55° C., then 900 cc. alcohol is added and the mixture kept covered at 48° C. It is brought under the precipitating machine, which contains Zenith metering pumps. The stirrer is started, 1 cc. of B is poured separately at first to ensure an excess of bromide from the start. The stirrer is made of a flat fiber surface held at the end of a stainless steel rod; it should keep the mass turning regularly in a vortex as fast as possible without spilling and without bubble formation, but its exact speed is not critical. From now on only red light should be allowed to reach the reacting mass. The emulsion is not very sensitive to light, and a bright red light (25 watt ruby bulb) is perfectly safe at all stages of its handling, even before development.

The two pumps A and B are geared together and used to deliver simultaneously 1911 cc. of A and 1950 cc. of B, so there is always a 2% excess of B over A. Great care is taken not to splash any A and B liquors on the stirrer's rod, which stands uncovered by the mass in the center of the vortex. For this purpose, the flow is set quite slow at first, and the tips of the glass tubes that are pouring A and B are pushed under the surface of the mass. The flow may then be speeded up. It is slowed down again when the required volumes have been nearly all delivered, and the tips are removed from below the surface before the flow is stopped to prevent the lighter emulsion from ascending in the pouring tubes.

If such precautions are not taken, drops of A and B react on the stirrer's rod where they meet in the almost complete absence of gelatine, and a coarse precipitate appears, which may partly settle at the bottom of the mass if this is left standing for a while. This precipitate explains most of the coarse fog obtained previously with this formula. As seen in the accompanying figures coarse fog is now almost entirely absent.

Precipitation takes about 35 minutes. It probably could be speeded up several times by using larger pumps.

No thermostat is used during the above precipitation. Owing to the heat of reaction, the temperature remains constant at 48° C. throughout. In special tests, by surrounding the pot with cold water, the mass was kept as cold as was possible without it setting, that is at about 25° C. In another case, it was kept heated at 70–75° C. The low temperature reduced grain size, fog, and sensitivity a little, but the difference appeared negligible after a few weeks' keeping. The high temperature acted the opposite way, and fog became excessive on keeping. Safe temperature limits are therefore 35 to 48° C. during precipitation. The presence of 300 gm. $Na_2SO_4.10H_2O$ in solution C was tried, but it only induced supplementary fog and coarser grain.

The precipitated emulsion is cooled in a cold water bath to 12–15° C. with hand stirring. If stirred at lower temperatures, a weak jelly is broken into small pieces, which never set in a single block suitable for shredding. After it has been kept overnight in a refrigerator at 0–5° C., the mass is shredded by being placed in large lumps in a press made of a 3 in. diameter fiber tube 12 in. high with its bottom closed by a net of crossed stainless steel wire 0.7 mm. in diameter forming squares of 3 mm. side. The jelly is forced down by the bottom of a glass bottle that fits in loosely, and it comes down as long noodles or shreds which are washed thoroughly in cold running water at less than 5° C. preferably, and not more than 10° C. Washing lasts two to four hours in two stainless steel pots of 5 to 7.5 l., with frequent stirring. A good rule is as follows. A noodle is melted between closed hands. Then the hands are rubbed, half-opened, and are smelled. A very small trace of alcohol is then easily detected. When the smell of alcohol disappears, washing is usually halfway or two thirds through.

Shreds are collected, drained, and may be kept in the refrigerator for several days at 0–5° C. *One third* of the mass is taken. The other two thirds will be taken later and treated in the same way in their turn. The third is melted at 50° C. and to it are added:

Triethanolamine	13.5 gm.,
Thymol	0.5 gm.,
Alcohol	100 cc., making one solution.

The quantity of triethanolamine is critical; the antiseptic thymol may not be very useful and we are now trying to do without it; some alcohol helps in avoiding bubbles, which a wetting agent might do as well.

The remelted emulsion with its additions is poured at 35–40° C. from the bottom tip of a stainless steel medical "irrigator", through a rubber tube. Great care is taken to avoid air bubbles, hence the use of siphoning the liquid off the bottom. It is poured on a flat tray formed on a piece of double glass ($\frac{1}{8}$ in. thick), 24 in. × 36 in., laid flat with a good spirit level in the darkroom. The sides of the tray are lucite bars cemented with 8% gelatine, or with cellulose acetate cement. The tray measures 78 × 53 cm.

The emulsion is about 3 mm. thick and sets in half an hour or so. It is fanned by an electric ventilator at its lowest speed, giving a wind of 1 to 2

m./sec. The temperature is about 25° C. in the darkroom. The humidity should be kept at 67 ± 3%; it is controlled by a hygrostat consisting of a strip of cellophane 130 cm. long which makes a contact when too dry thus opening an electric valve controlling hot water, and setting a small fan running to activate evaporation. Drying ought to take two days; otherwise the emulsion crevices, cockles, wrinkles, and lifts off the glass irregularly. The sheet of dried emulsion is easily lifted off the glass. It is cut into sheets 2 in. × 4 in. over 300 μ ± 10%. A maximum number of 75 sheets is obtained. The sheet is more glossy on the side that was touching the glass, and naturally bears traces of any bubbles in its mass, or of marks in the glass.

The two remaining thirds of the emulsion are both treated in the same way in their turn, so that a single recipe may yield a maximum of 225 sheets, weighing about 1300 gm. in all. Residues are collected for silver recovery.

III. UTILIZATION OF EMULSION SHEETS

Homogeneous Stacks

Until now several kilograms of stacked sheets made by the above two-jet formula or by its earlier variants, or by the three-jet formula, have been flown. The stacks that are used are homogeneous. Save for a thin layer of air that cannot be avoided, and that was about 10 μ thick in one measured case (11), they are made exclusively of emulsion from side to side. Bradt and Peters; Freier, Lofgren, Ney, and Oppenheimer; Hoang; Schein; and others have used heterogeneous stacks made of emulsions coated on glass, sometimes with other materials, such as brass or lead, interposed. O'Dell, Shapiro, and Stiller (25) have discussed their use. Powell (26) recently suggested and tried the use of stacks consisting mainly of G5 pellicles. Lal, Pal, and Peters (21) give elaborate details on their processing. At least in the case of these last authors, paper is interposed between the sheets to avoid sticking; the distance between the sensitive surfaces may reach 150 μ according to their statements.

In the homogeneous stacks made up of our baseless sheets, we sometimes had trouble from sheets that were somewhat tacky and that could not be separated—especially when using the three-jet formula, which led to greater softness that was probably related to the larger grain diameter. However, with the very fine grain of the two-jet formula above, the substance is hard and behaves very much like gelatine itself. The sheets adhere slightly to each other so that when pressed together, they cannot be shifted sidewise; they are easily separated, unless the package has been subjected to excessive moisture.

Homogeneous stacks have been suggested by Kinoshita (20), in 1910, for following particles whose range would exceed a single layer's thickness, and he managed to prepare and superpose two thin and baseless sheets obtained by melting a plate's coating after swelling it in water. It is not clear whether he followed tracks in these sheets, since apparently he did not recognize tracks in single sheets.

Demers (9, 10, 11) since 1949 has used homogeneous stacks to follow cosmic ray tracks, strong and weak, through several sheets.

Irradiating Techniques

These sheets keep well for at least one year in a refrigerator, tightly packed together in black paper with several turns of strings about them. Packages for cosmic ray irradiation are pressed between dural sheets 1 mm. thick and somewhat larger than the sheets. Some packages are irradiated lying flat and are kept oriented during the flight by a compass improved over the one described earlier (11). Some are exposed with their plane vertical. In all cases the packages are surrounded by a transparent plastic box large enough so that the sun's rays will keep them warm. The temperature is kept between probably 0° and 25° C.

Flights, launched from the University of Montreal grounds, are now made by an improved technique (13), which allows us to keep a light load at a ceiling for several hours. Some of the flights lasted 13½ hr. The integral pressure vs. time curve is now obtained by a radioactive barometer (15). The flight recovered at Lefaivre, Ont., lasted 8 hr. 50 min. above ground, 7 hr. above 0.13 atm., 6 hr. above 0.038 atm., 5 hr. above 0.037 atm., and reached 0.019 atm. or 27.4 km.

Development

Previously described tests (12) have shown that increasing the concentration of sodium sulphite and of potassium bromide in Eastman Developer D8 decreased the ratio sensitivity/fog determined from grain counts. Also D19 containing elon is more detrimental than D8 containing only hydroquinone. All these features point to the detrimental effects of physical development, which is enhanced by sodium sulphite, potassium bromide, and elon (see Voyvodic, p. 228 (28)). After the test on the gelatine samples described above, it was deemed worth while modifying D8 by subtracting some quantity of sodium sulphite and potassium bromide from it. As a rule the baths were employed after dilution with six times their weight of water, and development was at 0–2° C. and lasted 7½ hr. Here are the formulas tested. In them, water and hydroquinone were the same throughout.

	D8	*D8* modified			
Water, cc.	750				
Dissolve in succession:					
Na_2SO_3, gm.	90	30	20	20	40
Hydroquinone, gm.	45	—	—	—	—
NaOH, gm.	37.5				
KOH, gm.		32.5	30	30	30
KBr, gm.	30	8	4	0	16
Water to make	1000 cc.	—	—	—	—

The decrease of sodium sulphite decreased the grain size and the fog but increased the red stain. The red stain, being not granular under the microscope, is of inconvenience only because it reduces light intensity. It induces no turbidity. A more complete removal would probably be advantageous under

proper conditions of mixing (see later), but the present tests suggest the necessity of preserving 20 or 30 gm. of sodium sulphite in the modified formula.

The case of potassium bromide was different: in its complete absence, we found that granular fog is bad; but there seems to be an optimum amount between 4 and 8 gm. giving much less fog than with D8. Potassium hydroxide was used in the hope that potassium ions might be less detrimental than sodium. The best modification, with 25 gm. sodium sulphite and 6 gm. potassium bromide, reduces fog by a factor estimated as 2 or 3 with respect to D8.

Further improvements were sought by changing the active substance. From books on photography, it was found that pyrocatechol and chlorohydroquinone, two substances akin to hydroquinone, are strong and clean developing agents. They cost two or three times more than this last substance, hence probably the fact that they are little used. Both gave very superior results, when replacing hydroquinone in equal weights in the above modified formulae. From their use on test sheets that had not been flown, and that were not of the best quality, it was not possible to decide between them.

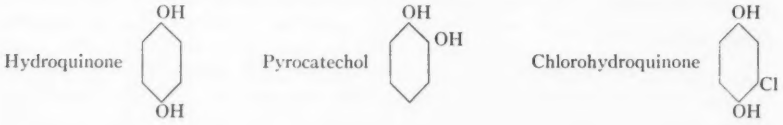

Recommended Processing

The procedure used on the 52 cosmic ray sheets from the Lefaivre ascent, which brought out minimum ionization tracks, was as follows. The developer used consisted of:

Water 750 cc.

Dissolve in succession:

Na_2SO_3 30 gm.
Chlorohydroquinone (pure) 45 gm.
KOH 32.5 gm.
KBr 8 gm.
Water q.s. 1000 cc.

This stock solution is diluted 1:6 by weight, i.e., in six times its weight of water, used at 0–2° C. in a 7.5 l. covered stainless steel pot, and kept in an electric refrigerator. The sheets were hung side by side between turns of two coils made of stainless steel wire of diameter 0.7 mm. held on horizontal glass rods. They were stirred gently, for fear of breaking the sheets, by revolving the pot a few times, in the course of $7\frac{1}{2}$ hr.

This developer was brown from the start and it induced a red stain. From recent tests made by Miss Simone Kittel in this laboratory, it is now understood that the original brown color came from the presence of undissolved chlorohydroquinone at the time when the caustic was added. If care is taken to dissolve chlorohydroquinone completely (at 40–50° C.) before the caustic is added, an almost white solution results, causing no red stain. Then it becomes possible to use as little as 10 gm. of sodium sulphite without inducing red stain.

After 7½ hr., the developer is siphoned off, and replaced by an ice-cold stop bath:

Acetic acid 1 to ½%.

At this stage the sheets are hard like rubber, somewhat swollen, and they have kept their shape. Too acid a bath may cause breakage of the sheets, probably through the evolution of gas bubbles.

After some 15 min. the fixer replaces the hardener:

Kodak Rapid Hardening Fixer, 1 volume,
$Na_2S_2O_3$, 30% by weight in water, 1 volume.

This formula gives little distortion. The pure Kodak Fixer makes the sheets too brittle, they break and are easily distorted. Distortion is still worse if pure hypo is used.

Some substance present in the Kodak product—which remains to be identified—sometimes causes tumefaction of the sheets and the appearance of a white opaque precipitate in them, which never dissolved out, and which is presumably a silver complex. This accident occurs when the sheets stay too long in contact with the spent bath. This may occur if a sheet falls to the bottom, if two sheets stay in contact for a long time, or if circulation is slowed down by a paper bag around the sheets and then the paper and the sheets get stuck together. For these reasons a more standard fixer of proper hardening properties would be preferable. With the above fixing bath used in large quantities, and with gentle occasional stirring, fixing is completed in two to five hours.

The fixer is withdrawn and thorough washing is done, always in the same container, for two to four hours, for some time after the sheets retain absolutely no taste of thiosulphate. Water temperatures as high as 20° C. seem to have no ill effects after the recommended fixing bath.

The sheets are then removed from their coils and laid, a few at a time, in a conditioning solution in a flat tray:

Water 300 cc.
Alcohol 200 cc.
Glycerine 40 gm.

They are gently stirred, and after 10 min., they are taken with the hands and laid centrally on a piece of glass 0.8 mm. thick, 3¼ in. × 5 in., care being taken not to trap any air bubbles. They are covered with a piece of Kraft absorbent paper wetted with the conditioning solution, and a roller is passed on them with light pressure to remove the excess of liquid.

They are left to dry horizontally in a dust-free atmosphere, under a tent of gauze if necessary. Drying should be very slow, taking at least a day; then the sheet is usually well adherent to the glass.

When dry, they are rubbed with a Kleenex pad and alcohol to remove surface physical fog. Then they are placed one by one at leisure in the atmosphere of a covered tray containing water at its bottom; this 100% humidity treatment swells them, and they can be lifted off the glass, turned over after another stay in the conditioning solution, and stuck again, upside down this time, on the piece of glass.

When dry again, their back side can be cleaned also; they can be kept this way, or turned over again. These swelling and resticking procedures can be repeated apparently without distorting the sheet.

The 100% humidity treatment is useful to stick back a sheet that has peeled off. A higher glycerine content may be necessary in bad cases. Sheets that have been fixed without a hardener are softer and have less chance of peeling off from dryness.

The resulting sheets had an optical density of 0.6 to 0.9. They were evenly developed throughout their thickness and surface, except for a segment of a circle defined by the holding spring.

IV. PROPERTIES OF THE EMULSION

Geometrical Transformations of the Sheets

Some of the sheets have changed their shape slightly. Part of this change we ascribe tentatively to variations in thickness of the original sheet. But most sheets retain their shape quite exactly. Their lateral dimensions are changed regularly by a factor $(1 + \epsilon)$, with extension ϵ between 2 and 9%. More precisely, if we call y the direction that was vertical during processing, x the perpendicular direction in the sheet's plane, and z the direction of the sheet's thickness, then the following equations hold (11):

$$x' = x/(1 + \epsilon_x), \qquad y' = y/(1 + \epsilon_y), \qquad z' = zf.$$

The accents refer to coordinates at the time of irradiation, and the unaccented quantities, to those at the time of observing, f is the shrinkage factor, nearly equal to 2.

Measurements on a few sheets showed $\epsilon_y = 9\%$, $\epsilon_x = 6\%$, assuming that dimensions before development were exactly 4 in. $\times$ 2 in. In other sheets thicker and made at a lower temperature, $\epsilon_y = 4\%$ and $\epsilon_x = 2.5\%$. This suggests a slight plastic flow of the sheet under its own weight during processing (in the y direction). This matter should be investigated more closely, since it is thought that hardening occurs only after removal of the silver bromide. This belief is based on attempts made at preparing a hardened nuclear emulsion by adding chromium and aluminum salts at the time of pouring it; these attempts all failed.

This small anisotropy ($y/x = 109/106$ or $104/102.5$) could perhaps be removed by holding the sheets horizontal as proposed and experimented by Lal, Pal, and Peters; their processing was done by laying the sheets on a paper covering the bottom of individual trays. According to these authors fixing expanded the G5 sheets by $\epsilon = 50\%$ but gradual dehydration in alcohol brought them back to the original size and shape within $\epsilon = 0.5\%$, and negligible distortion resulted.

Grain Size and Discrimination

Emulsions made by the above formula were examined by Mr. A. Nantel of the Institut de Microbiologie with the electron microscope. The grains appeared more or less rounded with an average diameter d of nearly 0.08 μ. According to the Jdanow formula (see Voyvodic, p. 222), maximum grain

density should be about 900 per 100 μ of path, or about 60 times the minimum that we observe for minimum ionization $I_0 = 550$ e.v./μ. Thus throughout a large range of ionizing values extending from I_0 to considerably more than $I = 60I_0$, we may expect some variation of appearance of track with variation of I, either in measurable grain density, in optical density, or in width.

This agrees with measurements on fission tracks by photometric means, in similar but less sensitive two-jet emulsions made earlier, where considerable variations in optical density were used for a precise study of I in the range between 100 and 30000 I_0, see Mathieu and Demers (23). Apparently there exists no other emulsion of comparable properties, since similar photometric measurements have not been reported elsewhere.

The wide range of the discrimination may be appreciated from inspection of the accompanying figures.

The grain size after development is appraised to be 0.1 to 0.2 μ in the sheets under discussion here, for single grains forming weak tracks. With dense tracks, clogging sets in and the core of a very dense iron track at its maximum width may be 2 μ wide.

Threshold of Sensitivity of Individual Grains

Assuming the above size $d = 0.08$ μ for those silver bromide crystals that possess a latent image after passage of a minimum ionization track through them, we may calculate the minimum energy loss and the minimum number of electrons set free in the crystals that will produce a detectable effect. Assume that $I_0 = 550$ e.v./μ in the emulsion, 775 e.v./μ in silver bromide, the minimum loss is 62 e.v. for the longest track possible through the grain. Assume 4.5 to 7.5 e.v. lost per electron set free; from 8 to 14 electrons are set free. These numbers should be raised somewhat if fluctuations in energy loss intervene. This threshold sensitivity for single grains compares with that attained in the best negative light sensitive materials. Berriman (2), while discussing NT2*a*, stated that an increase of the grain size would be one way of reaching minimum sensitivity. The result has been obtained here by following the opposite procedure.

Distortion and Scattering Measurements

The regular over-all deformations described above are not accompanied by any large distortion of the tracks. In the portions of plates examined so far, C or S distortion of strongly dipping tracks, indicative of shear in the thickness of the layers, is moderate near the edges, where it is linked with the drying process. A few millimeters from the edges, it is usually so small as to escape detection even near the point of hanging. A mechanically elaborate microscope is not available, but an upper limit may be set approximately as follows: the whole length of a vertical track crossing from air A to glass V may agree with a straight line within 1 μ, length $AV = z = 140$ μ, $z' = 300$ μ. Very long tracks have been observed showing no detectable curvature or deflection over a 15 mm. length. See figures.

While no accurate scattering measurements have been attempted so far in these plates, it seems probable that they could be carried out quite successfully.

A gain in accuracy is expected on account of the smaller grain diameter. This gain would be most useful in minimum ionization tracks, as will be discussed briefly.

Whether an angular method or a sagitta method is applied, the ultimate accuracy attainable and the ultimate high energy limit in these measurements depend on the structure of the track. If the track is materialized more accurately, more accurate settings of a hairline on the track's image become possible, with fewer grains.

The influence of grain diameter d and of linear grain density D on the accuracy may perhaps be appraised from the following qualitative argument. Suppose two identical tracks, having the same length with the same number of intervals Δs, but with different values of d and D. The error ϵ_1 on angles derived from single readings in either method, arising from track structure, ought to be proportional to the linear grain dimension, namely d. Then, from the usual statistical law of the square roots of the number of independent events, it should be proportional to the number of grains in the interval to the power $-\frac{1}{2}$. On these grounds, and within a constant factor:

$$\epsilon_1 = d/D^{\frac{1}{2}}.$$

This agrees with a formula given by Goldschmidt-Clermont (18) for the angular method.

In the present emulsion take $d = 0.15\ \mu$, $D_0 = 15$. In G5, take $d = 0.6\ \mu$, $D = 36$, which are average values from Voyvodic. Thus ϵ_1 is 2.6 times smaller in the present emulsion. Very dense minimum tracks have been obtained by Marguin and Maitrot in G5, with $D \sim 0.8\ \mu$ and $D = 50$ (22); even in this case ϵ_1 is 2.9 times smaller in our emulsion. A small grain may be said to be more advantageous than a large grain density.

If the track structure were the only cause of error, then the error in determining mean scattering angles and energies would also be 2.6 times smaller, to take an average G5 plate as a standard, and the maximum energy attainable would be 2.6 times greater. If the maximum energy is 100 Gev. in G5, it would be 260 Gev. in the present emulsion.

Of course this is not quite the case since the total error ϵ is the statistical sum of ϵ_1, of stage noise error ϵ_2, and of observing error ϵ_3:

$$\epsilon = (\epsilon_1^2 + \epsilon_2^2 + \epsilon_3^2)^{\frac{1}{2}}$$

and with the more usual emulsions, ϵ_1 is not the most important term.

However, it is clear at any rate that the disadvantage of the somewhat low grain density at minimum ionization achieved so far is more than offset by the small value of the diameter, and that the present emulsion allows of good scattering measurements. The advantage should only become more marked if better stages and better observing conditions become available.

Fog

The sheets from the Lefaivre ascent, processed as described above, looked very clean under the microscope, while showing distinctly slow nucleonic branches. Fog is very small in them, and it is estimated, from a comparison

such as that of Fig. 5, that the number of fog grains is 10 times smaller than it was in certain previous sheets of formula 2 made and developed in 1949. Layers with intermediate fog values have been made earlier, but the decrease in fog attributed to the use of the new developer is probably by a factor of about 5.

This estimate is based on grains visible in a single field of view without change in focusing. However, the gain would still be larger if we excluded from the count those grains that belong to electron tracks or to other tracks. The remaining "true fog" grains are exceedingly few. In a field of view of diameter 160 μ, for a single focusing with a $\times 90$ apochromat 1.3 N.A. oil immersion, there may be as few as five grains of true fog. Sometimes this number, which may vary a little in a single sheet, is least in the center and largest near top and bottom. Electron tracks are few and not obvious. Photographs reveal more fog grains than are seen directly.

These conditions of very low fog probably arise from three causes: from the new developer chosen, which cuts down true fog; from the fading of the latent image (17), which erases old electron tracks; and lastly from geometrical effects connected with the smallness of grain size d, as follows. Suppose two emulsions 1 and 2 having the same number of fog grains per unit volume, but different values of d, with $d_1 < d_2$. When the resolving limit r of the microscope is comparable with d_2, but still allows the grains d_1 to be seen, nearly the same number of fog grains are seen per unit area in a single focusing in 1 and in 2. If $r < d_1$, more grains will be seen if the grains are coarser, because in emulsion 2, the same grain may be seen at several successive settings of the focus having depths differing by r. In emulsion 1, a grain can be seen at only one such setting.

If we try to appraise the inconvenience of fog, we may admit that it ought to be proportional first to the number of fog grains per unit volume present; second to their thickness d, since the thicker they are the greater their number visible per field of view assuming a very small value of r; and thirdly to their cross section or to d^2, which is a measure of the quantity of light and of the quantity of interesting detail in tracks that a grain may obscure when it is visible. Finally the fog's inconvenience per grain is proportional to its volume d^3. With $d_1 = 0.15$ μ and $d_2 = 0.6$ μ, fog grains are 64 times more cumbersome in the second emulsion.

Fog may also be evaluated from the "fogginess" or turbidity it induces. This should also be proportional to the number of grains per unit volume, and to the elementary volume d^3 when d is very small, or to area d^2 when d is very large with respect to wavelength.

Things may be presented in another way still. The resolving limit r should be chosen to be nearly equal to d, either for searching or for examining. With equal numbers of fog grains per unit volume, then if d is large, more fog grains are seen and resolution is coarse. If d is small, fog grains are fewer, resolution is better, and tracks of lower grain density can be recognized.

It is thought that the very low fog value achieved, together with a small improvement in intrinsic emulsion sensitivity, is responsible for bringing out minimum ionization tracks.

Fog grains are so few that they practically never interfere with grain counting in tracks even of the lowest density.

V. COSMIC TRACKS AT MINIMUM IONIZATION

The Identification of Minimum Ionization Tracks

Examination of a few stars in the sheets showed a peculiar abundance of very weak tracks with about 20 grains per 100 divisions. One division is worth between 1.12 and 1.18 μ of the emulsion being examined, according to the interpupillary distance of the observer. It was at once suspected that these were minimum ionization tracks.

These very weak tracks are not easily seen. They are almost perfectly invisible under a ×20 0.65 N.A. dry apo objective, and require a ×40 1.0 N.A. oil immersion fluorite or preferably a ×90 1.3 N.A. apo objective to be found and examined. When strongly dipping, some of them perhaps escape observation entirely, although typical minimum tracks inclined at more than 45° at the time of observing have been sighted. The very weak tracks associated with stars are certainly found more easily than those existing singly.

It is known that the number dN/dI of tracks found in cosmic stars per unit interval of ionization I exhibits a strong maximum at $I = I_0$. The absolute minimum of ionization I_0 will be taken as a unit. For $I > 1$, dN/dI decreases continually, at least until $I = 4$. If, therefore, in a new emulsion irradiated with cosmic rays, a maximum of dN/dD is observed for the smallest D values measurable, D being the number of grains per 100 μ, there is a very great chance that this lowest value of $D = D_0$ is the one for minimum ionization tracks.

The inference is perhaps not absolutely certain, because it involves the relation between D and I. However, in all very sensitive emulsions studied so far, this relation is simply a proportionality law at low values of I, and departures from this law in other emulsions disfavor an accumulation of tracks

FIG. 1. Star recorded in the new emulsion described; it is 4, 6_α in the Bristol nomenclature. No. 1 relativistic α excites a nucleus, probably one of oxygen, and goes out at nearly the same velocity, oxygen $\rightarrow$ Li + 2α slow + 1 fast proton. Seven minimum or nearly minimum particles appear, presumably six π^+ and π^- mesons and one proton. No. 5 is 5 mm. long and looks perfectly straight save near surface V (glass). The slight distortion near A (air) and V surfaces is attributed to a severe rubbing intended to remove an ink mark still visible on tracks 1 and 2. Track 5 being very long is shown in sections designated by small letters. Values marked $z =$ refer to the vertical coordinates as read on the fine adjustment drum, glass V being the origin. Letter F denotes the end of a track.

Note.—This image is a mosaic, each picture in it is printed from an "anamorphosis" 1:4 on a negative film. A circle becomes an ellipse of axes in the said ratio; see how defects and grains are flattened. Length along the axis of motion of the negative is shortened, grain density is increased. Side details (see delta rays on No. 11) and visibility are enhanced for a given area occupied by the photographic print. The pictures would lend themselves readily to scattering measurements because angles between directions near the axis of motion are multiplied by a factor 4. Angles between the tracks are transformed on a single print as seen in the larger picture in the upper left-hand corner. In this mosaic, the natural disposition of the tracks near the center was restored.

The continuous photographic instrument previously used to obtain *natural* pictures (11) was employed to obtain such *contracted* pictures, by increasing the plate speed. Details will be published elsewhere. Striae are visible on the prints, marking either the axis of motion of the film, or the direction of a slit, as a rule perpendicular to the first axis. These striae are defects of the system.

In this and in the other pictures, two values of the scale are indicated when necessary, the one in parentheses referring to the contracted dimension.

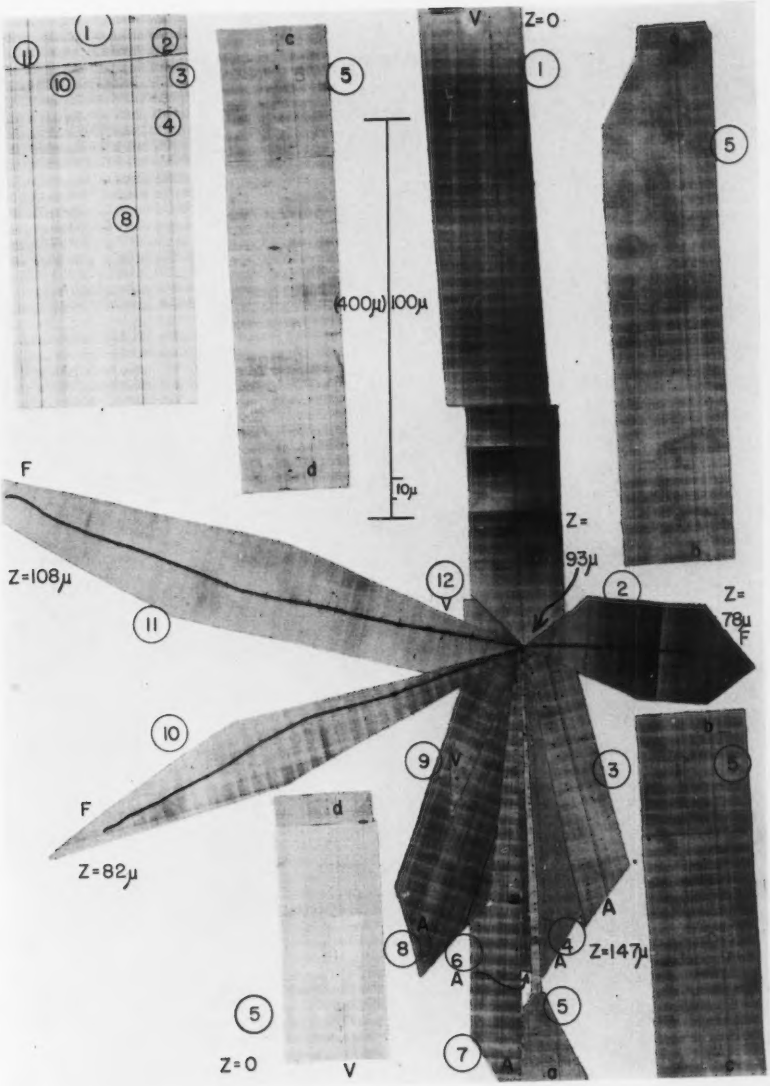
Z=0
V
(400μ) 100μ
10μ
Z=108μ
F
Z=
93μ
Z=
78μ
Z=82μ
Z=147μ
Z=0
V

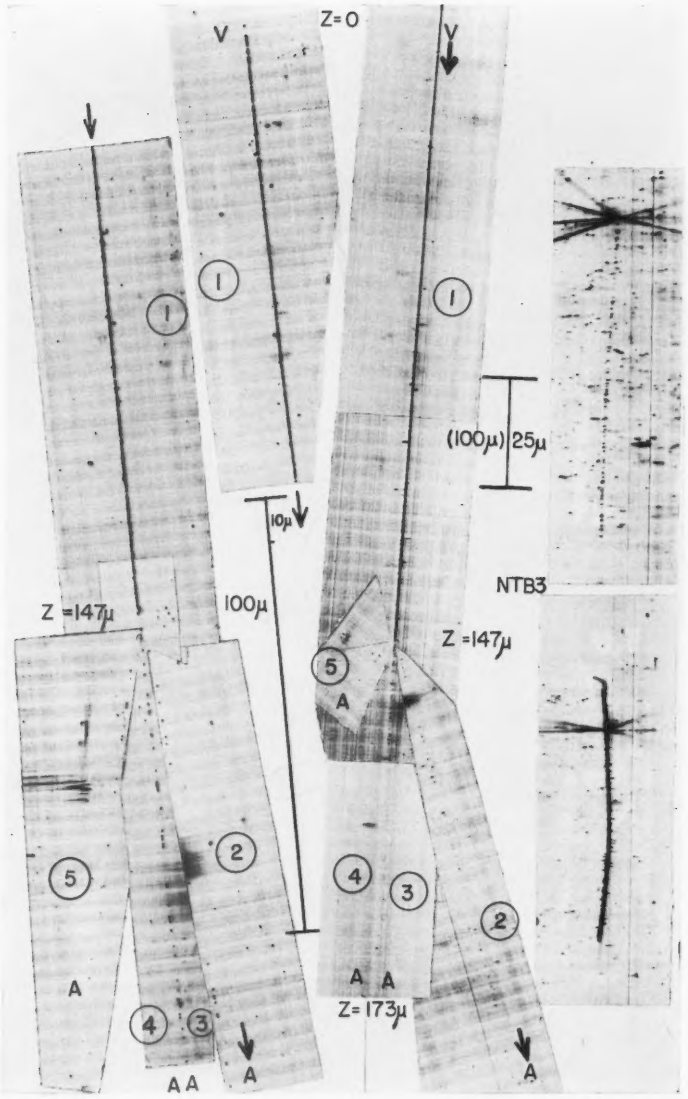

FIG. 2. *Left*—Natural picture of a star that may be interpreted as Li (relativistic) + H → 4H. If the incident is more charged than Li, some proton tracks are strongly dipping and will not be seen. Tracks 3 and 4 are nearly superposed. Tracks 1 and 2 totalled 16 mm. of observed path and showed no sign of curvature. *Center*.—Contracted picture of same. This mosaic keeps the angles of the contracted negatives. *Right*.—Contracted pictures of a star in NTB3, see natural picture in (11).

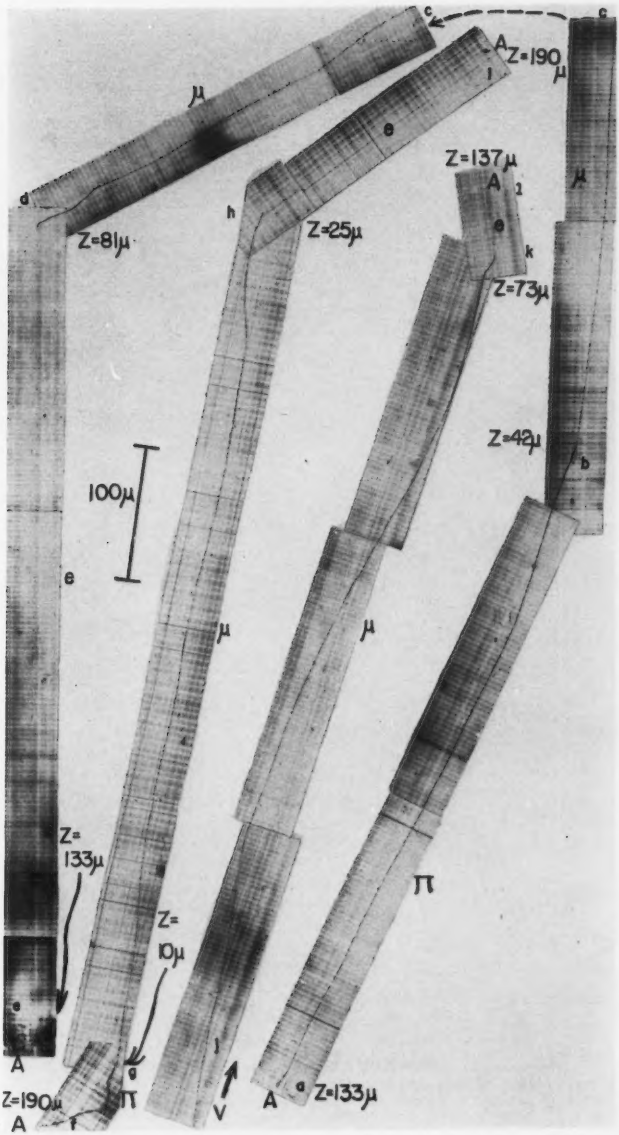

FIG. 3. Natural pictures of *two* $\pi\mu e$ *events* and of *one* μe *event* observed. One of the $\pi\mu e$ events is shown in two pieces. In two cases the electron track dips very steeply. Successive points in these events are identified by the same small letters in this and in following figures.

Inherent loss of detail in the reproduction is apparent in the electron tracks, which show up better in Figs. 4 and 5.

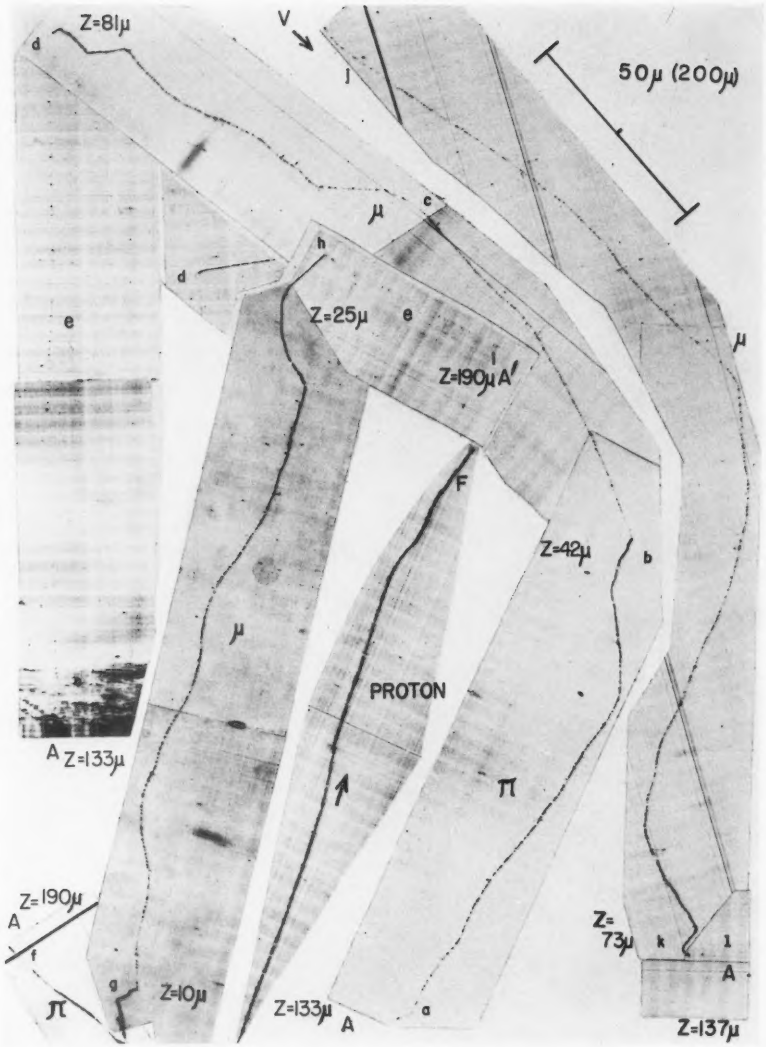

FIG. 4. Contracted pictures of same as Fig. 3. Angles of the contracted negatives are preserved in these mosaics. Wavy appearance is characteristic of mesons. The end of a slow proton found in the same sheets is shown for comparison. The difference in scattering and in density is rendered very obvious by the contraction.

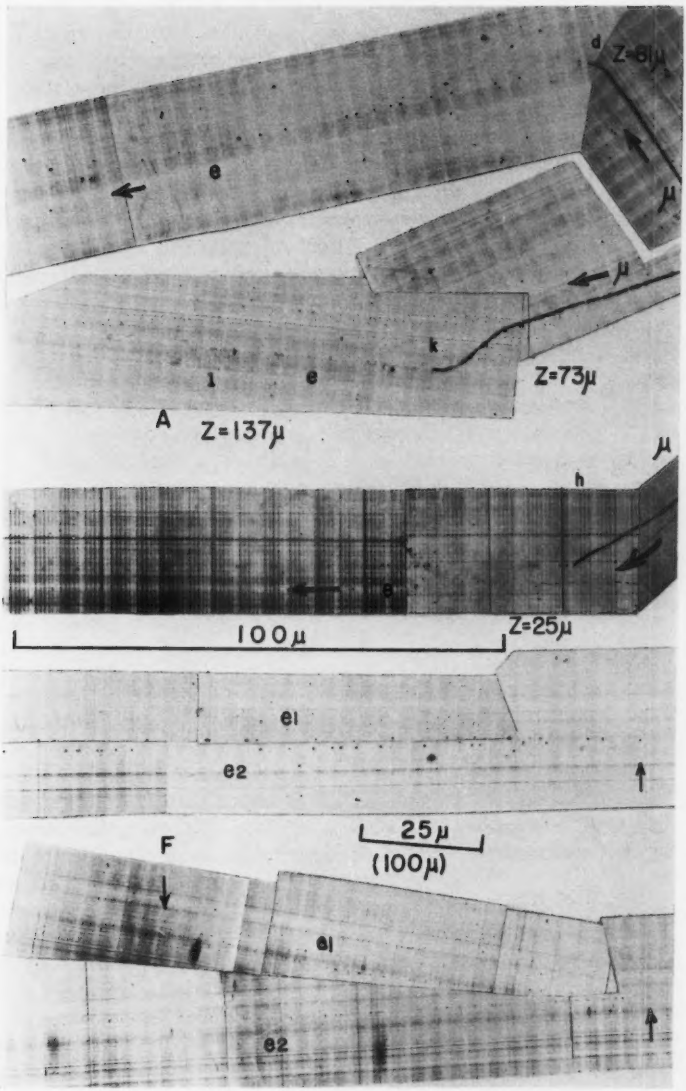

FIG. 5. *From the top.*—Natural pictures showing the beginning of the electron tracks of the three events of Figs. 3 and 4, on a larger scale. Beginning of an *electron pair*. *At bottom.*—Contracted picture of the same pair, one track ends abruptly at *F*, and may be a positon. On this picture, the scattering along the fast electron tracks may be recognized by using a ruler.

The low fog value attained may be appraised by comparing the above natural pictures with those of (11).

in categories having nearly the lowest recognizable densities. Furthermore, in previous sheets of similar make and grain size, similarly exposed, where sensitivity reached $I = 2$, no peculiar maximum of dN/dD at the lowest values of D detected was ever noticed. Fig. 6 shows the distribution observed in the present emulsions for dN/dD vs. D.

Another argument is derived from the proportion of stars containing such weak tracks. Out of a group of 50 stars having more than three branches, 17 showed at least one and on the average two tracks with $D = 13$ to 20 per 100 μ at the time of recording. This agrees well with the tables of Camerini *et al.*, which indicate that about one-third of such stars recorded at 70,000 ft. altitude contain at least one track of density between D_0 and 1.5 D_0, either as a p incident branch or as an s outgoing branch. In some cases also we have observed two or more branches grouped angularly in the same star.

One particularly clear case is shown in Fig. 1 which is interpreted as follows. A relativistic α-ray $D = 60$ comes in as No. 1 and goes out as No. 4 slightly deflected but almost unchanged in velocity. The three dense branches appear to be 1 Li and 2 α, suggesting the break-up of an oxygen nucleus; no recoil is visible. Seven shower tracks appear, four of them strongly collimated, with $D = 14$ to 25. Such a phenomenon would be very difficult to explain if these tracks were not nearly at minimum density.

Another star is more curious, Fig. 2. A very stiff heavy track No. 1 stops short and gives rise to four minimum tracks that are strongly collimated. The outgoing particles being relativistic, the incoming No. 1 ought to be relativistic also. From the number of tracks, the most obvious explanation is the reaction of an incident lithium ion, possibly primary, on a proton of the emulsion:

$$\mathrm{Li} + \mathrm{H} \rightarrow 4\mathrm{H}.$$

However $D \sim 160$ for No. 1 and the linear density of delta rays is about 12 per 100 μ, which suggest a charge of at least 4 on the incoming particle. Charge 6 would a priori be most probable, from the cosmic abundance of carbon. If the reaction is that of an ion of charge 4, 5, or 6 on a proton, it follows from charge balance that 1, 2, or 3 tracks have been missed. This is not impossible if the missing tracks are almost vertical under the microscope. This phenomenon would be very difficult to interpret if the four weak tracks were not nearly minimum ionizing protons.

Furthermore a perfectly characterized phenomenon was found. There are two unmistakable phenomena allowing recognition of minimum ionization tracks in a single event: namely a $\pi\mu e$ disintegration, and a Li_8 hammer track. Both phenomena contain an electron of several Mev. energy, which is relativistic and ionizes between 1 and 1.1 times minimum (between minimum and plateau ionization). So far two $\pi\mu e$ events were found, and one μe event. In two cases, the electron, though strongly dipping, is clearly recognized, indicating that minimum tracks can be seen in these emulsions under adverse angular conditions (angle of dip as large as 60° at the time of recording). See Figs. 3, 4, and 5.

The method of obtaining photomicrographs is somewhat unconventional, and is illustrated by Figs. 1 to 5 (10).

Distribution of Very Weak Tracks

Weak single tracks are so inconspicuous that until this point they had hardly attracted attention. This is inconvenient when looking for them; however this is almost bound to happen in any very small grain emulsion. One cannot have at the same time the benefit derived from a very small grain and a good discrimination on the one hand, and very dense and obvious minimum tracks on the other hand. However a small increase in minimum density might be of help in sighting weak tracks, without too great sacrifice in other interesting features of the emulsion.

Anyhow the difficulty of seeing weak tracks indicates how clean the emulsions look; fast mesons and electrons are present but interfere little with observations on other tracks and stars. The multitude of single relativistic tracks was revealed by a careful search under a ×90 apochromat 1.3 N.A. oil immersion with correct blue-green illumination and ×12.5 compensating eyepieces. In a sheet irradiated with its plane vertical, all single tracks dipping by less than 10 μ over 100 divisions were noted and their grains were counted over a single length of 100 divisions in order to leave unaltered one of the coordinates. The scanning was done by moving the plate exclusively along a single axis, along x for about half of the search, and along y for the other half; 296 tracks were found, or about 16.5 per mm. of axis, 107 per mm.^{2} of area, and 357 per mm.^{3} of volume examined, all dimensions being meant at the time of irradiation.

In the density distribution of Fig. 6 all tracks so encountered are included. The densest had 194 and the weakest 11 grains per 100 divisions. A strong

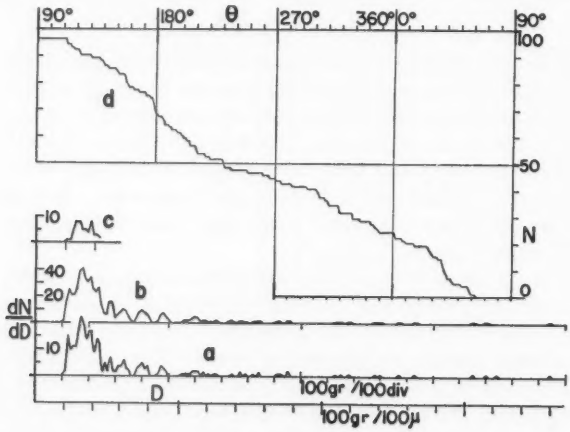

FIG. 6. (*a*) Frequency distribution of *linear grain densities* D in 297 tracks found singly. (*b*) Same as (*a*), but *perequation by 2* (successive sums of two consecutive values of dN/dD). (*c*) Same as (*a*) but for very weak tracks, found in stars, D in grains/100 μ, and $D < 23$. Scales of D: grains/100 divisions at the time of observing, and grains/100 μ at the time of irradiation. (*d*) Integral distribution N of very weak tracks found in stars. Abscissae are projected angles θ counted clockwise. Ordinates are number N having angle less than θ. Tracks are grouped (greatest value of slope $dN/d\theta$) about vertical at 0° and at 180°.

group stands out at low values of D, as expected for minimum ionization tracks. If statistical fluctuations in individual grain counts are taken into account, 16.5 grains per 100 divisions seem to be representative of the lowest density, or $D_0 = 15$ per 100 μ at the time of irradiation. Relativistic and nearly relativistic α rays as found by Bradt and Peters should form a group at $D = 55$ to 90 if statistics were better. The density of the relativistic α No. 1 in the star of Fig. 1 is nearly equal to $4D_0 = 60$. The angular distribution of single tracks was found to be approximately isotropic.

The density distribution was also obtained for all tracks contained in stars, having less than 25 grains per 100 divisions, and dipping by less than 80 μ per 100 divisions, see Fig. 6(c). The lower limit of the density distribution seems to be $D_0 = 14$ to 15. The convention was made to count all grains, as opposed to blob counting.

In the electrons seen arising from the two $\pi\mu e$ disintegrations, $D = 17$ after important and not too certain dip corrections. This would fit with a plateau value of density several per cent higher than minimum, since these electrons are expected to be very fast, having 10–20 Mev., and their value of $\gamma = E/mc^2$ being 20 to 40.

The angular distribution of all very weak tracks, density < 25 grains/100 divisions, found in stars is shown in Fig. 6(d); θ is the angle of the track projected on the xy plane of the emulsion, counted clockwise as seen in the microscope. The branch is the arm of the clock and the center of the star is the center of the clock; $\theta = 0°$ points to zenith. There are a few more tracks below than above the horizontal, and there is evidence of a grouping of branches about 0° and 180°, as is known to occur for branches at minimum ionization.

Pairs

The search under oil immersion was intended to find pairs. One pair was found almost at once, then no more were seen. It is shown in Fig. 5. The tracks, being irregular, are more difficult to find and to follow than the average single tracks.

The phenomenon was identified by the angular association of the two tracks, which seem to start as a single track of double density, and then to diverge from each other. Grain density $D = 14$ to 16.

One of the tracks stops short, which may be due to a sudden deflection almost upward or downward, or to annihilation. Coates and Herz (3) mentioned such disappearances as being the rule. However the mean free path for annihilation of positons is several centimeters from theory, and Voyvodic and Pickup (29) mention the phenomenon as being rather infrequent. Regions of low sensitivity might also explain it. In our case, other minimum tracks could be seen passing in the neighborhood of the point of disappearance.

ACKNOWLEDGMENTS

Thanks are due to Dr. A. Steigmann, of Atlantic Gelatine Co., and to its president Mr. S. Cohen, for correspondence exchanged and for special gelatine samples provided; to Mr. A. Nantel of the Microbiology Institute in this University, for electron microscope observations; to Miss Solange Boucher

who helped in nearly all phases of the work described; and to Miss Suzanne Lavallée who also helped in this work. Acknowledgments are gratefully made to the National Research Council, and also to Canadian Industries Limited and to Office Provincial des Recherches Scientifiques (Ministère de l'Industrie et du Commerce, Québec), for grants received.

REFERENCES

1. BERRIMAN, R. W. Nature, 162: 992. 1948.
2. BERRIMAN, R. W. Phot. J. 89, B: 121. 1949.
3. COATES, A. C. and HERZ, R. H. Phil Mag. 40: 1088. 1949.
4. DEMERS, P. P.M. 114, I, 4 pp. July 5, 1945. Montreal Laboratory, Natl. Research Council Can.
5. DEMERS, P. P.M. 114, II, 3 pp. September 20, 1945. Montreal Laboratory, Natl. Research Council Can.
6. DEMERS, P. Phys. Rev. 80: 86. 1946.
7. DEMERS, P. Can. J. Research, A, 25: 223. 1947.
8. DEMERS, P. Compt. rend. 231: 616. 1950.
9. DEMERS, P. Ann. ACFAS, 16 (1949): 74. 1950.
10. DEMERS, P. Phys. Rev. 78: 320. 1950.
11. DEMERS, P. Can. J. Research, A, 28: 628. 1950.
12. DEMERS, P. Science et inds. phot. 23(2): 1. 1952; Colloq. internationale de Phot. Sci. Paris, 1951. Revue d'optique, Paris. 1952. pp. 301-304.
13. DEMERS, P. Can. J. Phys. 31: 366. 1953.
14. DEMERS, P. Compt. rend. 237: 1228. 1953.
15. DEMERS, P. Ann. ACFAS, 20(1953). In press. 1954.
16. DEMERS, P. and HÉBERT, J. Colloq. internationale de Phot. Sci. Paris, 1951. Revue d'optique, Paris. 1952. pp. 304-309.
17. DEMERS, P., LAPALME, J., and THOUVENIN, J. Can. J. Phys. 31: 295. 1953.
18. GOLDSCHMIDT-CLERMONT, Y. Nuovo cimento, 7: 331. 1950.
19. JENNY, L. Bristol Phot. Conf. 259. 1950.
20. KINOSHITA, S. Proc. Roy. Soc. (London), A, 83: 432. 1910.
21. LAL, D., PAL, Y., and PETERS, B. Proc. Indian Acad. Sci. A, 38: 277. 1953.
22. MARGUIN, G. and MAITROT, M. J. phys. radium, 15: 123. 1954.
23. MATHIEU, R. and DEMERS, P. Can. J. Phys. 31: 97. 1953.
24. OCCHIALINI, G. P. S. Colloq. internationale de Phot. Sci. Paris, 1951. Revue d'optique, Paris. 1952. pp. 296-300.
25. O'DELL, F. W., SHAPIRO, M. M., and STILLER, B. Phys. Rev. 91: 496. 1953.
26. POWELL, C. F. Phil. Mag. 44: 219. 1953.
27. POWELL, C. F., OCCHIALINI, G. P. S., LIVESEY, D. L., and CHILTON, L. V. J. Sci. Instr. 23: 102. 1946.
28. VOYVODIC, L. Chapter V. *In* Progress in cosmic ray physics. Vol. II. *Edited by* J. Wilson. Interscience Publishers, Inc., New York. 1954.
29. VOYVODIC, L. and PICKUP, E. Phys. Rev. 85: 91. 1952.

SOMMAIRE

Nous décrivons la préparation d'une émulsion au gélatino-bromure et son emploi sous forme d'empilements homogènes de feuilles sans support. Un développement convenable y montre les traces au minimum d'ionisation avec des grains de diamètre 0.1 à 0.2 μ, et une densité linéaire de 15 grains par 100 μ. Nous discutons la série d'observations qui ont conduit à identifier les traces au minimum. Les reculs courts et les rayons delta courts sont visibles et la discrimination est excellente pour tous les pouvoirs ionisants. La relation entre le voile et la dimension des grains est analysée.

Plusieurs phénomènes cosmiques contenant des traces au minimum d'ionisation sont présentés: traces isolées, gerbes dures, paires et désintégrations $\pi\mu e$. La distorsion est très faible et on démontre que la finesse du grain rend possible des mesures de diffusion angulaire plus précises jusqu'à des énergies plus grandes. Dans cette émulsion à peu près toutes les mesures possibles sur les trajectoires deviennent réalisables avec une précision accrue.

NEW MEASUREMENTS ON THE $A^1\Pi \leftrightarrow X^1\Sigma$ BAND SYSTEM OF AlH[1]

By P. B. Zeeman and G. J. Ritter

ABSTRACT

The AlH band system at 4241 Å was produced in a large King Furnace and the bands were photographed in emission and absorption in the second and third orders of a 21 ft. concave grating. The vibrational and rotational constants were newly determined with improved accuracy.

INTRODUCTION

The 4241 Å system of AlH was first described by Howson (5), Mörikofer (8), and Eriksson, Hulthén, and Bengtsson (1). The bands were excited by them in an arc between aluminum electrodes in a hydrogen atmosphere. Various other workers also investigated these bands, particularly Holst and Hulthén (4). Holst (3) reported a new band system at 4980 Å. Recently Kleman, Lagercrantz, and Uhler (7) pointed out that the band at 4980 Å is none other than the (0–2) band of the 4241 Å system.

While experimenting with a large King Furnace at the National Research Council Laboratories, Ottawa, Canada, in search of bands of the evasive Al_2 molecule one of the writers observed the AlH bands with great intensity. Some interesting features in connection with predissociation were also observed. In the earlier work on the AlH molecule the wave numbers of only the (0–0), (1–1), (1–0), (0–1), and (1–2) bands were given by Eriksson, Hulthén, and Bengtsson (1) mostly to 0.1 kaysers only. No wave numbers of individual lines are given by Holst and Hulthén (4). In view of these facts it was considered important to measure the observed AlH bands, which include the (0–3) band not previously reported, with higher precision. The vibrational and rotational constants were determined by means of the graphical methods suggested by Herzberg (2, page 181); care having been taken to use large enough scales for the various graphs to ensure the highest possible accuracy. Accordingly it is believed that the constants listed in this paper are more complete and accurate than those existing at present in the literature.

EXPERIMENTAL

The King Furnace used was the same as that described by Zeeman (11). The AlH bands were observed when aluminum was introduced into a suitable liner inside the graphite furnace element. Initially the bands were observed as an impurity due to the hydrogen that was set free while the furnace was outgassed. In subsequent experiments pure hydrogen was filled into the furnace to a pressure of 40 to 50 cm. Hg. The bands were photographed at about 2100°C. both in emission and absorption. The exposure times were of the order one to five minutes on high contrast plates. The iron arc was used as comparison spectrum.

[1]*Manuscript received April 29, 1954.*

Contribution from the Merensky Institute for Physics, Stellenbosch, South Africa. (The experimental part of the work described in this paper was carried out at the N.R.C. Laboratories, Ottawa, Canada. The bands were measured and the manuscript prepared at the Merensky Institute for Physics.)

The (0–0), (0–1), (0–2), (0–3), (1–0), (1–1), (1–2), (1–3), and (1–4) bands were photographed in the second and third orders of the grating. All these bands were measured on high dispersion plates using an Abbe comparator. The wave numbers were computed with the aid of a correction curve. In Table I the wave numbers of the lines of only the (0–2), (0–3), (1–3), and

TABLE I

WAVE NUMBERS OF THE LINES OF THE (0–2), (0–3), (1–3), AND (1–4) BANDS OF THE VIOLET AlH BAND SYSTEM

	(0–2) band				(0–3) band		
J	$R(J)$	$Q(J)$	$P(J)$	J	$R(J)$	$Q(J)$	$P(J)$
0	20288.749	..	..	0	..	..	..
1	300.927	20276.852	..	1	..	..	..
2	313.297	277.173	20253.129	2	..	..	..
3	325.741	277.609	241.634	3	..	..	..
4	338.264	278.152	230.314	4	..	18767.347	..
5	350.812	278.805	219.147	5	18841.471	769.464	..
6	363.337	279.509	208.137	6	855.970	772.232	18701.023
7	375.750	280.225	197.226	7	871.195	775.411	692.435
8	388.016	280.876	186.404	8	885.957	778.994	684.354
9	400.080	281.455	175.630	9	901.230	782.703	676.993
10	411.825	281.826	164.832	10	916.336	786.555	669.484
11	423.121	282.040	153.979	11	931.646	790.565	662.603
12	433.875	281.826	142.966	12	946.676	794.584	655.600
13	443.953	281.146	131.736	13	961.250	798.447	648.898
14	453.184	279.915	120.124	14	975.320	802.066	642.231
15	461.385	277.959	108.098	15	988.774	805.292	635.410
16	468.365	275.088	95.444	16	19001.295	807.897	628.080
17	473.831	271.088	82.027	17	012.650	810.153	620.778
18	477.467	265.729	67.706	18	022.497	810.750	612.542

	(1–3) band				(1–4) band		
J	$R(J)$	$Q(J)$	$P(J)$	J	$R(J)$	$Q(J)$	$P(J)$
0	19855.432	..	..	0	18394.070	..	..
1	865.018	19843.894	..	1	404.020	18382.870	..
2	873.640	841.975	19820.883	2	413.306	381.648	18360.563
3	881.145	839.036	807.481	3	421.870	379.733	348.194
4	887.465	835.010	793.098	4	429.558	377.098	335.196
5	892.498	829.860	777.710	5	436.309	373.677	321.504
6	896.057	823.379	761.204	6	441.947	369.271	307.091
7	897.965	815.508	743.486	7	446.248	363.801	291.774
8	897.905	806.005	724.418	8	448.941	357.070	275.465
9	895.521	794.596	703.791	9	449.765	348.776	257.930
10	890.483*	781.028	681.367	10	447.937*	338.597*	218.120
11		764.802*	656.783*	11	443.843*	326.013*	195.182*
12			629.384*				

Indicates predissociated lines.

(1–4) bands are given. These bands are considered to be of more interest in view of previous work. In Fig. 1 a spectrogram of the (1–3) band is given. The band at 4980 Å mentioned before appeared both in emission and absorption simultaneously with the rest of the 4241 Å system. The values determined for the rotational and vibrational constants of this band agreed exactly with those calculated for the (0–2) band of the 4241 Å system. This assignment therefore seems firmly established.

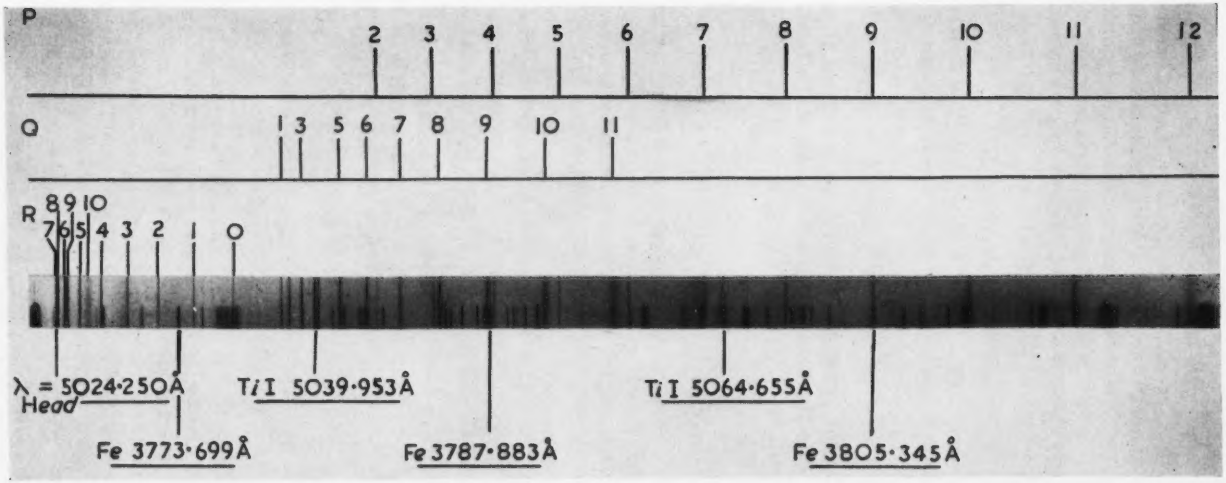

FIG. 1. Spectrogram of the (1–3) AlH band taken in the third order of the 21 ft. grating spectrograph.

The well-known breaking off of the rotational structure on account of predissociation which usually occurs in emission in low pressure arcs or discharge tubes occurs in the $v' = 1$ level of the AlH molecule. In the present experiments which were carried out at a fairly high pressure, no breaking off was observed in emission, but a progressive broadening of the lines as is shown in Fig. 1. The absence of the breaking off is due to the fact that thermal equilibrium exists in the source, and verifies the findings of Wurm (10) and Olsson (9) in connection with line broadening and thermal equilibrium.

ROTATIONAL ANALYSIS

The 4241 Å system of AlH is due to a $^1\Pi \leftrightarrow {}^1\Sigma$ transition as was shown by previous investigators. For the $^1\Sigma$ state we have the following expression for the rotational terms:

$$[1] \qquad F_v(J) = B_vJ(J+1) - D_vJ^2(J+1)^2 + H_vJ^3(J+1)^3.$$

For the $^1\Pi$ state on account of the Λ type doubling two rotational term series arise which follow the formulae (omitting the subscripts v):

$$[2] \qquad F_c(J) = B^c_{ett}\,J(J+1) - D^c_{ett}\,J^2(J+1)^2 + H^c_{ett}\,J^3(J+1)^3$$

and

$$[3] \qquad F_d(J) = B^d_{ett}\,J(J+1) - D^d_{ett}\,J^2(J+1)^2 + H^d_{ett}\,J^3(J+1)^3.$$

The constants B, D, and H have the usual meanings. In the case of the $^1\Pi$ state, the analysis of the empirical data yields the effective values B^c_{ett}, B^d_{ett}, etc. for a certain vibrational level v. In a first approximation the true B_v, D_v, and H_v values are obtained by taking the average of the B^c_{ett} and B^d_{ett}, etc. values.

The combination differences $\Delta_2F(J) = F(J+1) - F(J-1)$ are given by the following expression:

$$[4] \qquad \Delta_2F(J) = (4B_v - 6D_v)(J+\tfrac{1}{2}) - 8D_v(J+\tfrac{1}{2})^3 - 12H_v(J+\tfrac{1}{2})^5.$$

The values of the combination differences $\Delta_2F'(J)$ and $\Delta_2F''(J)$ were obtained by means of the usual relations:

$$[5] \qquad \Delta_2F'(J) = R(J) - P(J),$$

$$[6] \qquad \Delta_2F''(J) = R(J-1) - P(J+1).$$

If equation [4] is divided by $(J+\frac{1}{2})$ we obtain:

$$[7] \qquad \Delta_2F(J)/(J+\tfrac{1}{2}) = (4B_v - 6D_v) - 8D_v(J+\tfrac{1}{2})^2 - 12H_v(J+\tfrac{1}{2})^4.$$

If the term in H is neglected the constant D_v can be determined by plotting the left-hand side of equation [7] against $(J+\frac{1}{2})^2$. In the case of the $\Delta_2F''(J)$ values this graph was a straight line; but in the case of the $\Delta_2F'(J)$ values the graph was slightly curved towards the ordinate axis. Hence it became necessary to introduce the H-correction for the upper state. This was done in the following way. If equation [4] is divided by $(J+\frac{1}{2})^3$ and rearranged we obtain:

$$[8] \qquad [\Delta_2F'(J) - (4B_v' - 6D_v')(J+\tfrac{1}{2})]/(J+\tfrac{1}{2})^3 = -8D_v' - 12H_v'(J+\tfrac{1}{2})^2.$$

By using the preliminary B_v' value determined from the first graph and

plotting the left-hand side of equation [8] against $(J + \frac{1}{2})^2$ a straight line was obtained with slope $-12H_v'$ and intercept $-8D_v'$. In this way the constants H_d' listed in Table II were determined.

If we add $12H_v'(J + \frac{1}{2})^4$ to each value of $\Delta_2F'(J)/(J + \frac{1}{2})$ in equation [7], and plot the result against $(J + \frac{1}{2})^2$ we should obtain a straight line, with slope $8D_v'$ and intercept $(4B_v' - 6D_v')$. The slope gives an accurate value for D_v'. As an example of this procedure the graph for the (1–4) band is given in Fig. 2.

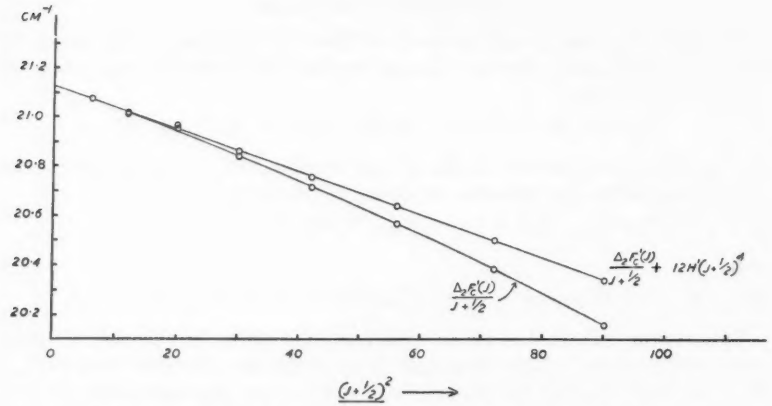

FIG. 2. Graphical determination of D_v' for the (1–4) band of AlH.

Although an accurate value of B_v' can be determined from the intercept of the last graph, preference was given to the value obtained from the graph of

$$\Delta_2F'(J) + 8D_v'(J + \tfrac{1}{2})^3 + 12H_v'(J + \tfrac{1}{2})^5 - 4\tilde{B}_v'(J + \tfrac{1}{2})$$

against J. This graph cuts the J-axis at $-\frac{1}{2}$ and this one fixed point considerably increases the accuracy with which the slope is determined.

In the above discussion only $\Delta_2F(J)$ values were used and the constants B'' and D'' of the $^1\Sigma$ state as well as the effective B', D', and H' values of the Π_d component of the upper state could be determined. The effective values B_c', D_c', and H_c' of the upper state can only be determined by making use of the Q branch as well, as is done below. It can be readily seen that

$$[9] \qquad \Delta_2F_c'(J) = Q(J + 1) - Q(J - 1) + R(J - 1) - P(J + 1).$$

By using this expression and proceeding in a similar way to the above the effective B_c', D_c', and H_c' values were determined. In Table II a summary is given of the rotational constants of the various observed vibrational levels.

The values in Table II were used to determine the constants in the formulae

$$B_v = B_e - \alpha_{e_1}(v + \tfrac{1}{2}) + \alpha_{e_2}(v + \tfrac{1}{2})^2 + \ldots$$

and

$$D_v = D_e + \beta_{e_1}(v + \tfrac{1}{2}) + \beta_{e_2}(v + \tfrac{1}{2})^2 + \ldots$$

The result is given in Table III.

TABLE II

ROTATIONAL CONSTANTS OF THE VIOLET AlH SYSTEM

State	v	B^c_{eff}, kayser	B^d_{eff}, kayser	B_v, kayser	D^c_{eff}	D^d_{eff}	D_v	H^c_{eff}	H^d_{eff}	H_v
					$\times 10^{-4}$ kayser			$\times 10^{-6}$ kayser		
$A^1\Pi$	0	6.0158_7	6.0255_6	6.0207_2	6.153_3	6.246_3	6.199_3	0.16_0	0.15_5	0.15_8
	1	5.2840_6	5.2928_0	5.2884_3	10.858_0	11.532_0	11.195_0	1.9_0	1.3_6	1.6_3
$X^1\Sigma$	0			6.2981_9			3.543_8			
	1			6.1157_3			3.490_0			
	2			5.9363_5			3.444_5			
	3			5.7600_5			3.402_5			
	4			5.5876_4			3.355_5			

TABLE III

EQUILIBRIUM ROTATIONAL CONSTANTS OF THE VIOLET AlH SYSTEM

State	B_e, kayser	α_{e_1}, kayser	α_{e_2}, kayser	D_e	β_{e_1}	β_{e_2}	r_e
				$\times 10^{-4}$ kayser			$\times 10^{-8}$ cm.
$A^1\Pi$	6.3868_8	0.7322_9		4.701_4	4.995_7		1.6482_6
$X^1\Sigma$	6.3906_6	0.1858_1	0.0016_1	3.570_6	-0.057_3	0.0028_2	1.6482_2

VIBRATIONAL ANALYSIS

The band origins of all the bands measured were determined as is described below in order to obtain the most accurate values for the vibrational constants. It can easily be seen that

[10] $$R(J-1)+P(J) = 2\nu_0+2(B_d'-B'')J^2-2(D_d'-D'')J^2(J^2+1)-2(H_d'-H'')J^4(J^2+3)$$

and that

[11] $$Q(J) = \nu_0+(B_c'-B'')J(J+1)-(D_c'-D'')J^2(J+1)^2-(H_c'-H'')J^3(J+1)^3.$$

The constants D', D'', etc. were substituted in equations [10] and [11] and the graphical procedure given by Herzberg (2, page 186) was followed to determine ν_0. The values of $(B'-B'')$ determined simultaneously were in close agreement with those obtained from the $\Delta_2F(J)$ values.

The Deslandres Table of the band origins of the violet AlH bands is given in Table IV. The vibrational constants of the lower state were evaluated by making use of the following relations given by Herzberg (2, page 96). For the separation of successive vibrational levels we have

[12] $$\Delta G_{v+\frac{1}{2}} = (\omega_0-\omega_0x_0+\omega_0y_0)-(2\omega_0x_0-3\omega_0y_0)v+3\omega_0y_0v^2,$$

for the second differences

[13] $$\Delta^2G_{v+1} = -(2\omega_0x_0-6\omega_0y_0)+6\omega_0y_0v,$$

and for the third differences

TABLE IV

DESLANDRES TABLE

v'' / v'	0		1		2		3		4	$\Delta G'_{v+\frac{1}{2}}$
0	23470.93	1625.20	21845.73	1569.05	20276.68	1514.50	18762.18			
	1082.80		1082.88		1082.68		1082.67			1082.76
1	24553.73	1625.12	22928.61	1569.25	21359.36	1514.51	19844.85	1461.37	18383.48	
$\Delta G'_{v+\frac{1}{2}}$		1625.16		1569.15		1514.51		1461.37		
$\Delta^2 G'_{v+1}$			−56.01		−54.64		−53.14			
$\Delta^3 G''_{v+3/2}$				1.37		1.50				

[14] $$\Delta^3 G_{v+3/2} = 6\omega_0 y_0,$$

if we assume $\omega_0 z_0 = \omega_e z_e = 0$. The $\Delta^2 G_{v+1}$ values from the Deslandres Table were plotted against v as is suggested by equation [13] and from the slope of the graph the value $\omega_0 y_0 = 0.238_9$ kayser was determined. Further, according to equation [12], if

$$\Delta G_{v+\frac{1}{2}} - 3\omega_0 y_0 v^2 + \overline{(2\omega_0 x_0 - 3\omega_0 y_0)} v$$

is plotted against v, where $\overline{(2\omega_0 x_0 - 3\omega_0 y_0)}$ is an approximate value of the slope, a straight line is obtained with gradient $\Delta(2\omega_0 x_0 - 3\omega_0 y_0)$ and intercept $(\omega_0 - \omega_0 x_0 + \omega_0 y_0)$. In this way the vibrational constants listed in Table V were obtained. These values determined from the Deslandres Table agreed well with the values obtained from the method first suggested by Jenkins and McKellar (6) in which use is made of corresponding lines of two bands having the same upper or lower states.

TABLE V

VIBRATIONAL CONSTANTS AND FORCE CONSTANTS* OF THE VIOLET AlH BANDS

State	ν_{00}, kayser	ω_0, kayser	ω_e, kayser	$\omega_0 x_0$, kayser	$\omega_e x_e$, kayser	$\omega_0 y_0$, kayser	k_e, dynes/cm.
$X^1\Sigma$	0	1653.65_3	1682.56_3	28.73_2	29.09_0	0.238_9	$1.6200_3 \times 10^5$
			$\Delta G_{\frac{1}{2}} = 1082.76$				
$A^1\Pi$	23470.93	..		..	..	..	..

Conversion factors were taken from (2).

ACKNOWLEDGMENTS

G. Ritter wishes to acknowledge a scholarship received from the South African Council for Scientific and Industrial Research.

P. Zeeman wishes to thank the National Research Council, Ottawa, Canada, for the postdoctorate fellowship awarded to him. The writers also wish to thank Dr. G. Herzberg for his guidance and interest in the work.

REFERENCES

1. ERIKSSON, G., HULTHÉN, E., and BENGTSSON, E. Nova Acta Regiae Soc. Sci. Upsaliensis, Ser. IV, 8. 1932.
2. HERZBERG, G. Molecular spectra and molecular structure. Vol. I. Spectra of diatomic molecules. 2nd ed. D. Van Nostrand Company, Inc., New York. 1950.
3. HOLST, W. Z. Physik, 90: 735. 1934.
4. HOLST, W. and HULTHÉN, E. Z. Physik, 90: 712. 1934.
5. HOWSON, E. Astrophys. J. 36: 286. 1912.
6. JENKINS, F. and MCKELLAR, A. Phys. Rev. 42: 464. 1932.
7. KLEMAN, B., LAGERCRANTZ, A., and UHLER, U. Arkiv Fysik, 2 (34): 359. 1950-51.
8. MÖRIKOFER, W. Diss. Basel. 1925.
9. OLSSON, E. Z. Physik, 104: 402. 1937.
10. WURM, K. Z. Physik, 76: 309. 1932.
11. ZEEMAN, P. Can. J. Phys. 32: 9. 1954.

LETTERS TO THE EDITOR

Under this heading brief reports of important discoveries in physics may be published. These reports should not exceed 600 words and, for any issue, should be submitted not later than six weeks previous to the first day of the month of issue. No proof will be sent to the authors.

The Occurrence of Ionized Nitrogen Bands in the Twilight Spectrum

It is important to establish whether or not N_2^+ ions are present in the undisturbed ionosphere and to what extent, if any, these ions contribute to the total ionization of the *E*-layer. The appearance of N_2^+ bands in the twilight spectrum is an indication of the presence in the atmosphere of molecular nitrogen ions.

The twilight spectrum has been photographed in the region of the (0, 0) N_2^+ band at 3914Å from Ottawa and Resolute Bay, N.W.T., with a plane grating spectrograph which has a dispersion of 40 Å/mm. Thirty-five satisfactory plates were obtained at Ottawa in the period July 28 to October 23, 1953, and 57 good plates were obtained at Resolute Bay in the period March 7 to April 6, 1954. The long twilight period in the spring at the latter location made it possible to secure several plates each evening. The exposures at Ottawa were timed so that at the beginning the lowest sunlit level of the atmosphere along the line of observation was at a height of 60 km. Since several twilight plates were secured each evening at Resolute Bay, the sunlit level along the line of observation varied from plate to plate. Magnetic records from Ottawa and Resolute Bay were secured from the Dominion Observatory and all disturbances during the periods of the twilight exposures noted.

On examining the spectra and the magnetic data we can make the following statement. During the periods studied, the ionized nitrogen band at 3914Å was not present in the twilight spectrum unless a magnetic disturbance occurred during the period of the exposure. Dufay (2) has pointed out that the 3914Å band is variable in intensity and that its intensity is a function of magnetic conditions. However, we would like to state explicitly that the band was seen in our spectra only during magnetically disturbed periods.

If the 3914Å band is not present in the twilight spectrum during magnetically quiet peroids, then either there are very few nitrogen molecular ions in the normal atmosphere, too few to contribute appreciably to the ionization of the *E*-region, or these ions are removed so rapidly by some process that the number of quanta radiated in the 3914Å band is small. This latter possibility has been discussed by Bates (1). In the absence of concrete information on the rate of removal of N_2^+ ions, we can only present the above observations.

1. Bates, D. R. Proc. Roy. Soc. (London), A, 196: 562. 1949.
2. Dufay, M. Ann. phys. 8: 813. 1953.

Received June 24, 1954.
Defence Research Telecommunications Establishment,
Defence Research Board,
Ottawa, Ontario.

M. Costello
H. Serson
R. Montalbetti
W. Petrie

CANADIAN JOURNAL OF PHYSICS

Notes to Contributors

Manuscripts

(i) ***General.*** Manuscripts should be typewritten, double spaced, on paper 8½×11 in. **The original and one copy are to be submitted.** Tables (each typed on a separate sheet) and captions for the figures should be placed at the end of the manuscript. Every sheet of the manuscript should be numbered.

Style, arrangement, spelling, and abbreviations should conform to the usage of this journal. Names of all simple compounds, rather than their formulas, should be used in the text. Greek letters or unusual signs should be written plainly or explained by marginal notes. Superscripts and subscripts must be legible and carefully placed.

Manuscripts should be carefully checked before they are submitted; authors will be charged for changes made in the proof that are considered excessive.

(ii) ***Abstract.*** An abstract of not more than about 200 words, indicating the scope of the work and the principal findings, is required, except in Notes.

(iii) ***References.*** References should be listed **alphabetically by authors' names,** numbered, and typed after the text. The form of the citations should be that used in this journal; in references to papers in periodicals, titles should not be given and only initial page numbers are required. All citations should be checked with the original articles and each one referred to in the text by the key number.

(iv) ***Tables.*** Tables should be numbered in roman numerals and each table referred to in the text. Titles should always be given but should be brief; column headings should be brief and descriptive matter in the tables confined to a minimum. Numerous small tables should be avoided.

Illustrations

(i) ***General.*** All figures (including each figure of the plates) should be numbered consecutively from 1 up, in arabic numerals, and each figure referred to in the text. The author's name, title of the paper, and figure number should be written in the lower left corner of the sheets on which the illustrations appear. Captions should not be written on the illustrations (see Manuscript (i)).

(ii) ***Line Drawings.*** Drawings should be carefully made with India ink on white drawing paper, blue tracing linen, or co-ordinate paper ruled in blue only; any co-ordinate lines that are to appear in the reproduction should be ruled in black ink. Paper ruled in green, yellow, or red should not be used unless it is desired to have all the co-ordinate lines show. All lines should be of sufficient thickness to reproduce well. Decimal points, periods, and stippled dots should be solid black circles large enough to be reduced if necessary. Letters and numerals should be neatly made, preferably with a stencil (**do NOT use typewriting**), and be of such size that the smallest lettering will be not less than 1 mm. high when reproduced in a cut 3 in. wide.

Many drawings are made too large; originals should not be more than 2 or 3 times the size of the desired reproduction. In large drawings or groups of drawings the ratio of height to width should conform to that of a journal page but the height should be adjusted to make allowance for the caption.

The original drawings and one set of clear copies (e.g. small photographs) are to be submitted.

(iii) ***Photographs.*** Prints should be made on glossy paper, with strong contrasts. They should be trimmed so that essential features only are shown and mounted carefully, with rubber cement, on white cardboard.

As many photographs as possible should be mounted together (with a **very** small space between each photo) to reduce the number of cuts required. Full use of the space available should be made and the ratio of height to width should correspond to that of a journal page; however, allowance must be made for the captions. Photographs or groups of photographs should not be more than 2 or 3 times the size of the desired reproduction.

Photographs are to be submitted in duplicate; if they are to be reproduced in groups one set should be mounted, the duplicate set unmounted.

Reprints

A total of 50 reprints of each paper, without covers, are supplied free. Additional reprints, with or without covers, may be purchased.

Charges for reprints are based on the number of printed pages, which may be calculated approximately by multiplying by 0.6 the number of manuscript pages (double-spaced typewritten sheets, 8½ × 11 in.) and making allowance for illustrations (not inserts). The cost per page is given on the reprint requisition which accompanies the galley.

Any reprints required in addition to those requested on the author's reprint requisition form must be ordered officially as soon as the paper has been accepted for publication.

Contents

Printed in Canada *by* University of Toronto Press